

## AN ABSTRACT OF THE THESIS OF

Laurel A. Muehlhausen for the degree of Master of Science in Oceanography  
presented on December 1, 1988.

Title: BIOMARKER ANALYSIS OF MARINE AND TERRESTRIAL ORGANIC  
CARBON SOURCES AND A PALEOTEMPERATURE RECORD FROM MANOP  
SITE C SEDIMENTS, EQUATORIAL PACIFIC.

Abstract approved: Redacted for privacy

Fredrick G. Prahl

Lipid extractions were performed on eleven, 0-26ka, sedimentary samples obtained from W8402A-14GC, a central equatorial Pacific core (MANOP site C; 1°N, 139°W). Biomarker data demonstrates that both marine and terrestrial sources contributed to the total organic carbon maximum observed at the last glacial maximum (LGM) 18,000 years b.p.. Long-chain ( $C_{37}$ ,  $C_{38}$ ,  $C_{39}$ ) unsaturated alkenones provide a measure of Prymnesiophyte algal productivity and can also be utilized to estimate paleotemperature based on the  $U^{k'}_{37}$ -index first defined by Brassell et.al. (1986). Terrestrial input estimates based on a series of long-chain ( $C_{20}$ - $C_{30}$ ) even-carbon-number predominated fatty acids indicate that significant eolian transport and deposition occurs even to this remote, open-ocean site. However, the terrestrial organic carbon input is relatively low ( $\leq 20\%$ ) and correlated with total organic carbon (TOC). Hence, it does not interfere with utilization of TOC as a paleoproductivity indicator. Considered as a whole, the data suggest that a Prymnesiophyte productivity maximum (22-20ka) preceded full glacial conditions such as global cooling and increased winds, and a species succession from calcite- to opal-producing phytoplankton occurred at the time of the LGM in response to changing nutrient concentrations. The greatest terrestrial organic carbon input coincides with the LGM (18ka) and is related to increased wind-strength and inferred increased continental aridity. The near-surface TOC maximum is undergoing post-depositional degradation, diminishing its chances for preservation in the geologic record, as evidenced by a bacterial indicator (branched  $C_{15}$  and  $C_{17}$  fatty acids) and a less source-specific, highly degradable component of organic carbon (easily-extractable,  $C_{14}$ ,  $C_{16}$  and  $C_{18}$  fatty acids).

BIOMARKER ANALYSIS OF MARINE AND TERRESTRIAL  
ORGANIC CARBON SOURCES AND A PALEOTEMPERATURE RECORD  
FROM MANOP SITE C SEDIMENTS, EQUATORIAL PACIFIC.

by

Laurel A. Muehlhausen

A THESIS

submitted to

Oregon State University

in partial fulfillment of  
the requirements of the  
degree of

Master of Science

Completed December 1, 1988

Commencement June 1989

APPROVED:

Redacted for privacy

\_\_\_\_\_  
Professor of Oceanography in charge of major

Redacted for privacy

\_\_\_\_\_  
Dean of Oceanography

Redacted for privacy

\_\_\_\_\_  
Dean of Graduate School

Date thesis is presented December 1, 1988

Typed by Laurel A. Muehlhausen and Heidi Hoffmann

for Laurel A. Muehlhausen

## ACKNOWLEDGEMENTS

Many people have provided assistance to me in the course of this work. Kathryn Brooksforce carried out the total organic carbon and carbonate carbon analyses on the LECO. Drs. Hans Schrader, Nick Pisias and Fred Prah (NSF grants OCE-8600418-01 and OCE-8812340) all had the good fortune to pay my GRA at some time. Dr. Mitch Lyle provided financial assistance for travel to other institutions and a national convention. Dr. B.R.T. Simoneit provided access to the gas chromatography-mass spectrometer. Another Laurel, Pat, Luis, Fred and D.Z. all contributed to my organic geochemical lab skills. Thanks, but I still say they taught me in 5th grade not to sniff paint thinner.

I wish to thank the members of my committee, Drs. Fred Prah, Mitch Lyle and Erwin Suess for their guidance and careful editing. Dr. Donald Amort served cheerfully as my graduate school representative.

I would like to thank CONMAR for hiring me to do an extended cruise in the Caribbean and Gulf of Mexico. Not many blonds can say they were once a member of the Mexican Navy. Mitch Lyle and Nick Pisias were responsible for my participation on the Multitracers cruise. Drs. Dave Nelson and Lou Gordon made it possible for me to chase penguins across ice floes in the Weddell Sea.

Reflecting on my years at OSU, great friendships have made all the difference. Thanks to Beaner, Jack and Ward for our little dinner parties and believing that you do not have to stay on the conveyor belt to be happy in life. I was deserving of the WSE award at least once. Many shared with me the woes of being a first-year student; Sara and Kevin, I'm glad you were there. Members of the "Rad Lab" taught me many useful things and provided great friendships. Mitch and I had several memorable adventures, rock-climbing, and skiing the bar rather than the rain to mention a few, as well as helpful discussions. Without any specifics I'd like to mention Jenny and Jeff, Anne, Bruce, Cherry, Dana, Dave Murray, Marta, Curt, Moser, Val, Kim, Joy, Sue, and Jackie. No offense to the many who go unnamed. Friendships formed outside Burt Hall added greatly to the status of my sanity; Lisa, Jeff,

Heidi, Mahoney, Tom Faus-what?, Poet, John Leland, Anterra, and Rodney, I'm glad I met ya. Thanks to my many friends at the gyms on-campus and downtown for sharing my music and my sweat. Carol, thanks for answering the phone and writing all these years.

From my undergraduate days at UM-Duluth, I wish to thank Drs. Dave Darby, John C. Green and Thomas C. Johnson of the Geology Department. Many friends there were important to me including Judy, Mary Beth, Dee, Brian, John, Ed, and Eric. Ronda, Friday afternoons would not have been the same without 79-cent burgers at Grandma's.

My family has been very supportive over the years, responding quickly and unquestioningly to urgent phone requests for money and advice about the funny noises emanating from my car, sending plane tickets assuring a white Christmas in Minnesota, and caring enough to travel to Oregon to see where I live and study. Paul, I'm proud to have you for my brother. Of all the things they taught me, the importance of completing something once you start it has had the greatest impact on the ultimate success of this research. This one's for you.

## TABLE OF CONTENTS

|   |    |
|---|----|
| A BRIEF SUMMARY OF THE ROLE OF SEDIMENTARY ORGANIC CARBON AND SITE C BACKGROUND     | 1  |
| Introduction  | 1  |
| Study site  | 9  |
| Sampling strategy   | 10 |
| METHODS   | 12 |
| MARINE, TERRESTRIAL, BACTERIAL AND MARINE/MIXED BIOMARKERS: DEFINITIONS AND DATA    | 20 |
| Data normalization  | 20 |
| Marine primary productivity biomarker   | 24 |
| Site C alkenone data  | 26 |
| U <sup>k</sup> <sub>37</sub> -index definition                                      | 29 |
| Alkenone preservation   | 30 |
| Other alkenone parameters   | 32 |
| K <sub>27</sub> /K <sub>38</sub>  | 33 |
| EE/K <sub>37</sub>  | 37 |
| Terrestrial organic carbon inputs to marine sediments                               | 43 |
| Terrestrial biomarker   | 44 |
| Bacterial and marine/mixed inputs   | 45 |
| Bacterial biomarker   | 45 |
| Marine/mixed indicator  | 46 |
| SOURCES AND SIGNIFICANCE OF THE NEAR-SURFACE TOC PEAK                               | 50 |
| INCREASED UPWELLING ASSOCIATED WITH THE LAST GLACIAL MAXIMUM                        | 55 |
| The U <sup>k</sup> <sub>37</sub> -index predicted paleotemperature record at Site C | 55 |
| Proposed phytoplankton succession   | 60 |
| PALEOPRODUCTIVITY   | 66 |
| Total organic carbon  | 66 |
| Prymnesiophyte productivity   | 67 |
| Terrestrial paleoinput  | 67 |
| Bacterial and marine/mixed indicators   | 70 |
| THE IMPACT OF TERRESTRIAL ORGANIC CARBON INPUTS ON MARINE SEDIMENTARY RECORDS       | 71 |
| Terrestrial source regions and transport paths                                      | 71 |
| Estimation of terrestrial organic carbon inputs                                     | 76 |
| Relative marine contribution to TOC   | 82 |
| Impact on sedimentary organic carbon records  | 82 |
| CONCLUSIONS   | 86 |
| Suggestions for future studies  | 86 |
| BIBLIOGRAPHY  | 89 |

|  |     |
|--|-----|
| APPENDIX A: Individual compound concentrations ( $\mu\text{g/g}$ dry sediment weight, <u>not</u> carbonate-corrected). | 97  |
| Easily-extractable lipids, fatty acid methyl esters.   | 97  |
| Acid-released lipids, fatty acid methyl esters.  | 98  |
| Easily-extractable lipids, long-chain alkenones.   | 99  |
| APPENDIX B: Sediment sample properties.  | 100 |

## LIST OF FIGURES

| <u>Figure</u>   | <u>Page</u> |
|---|-------------|
| Figure 1. MANOP site C bathymetry and location of sediment core W8402A-14GC.  | 2           |
| Figure 2. Relative amounts of (a)acetic acid leachable and (b)aluminum associated with clays in W8402A-14GC, MANOP site C (Lyle, unpublished data).   | 5           |
| Figure 3. Regression analysis of barium against total organic carbon in MANOP site C sediments (data from Murray, 1987).  | 7           |
| Figure 4. Downcore profile of total organic carbon (carbonate-free) and manganese in W8402A-14GC showing the last glacial maximum (LGM; indicated by **) and the depths sampled for this lipid survey (squares).  | 11          |
| Figure 5. Flowchart showing laboratory protocol used to extract lipids from MANOP site C sediments.   | 13          |
| Figure 6. A representative downcore record from MANOP site C comparing various data normalizations: (a)ng/g dry sediment, (b)ng/TOC, (c)ng/g dry sediment, carbonate-corrected, and (d)accumulationrate in $\mu\text{g}/\text{cm}^2/\text{kyr}$ .   | 22          |
| Figure 7. Representative gas chromatograms of the long-chain alkenones (a) and the fatty acid methyl esters from the (a)easily-extractable and, (b)acid-released lipids detected in W8402A-14GC (MANOP site C sediments).   | 27          |
| Figure 8. Long-chain alkenone parameters (a) $K_{37}/K_{38}$ and (b) $EE/K_{37}$ measured in cultures of <i>E. huxleyi</i> at various growth temperatures (square). Values measured from MANOP site C (closed diamond) and Washington coastal (triangle) sediments as well as a site C sediment trap (open diamond) are superimposed (figure from Prah1 et.al., 1988).                | 35          |
| Figure 9. Time-series of (a) $K_{37}/K_{38}$ and (b) $EE/K_{37}$ measured in MANOP site C sediments. Also plotted are a single site C sediment trap value (inverted triangle) and the range of values measured in <i>E. huxleyi</i> grown at 25°C (shaded area) from data in Prah1 et.al.(1988).  | 39          |
| Figure 10. Regression analyses of the alkenone parameters: (a) $K_{37}/K_{38}$ against the sum of all long-chain alkenones ( $\Sigma\text{alkenones}$ ), (b) $K_{37}/K_{38}$ against carbonate-free total organic carbon, (c) $EE/K_{37}$ against the sum of all long-chain alkenones ( $\Sigma\text{alkenones}$ ), and, (d) $EE/K_{37}$ against carbonate-free total organic carbon. | 41          |



|  |    |
|--|----|
| Figure 11. Ratio of acid-released to easily-extractable short FAME's: marine/mixed indicator (triangle) and bacterial (square) indicators vs. depth and age.   | 49 |
| Figure 12. Downcore concentration records from MANOP site C of (a)total organic carbon, (b)the easily-extractable marine/mixed indicator (triangle) and the easily-extractable bacterial indicator (diamond), (c)the acid-released marine/mixed indicator (inverted triangle), and the acid-released bacterial indicator (square), (d)the $U^{K'}_{37}$ -index predicted paleotemperature, (e)the marine indicator, and (f)the easily-extractable terrestrial indicator (open square) and the acid-released terrestrial indicator (open triangle). | 51 |
| Figure 13. Regression analysis of $U^{K'}_{37}$ -index predicted paleotemperatures against $\Sigma$ alkenones.   | 57 |
| Figure 14. Representative gas chromatograms comparing the relative concentrations of the long-chain alkenones from (a)Washington state coastal sediments and (b)MANOP site C sediments (Washington coast sediment data from Prahl et.al, 1988).  | 59 |
| Figure 15. Comparison of time-series from MANOP site C sediments: (a)TOC, a general productivity indicator, (b) $\Sigma$ alkenones, the Prymnesiophyte indicator, and (c)opal, a siliceous phytoplankton indicator.  | 62 |
| Figure 16. Regression analysis of TOC (weight percent, carbonate-free) vs. $\Sigma$ alkenones (ng/g, carbonate-free).  | 64 |
| Figure 17. Maps of the Pacific Ocean showing (a)location of MANOP site C and other cores mentioned in this discussion and the surrounding land masses, (b)oceanic surface currents around site C (figure after Pisias and Rea, 1988), and, (c)modern prevailing winds (figure from Pickard and Emery, 1982).   | 72 |
| Figure 18. Linear regression of the easily-extractable terrestrial indicator ( $\Sigma$ FAME's) against total organic carbon (both carbonate-free).  | 77 |
| Figure 19. Terrestrial (striped area) and marine (dotted area) organic carbon inputs to MANOP site C sediments estimated from Zafiriou et.al. (1985) aerosol data.   | 83 |
| Figure 20. Estimated terrestrial (circle) and marine (diamond) inputs as their absolute contributions to TOC (square).   | 85 |

## LIST OF TABLES

| <u>Table</u>   | <u>Page</u> |
|--|-------------|
| Table 1. Solvent volumes employed for silica gel column chromatography.  | 14          |
| Table 2. Data measuring recovery ( $\alpha$ -C <sub>24</sub> , i-C <sub>20</sub> FA) and methylation ( $\alpha$ -C <sub>21</sub> FA) efficiencies for each of the eleven sediment samples analyzed from W8402A-14GC. | 17          |
| Table 3. Biomarker concentrations in MANOP site C sediments.   | 21          |
| Table 4. Long-chain lipid parameters determined from <i>E. huxleyi</i> grown in the laboratory (from Prahl et.al., 1988).  | 34          |
| Table 5. Long-chain lipid parameters measured in MANOP site C sediments.   | 38          |
| Table 6. Estimation of relative terrestrial organic carbon input to MANOP site C sediments.  | 81          |

# BIOMARKER ANALYSIS OF MARINE AND TERRESTRIAL ORGANIC CARBON SOURCES AND A PALEOTEMPERATURE RECORD FROM MANOP SITE C SEDIMENTS, EQUATORIAL PACIFIC.

## A BRIEF SUMMARY OF THE ROLE OF SEDIMENTARY ORGANIC CARBON AND SITE C BACKGROUND

Introduction. The organic carbon fraction of marine sediments may be useful as an indicator of past marine productivity and terrestrial carbon inputs. This information aids in paleoclimatic reconstruction, improves our understanding of the modern Earth, and helps to predict future climatic conditions, particularly those related to CO<sub>2</sub> changes (e.g. Sarnthein et.al., 1988). Ocean sediments are an important store of organic carbon and need to be considered when constructing global carbon cycles (Garrels and Perry, 1974), particularly in regards to variable carbon reservoirs that affect global CO<sub>2</sub>. As reviewed by Sarnthein et.al. (1988), low latitude upwelling and the resultant high equatorial productivity is crucial to the exchange of CO<sub>2</sub> between the oceans and the atmosphere. When preserved, organic carbon stores can become major resources in the form of petroleum and related products (Hunt, 1979; Tissot and Welte, 1978).

Many techniques and measurements have been applied to quantify the organic carbon record in marine sediments and its sources. Previous studies have commonly assumed that the total organic carbon (TOC) measured in marine sediments comes entirely from marine sources and therefore quantitatively records paleoproductivity. Müller and Suess (1979) have developed a method which takes into account the variation in accumulation rates at different oceanic locations. This method features an empirical equation relating TOC, sedimentation rates, and bulk physical properties of the sediment to more accurately reconstruct paleoproductivity and TOC fluxes (Müller and Suess, 1979; Müller et.al., 1983). Because the isotopic composition of organic carbon reflects its source to some degree (Degens, 1969),

Figure 1. MANOP site C bathymetry and location of sediment core W8402A-14GC. Figure from Murray (1987).

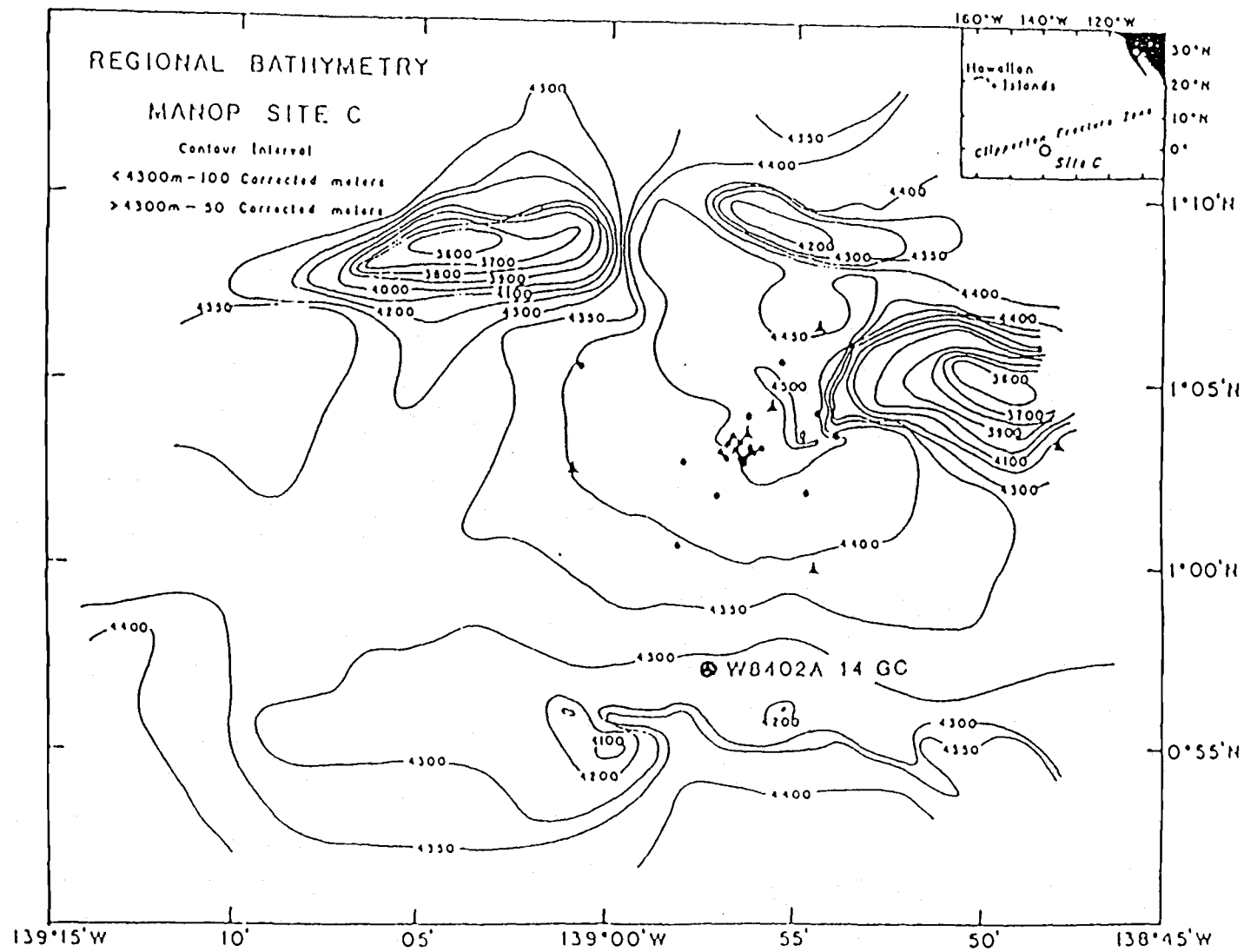


Figure 1.

$\delta^{13}\text{C}$  data have been applied to distinguish between marine and terrestrial contributions to sedimentary TOC (Müller et.al., 1983).

Other indicators not based on organic carbon have also been utilized to reconstruct paleoproductivity records and to estimate terrestrial organic carbon contributions to oceanic sediments. These proxy indicators may be obtained from elemental analyses and use aluminum (Al) to trace terrestrial inputs (e.g. Uematsu et.al., 1983), or barium (Ba) to estimate biogenic marine inputs (Dymond, 1985). However, aluminum may be unreliable as a terrestrial indicator for sediments with low terrestrial clay inputs. Acetic acid leach studies of MANOP site C sediments (Figure 1) show that up to 10% of total Al is easily-leached (Figure 2) and therefore not bound within the lattice of clay minerals derived from continental weathering. In addition, the near surface peak and relative constancy at depth observed in the easily-leached Al and clay-associated Al profiles (Figure 2) suggests that Al is reactive and diffusing out of the upper 15cm of this core. The high level of reactivity of the aluminum in the clay indicates that the clay is authigenic and therefore not indicative of terrestrial inputs (Lyle, pers.comm.). A general correlation between Ba and TOC in sediment trap material originally led to the suggestion that Ba was important for productivity and that Ba records could be used to estimate paleoproductivity (Dymond, 1985). However, in the case of site C, a Ba vs. TOC regression analysis of sediment data results in a correlation coefficient of only 0.02 (Figure 3), demonstrating that Ba and TOC systematics are not well understood and should be further studied before they can be used to estimate paleoproductivity.

While these input indicators can be good approximations, it is necessary to apply other methods in analyzing the MANOP site C organic carbon record (Figure 1). The TOC records observed in sediments are the result of several interdependent processes including primary productivity, passage downward through the water column, sedimentation and post-depositional alterations. Each transformation causes a net loss of organic carbon due to respiration such that only 0.01 to 0.1% of the original primary production is ultimately preserved in the sediments (Müller and Suess, 1979). Comparison of MANOP

**Figure 2. Relative amounts of (a)acetic acid-leachable and (b)aluminum associated with clays in W8402A-14GC, MANOP site C (Lyle, unpublished data).**

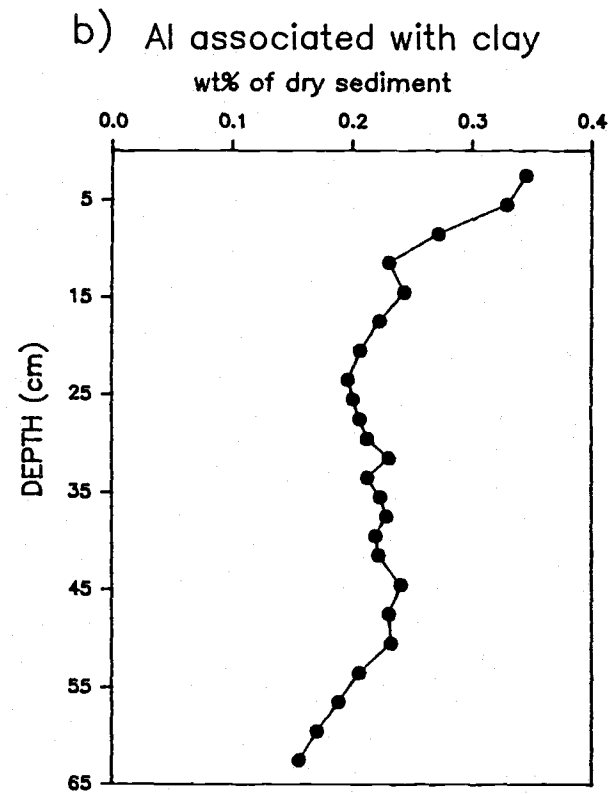
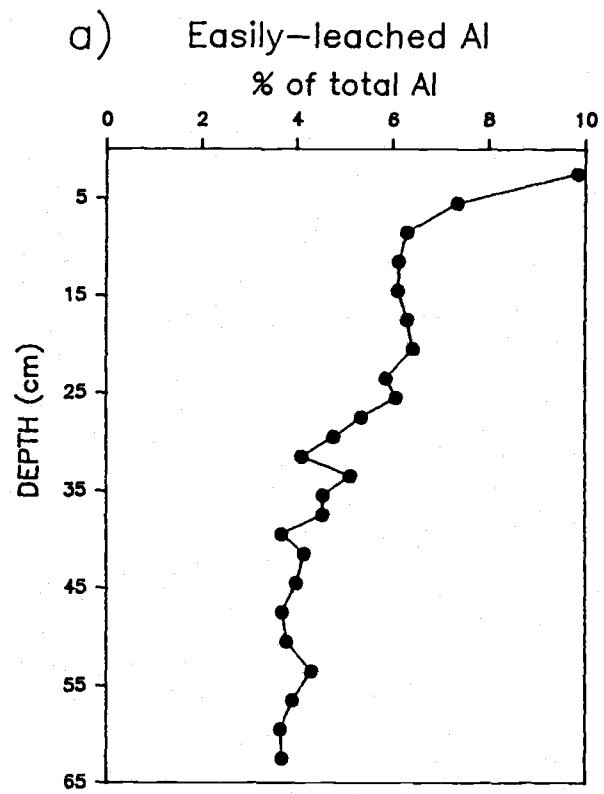
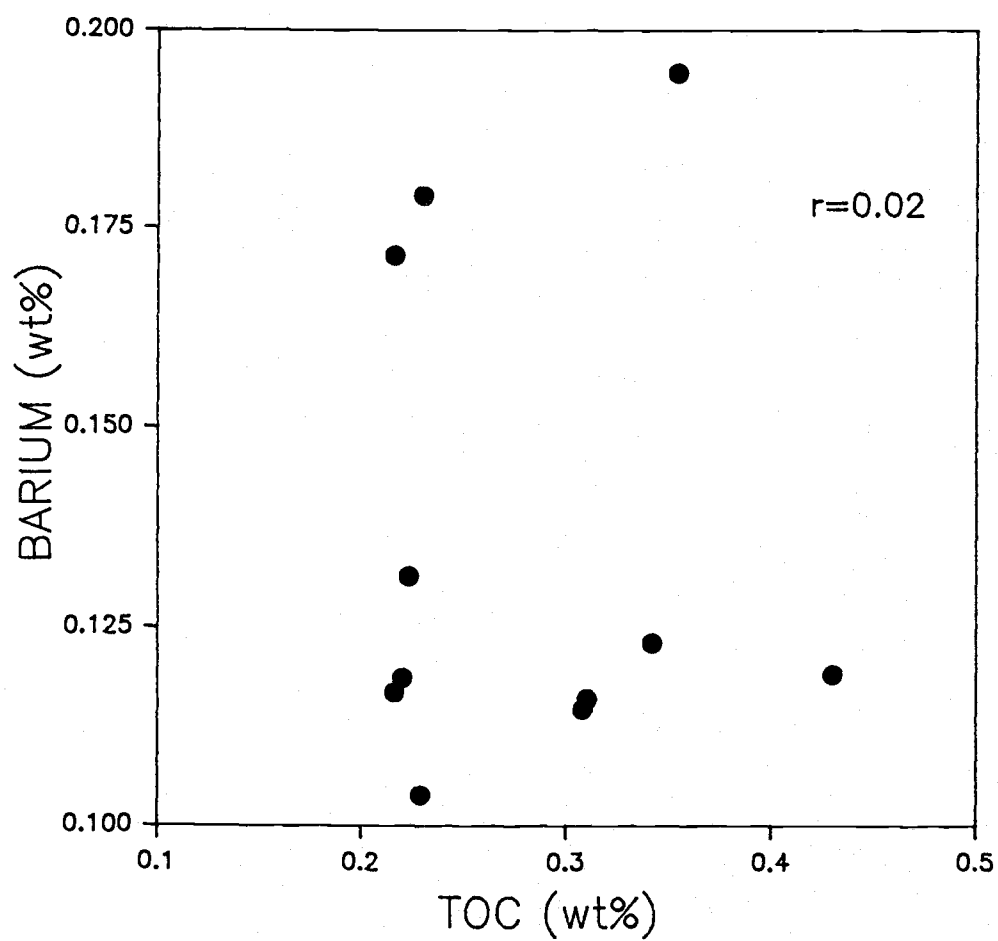


Figure 2.



Figure 3. Regression analysis of barium against total organic carbon in MANOP site C sediments (data from Murray, 1987).



site C sediment trap and surface sediment flux data led Murray (1987) to estimate that 98-99% of total organic carbon reaching the deep-water column and near-surface sediments is recycled and released as CO<sub>2</sub>. Only a small fraction of primary production ( $\approx 1\%$ ) escapes the euphotic zone.

Some workers cite pore-water chemistry data to infer that primary organic carbon inputs are highly altered by preservational and/or degradational affects such that TOC records do not accurately reflect productivity (Emerson et.al., 1985). Not all biochemical components of organic carbon are affected to the same degree, i.e., differential preservation can occur, and depending on the unique conditions within the water and sediment columns, the original makeup of the TOC can be altered considerably. For example, in the open ocean such as MANOP site C (Figure 1) low organic carbon abundances and high levels of alteration may mask carbon sources. According to end-member mixing models based on organic carbon isotope interpretations, bulk organic carbon derived from marine plankton has an isotopic range of -18 to -21‰, and terrestrially-derived organic carbon has an isotopic range of -25 to -27‰ depending on geographic latitude (Emerson et.al., 1987). Therefore, a  $\delta^{13}\text{C}_{\text{org}}$  measurement of organic carbon averaging  $19 \pm 0.5\text{‰}$  (MANOP site C sediments, McCorkle, 1987) would not indicate significant input of terrestrially-derived organic carbon. However, as recently suggested, preferential preservation of an isotopically-heavy proteinaceous material derived from foraminifera in this calcareous ooze (MANOP site C, 85% CaCO<sub>3</sub>) could mask significant terrestrial carbon inputs (Prahl and Muehlhausen, 1988).

Molecular biomarkers are source-specific organic compounds or a series of compounds used to identify organic carbon sources. They are components of the TOC and therefore can be expected to provide a better representation of organic sedimentary inputs than do mineralogic or elemental proxy indicators. Thus, it may be that biomarker methods can provide more definitive information about paleoproductivity, the degree of alteration, and other organic carbon inputs.

The following study of lipid distributions with depth in a sediment core (W8402A-14GC, MANOP site C) with a well-constrained age-scale demonstrates the usefulness of biomarker information despite very low TOC (ave. = 0.28 wt.%). Molecular biomarker information is utilized to establish the individual importance of marine and terrestrial organic carbon inputs over the last 26kyr. Geochemical information signaling in situ sedimentary processes such as microbial degradation is also revealed. An absolute paleotemperature scale is estimated, based on changes in unsaturation patterns in long-chain alkenone compositions. Based on these observations, I suggest a scenerio of coupled but non-contemporaneous response of the oceans and continents to the development of global glacial conditions.

Study site. A 330cm-long large-diameter gravity core (W8402A-14GC; 0°5 7.2'N, 138°57.3'W) was collected from the equatorial Pacific in 4287m water depth during the Manganese Nodule Program (MANOP), in February of 1984, (Figure 1). The study area is typical of the calcareous ooze province of the equatorial Pacific and was named "site C" after the sediment type. MANOP site C underlies the region of equatorial upwelling and is located within the equatorial production zone (defined as the zone extending from 90°W to 180°W and from 10°S to 10°N) estimated to provide up to 30% of "new" organic carbon production in the world's ocean (Chavez, 1987; Chavez and Barber, 1987). Given the magnitude of carbon production in this area, elucidating the quantity, type and source of organic carbon inputs to these sediments will help clarify global organic carbon budgets and will illustrate the problems associated with understanding the burial of organic carbon in the deep sea.

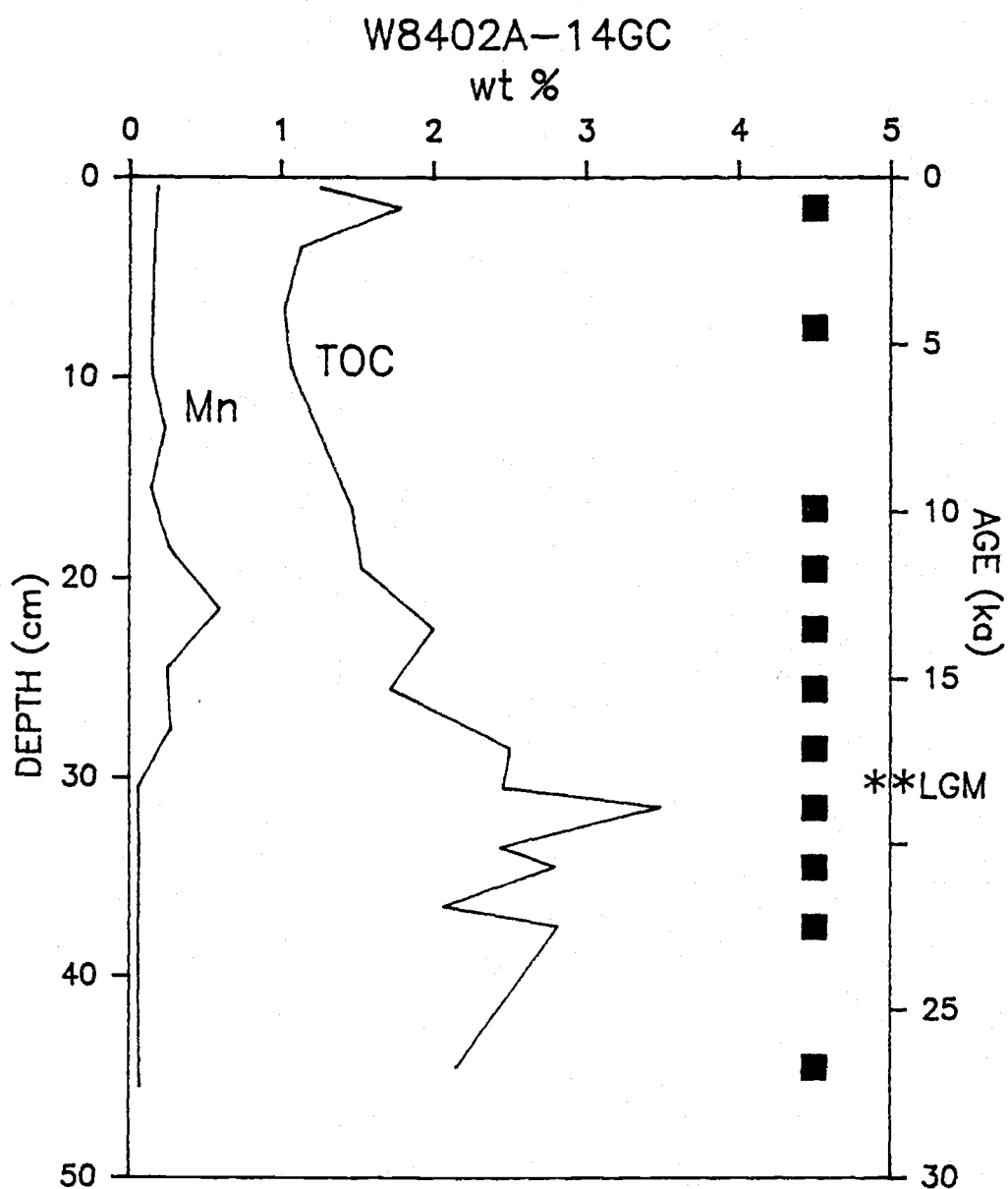
On average, W8402A-14GC contains  $85 \pm 7\%$   $\text{CaCO}_3$  and  $0.16 \pm 0.07\%$  TOC (Murray, 1987). Within the upper 45cm examined in the present study,  $\text{CaCO}_3$  and TOC are higher than average, i.e. 87% and 0.22%, respectively (appendix A). Sedimentation rates based on an oxygen isotope stratigraphy average 1.69 cm/kyr for the upper 45cm (Murray, 1987). Other data from previous investigations of W8402A-14GC to be utilized in this study include dry bulk

densities, elemental analyses (x-ray fluorescence), and siliceous microfossil identification and quantitation (Murray, 1987).

Sampling strategy. In order to obtain high time resolution (1500yrs) and a workable sample size, eleven intervals were subsampled in the upper 45cm of the core spanning the last 26kyr (Figure 4). This interval includes two TOC maxima, one near the sediment surface and another at 31cm depth, corresponding in age to the last glacial maximum (LGM) 18,000 years ago (Figure 4). TOC maxima have been correlated with glacial periods over the last 300kyr on a world-wide basis for the equatorial ocean (Lyle et.al., 1988). The upper TOC peak lies within the 0-7cm sediment mixed-layer (Emerson et.al., 1987). The present study will examine the biomarkers from these two sedimentary TOC peaks to determine the carbon inputs.

This interval also spans the redox boundary as delineated by a manganese (Mn) peak (Jahnke et.al. 1982) at 20cm (Figure 4). Above the Mn redox boundary, oxic degradation occurs within the sediments; below this zone, oxidation is mediated by much less efficient electron acceptors such as nitrate or Mn, and organic carbon degradation may be greatly reduced (Froelich et.al., 1979). Thus in situ organic carbon degradation may be occurring in the upper portion of the sampled interval but would greatly diminish below the current redox boundary.

Figure 4. Downcore profile of total organic carbon (carbonate-free) and manganese in W8402A-14GC showing the last glacial maximum (LGM; indicated by \*\*) and the depths sampled for this lipid survey (squares). Manganese data from Murray (1987); organic carbon data from Murray (1987) and samples analyzed in this study.



## METHODS

The laboratory protocol is presented in a flow chart in Figure 5. Eleven wet sediment samples, each weighing approximately 20g, were obtained in February, 1987 from core W8402A-14GC (MANOP site C), which has been stored under refrigerated conditions (4°C) at the Oregon State University core repository since its collection in February, 1984. Each 1cm wide sample approximates a 600-year time slice with 1800-year separations (neglecting bioturbation), based on the sedimentation rate and oxygen isotope datums determined for this core by Murray (1987). Based on  $^{14}\text{C}$  data, Emerson et.al. (1987) estimate a 7cm mixed layer depth in MANOP site C sediments which could result in smearing a 1cm wide sample such that up to 3500 years may be represented in a given subsample if homogenization is complete. Sample depths refer to the center of the sampled interval, e.g. 1.5cm denotes the sample recovered from the core depth 1 to 2cm.

Clean techniques were employed throughout the sample workup procedure with all glassware acid-washed and solvent-rinsed (methylene chloride) prior to use. High purity solvents (Burdick and Jackson, distilled in glass) were used and all inorganic reagents were solvent cleaned prior to use. Blanks of each extraction protocol indicated some contamination but none occurred in the column chromatographic fraction to be discussed in this thesis (L3, Table 1). For example, two phthalate peaks were identified by GC-MS (gas chromatography-mass spectrometry; use of GCMS courtesy of B.R.T. Simoneit) in the L4 fraction (Table 1). Phthalates are widely used plasticizers and are common contaminants. A certain amount of contamination could have been introduced during onboard core collection and subsequent storage in the PVC (polyvinyl chloride) coreliner but samples for lipid analysis were taken from the center of the sediment core that had not been exposed to the coreliner walls to reduce these effects.

The wet sediment samples were extracted (48 hours) with a soxhlet extractor using an azeotropic mixture (1:3) of toluene and methanol. These extracts are designated the "easily-extractable" fraction (Figure 5). After

Figure 5. Flowchart showing laboratory protocol used to extract lipids from MANOP site C sediments.

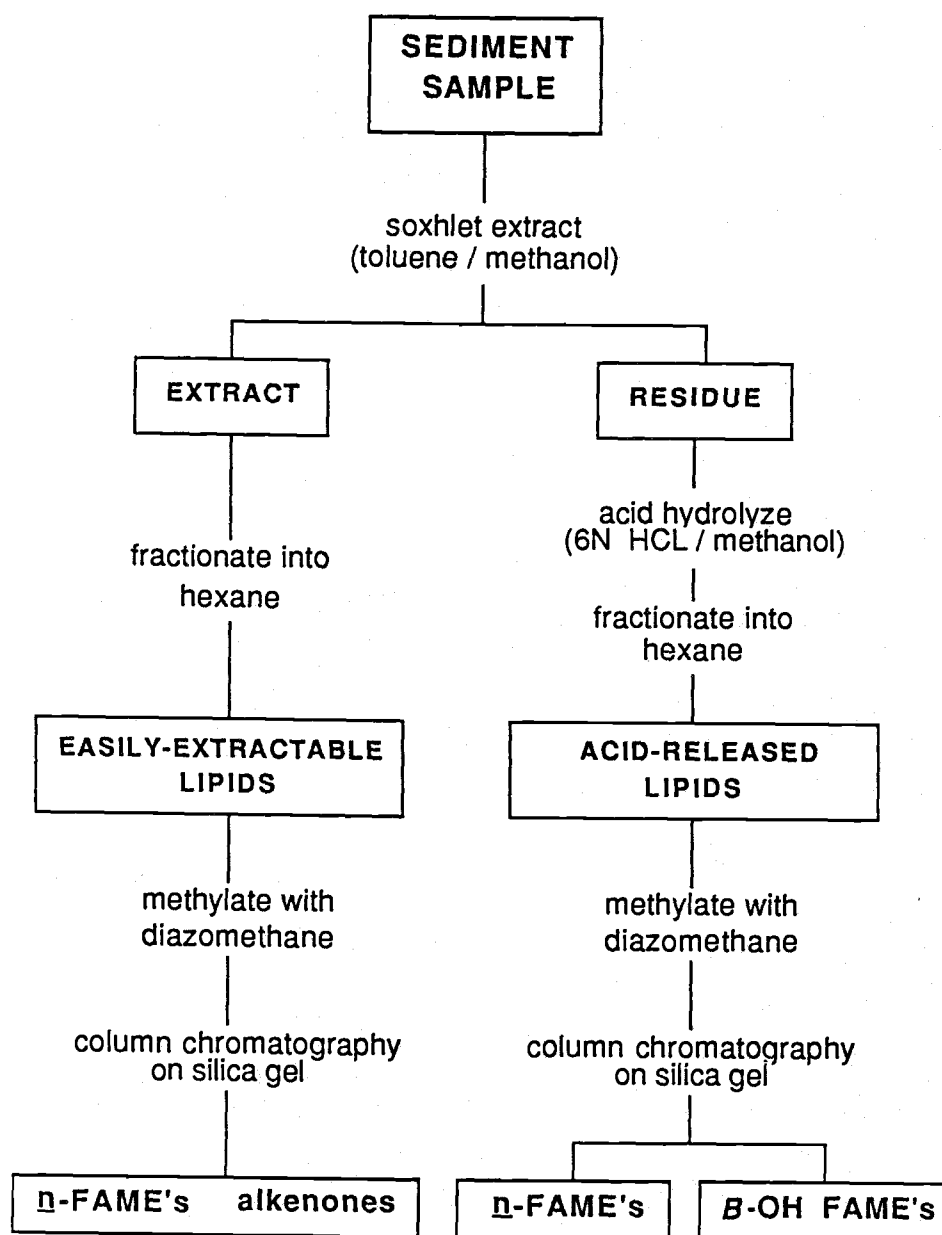


Table 1. Solvent volumes employed for silica gel column chromatography. The lipid classes detected in these fractions are listed below.

A. Easily-extracted

- L1: 30ml Hexane
- L2: 40ml 25% Toluene/hexane
- L3: 40ml 50% Toluene/hexane; 15ml 5% Ethyl acetate/hexane
- L4: 5ml 5% Ethyl acetate/hexane; 20ml 10% Ethyl acetate/hexane
- L5: 20ml 15% Ethyl acetate/hexane
- L6: 25ml 20% Ethyl acetate/hexane
- L7: 15ml Ethyl acetate; 20ml Methanol

B. Acid-released

- L1: 30ml Hexane
- L2: 40ml 25% Toluene/hexane
- L3: 40ml 50% Toluene/hexane
- L4: 20ml 5% Ethyl acetate/hexane; 20ml 10% Ethyl acetate/hexane
- L5: 20ml 15% Ethyl acetate/hexane
- L6: 25ml 20% Ethyl acetate/hexane
- L7: 15ml Ethyl acetate; 20ml Methanol

Key to fractions:

- L1: aliphatic hydrocarbons
- L2: polyaromatic hydrocarbons; alkenes
- L3: *n*-fatty acids as methyl esters; long-chain alkenones
- L4:  $\alpha$ , $\omega$ -dicarboxylic acids as methyl esters
- L5:  $\alpha$ , $\beta$  and  $\omega$ -hydroxy fatty acids as methyl esters; fatty alcohols as silyl ethers; 4-methyl steroidal alcohols as silyl ethers
- L6:  $\alpha$ , $\beta$  and  $\omega$ -hydroxy fatty acids as methyl esters; 4-desmethyl steroidal alcohols as silyl ethers
- L7: highly polar molecules



drying at room temperature and weighing, the residual sediment was transferred from the extraction thimble, placed in 150ml methanol and treated with 25ml of 12N HCL, added dropwise with stirring over 20-25 min. to insure complete carbonate dissolution ( $\text{pH} \approx 4$ ). The acidic methanol solution was refluxed for 48 hours, yielding the extract fraction designated "acid-released". The remaining carbonate-free sediment residue was separated from the lipid extract by filtration through a nominally  $1\mu$  glass-fibre filter. The easily-extractable and acid-released fractions from each sample were individually handled in the same manner as described next.

Lipid extracts were fractionated into nonpolar and polar entities with hexane and redistilled solvent-cleaned water, the hexane fraction washed with a 50% saturated NaCl solution, dried over solvent-cleaned  $\text{Na}_2\text{SO}_4$  and concentrated to near-dryness by rotoevaporation. The water fraction including pore water from the sediment and highly polar lipids was discarded. Etheral solutions of diazomethane were prepared from N-methyl-N'-nitro-N-nitrosoguanidine (97%, Aldrich Chemical Company) and employed to methylate (Schlenk and Gellerman, 1960) the total extracts of both the easily-extractable and acid-released fractions. Separation of bulk extracts into lipid classes by silica gel (Kieselgel 60, 70-230 mesh ASTM, Merck) column chromatography began with hexane and employed progressively more polar solvents for a total of seven fractions (Table 1).

The fatty acid methyl esters (FAME's) and long-chain alkenones to be discussed in this thesis coeluted in the same fraction (L3) from the easily-extractable lipids. As the gas chromatographic elution times of the FAME's and long-chain alkenones are sufficiently offset to avoid any interference, the elution of these two important chemical families in the same fraction reduces the number of GC runs necessary for quantification, saving time and other resources. Only fatty acid methyl esters are detected in the L3 fraction of the acid-released lipids; long-chain alkenone recovery is complete prior to acid treatment. However, significant additional fatty acid information is obtained after acid treatment (Appendix A).

Compounds were quantified by capillary gas chromatography (GC) on a Hewlett-Packard model 5890A gas chromatograph equipped with a DB-5 fused silica column (J&W Scientific; film thickness = 0.25 microns; column dimensions: 30m X 0.257mm). Hydrogen was utilized as the carrier gas in all cases and the head pressure was maintained at 10psi. Long-chain alkenones were analyzed using on-column injection; fatty acid methyl esters were analyzed using split/splitless injection. The injection port for split/splitless injections was set at 290°C, the on-column port was at ambient conditions ( $\approx 25^\circ\text{C}$ ), and the detector was set at 325°C regardless of injector conditions. On-column injections were programmed from 95 to 300°C at the rate of 5°C/min and held at 300°C for 40 minutes to allow complete elution of the long-chain alkenones. Split/splitless injections were programmed from 75 to 130°C at 10°C/min with a second temperature ramp to 300°C at 5°C/min, holding for 40 minutes at 300°C. Compound identification was accomplished by comparing to the retention times of a mixture of authentic fatty acid methyl ester standards ( $\text{C}_{12}$  through  $\text{C}_{22}$ ,  $\text{iC}_{16}$ ,  $\text{aiC}_{17}$ ,  $\text{aiC}_{19}$ ,  $\text{iC}_{20}$ ,  $\text{aiC}_{21}$ ,  $\text{C}_{24}$ ,  $\text{C}_{26}$ ,  $\text{C}_{28}$  and  $\text{C}_{30}$ ) with verification by gas chromatography-mass spectrometry. GC performance and response was monitored several times daily with a standard consisting of an  $n$ -alkane series ranging from  $\text{C}_{14}$  to  $\text{C}_{40}$ , hexamethylbenzene and  $5\alpha(\text{H})$ -cholestane. Sample fractions were dissolved in iso-octane containing a known concentration of hexamethylbenzene to allow quantitation by an internal standard method.

Prior to each extraction (easily-extractable or acid-released), the following standards were added to the sediment samples to determine the recovery efficiency of the extraction procedures: 3-methyl tricosane ( $\text{aiC}_{24}$ ) and 18-methyl nonadecanoic acid ( $\text{iC}_{20}$  fatty acid). After extraction and just prior to methylation, another fatty acid standard, 18-methyl eicosanoic acid ( $\text{aiC}_{21}$  fatty acid) was added to check for methylation efficiency. As listed in Table 2, the  $\text{aiC}_{24}$  alkane indicates good, consistent recoveries (easily-extractable:  $80\pm 7\%$ ; acid-released:  $79\pm 6\%$ ). The acid-released fatty acids also show good recoveries ( $73\pm 10\%$ ,  $\text{iC}_{20}$  fatty acid). The recovery rate of easily extractable fatty acids averaged  $69\pm 5\%$  ( $\text{iC}_{20}$  fatty acid) with the exception of the samples centered at 16.5 and 19.5cm. In some cases, more than 100%

Table 2. Data measuring recovery ( $\text{aiC}_{24}$ ,  $\text{iC}_{20}\text{FA}$ ) and methylation ( $\text{aiC}_{21}\text{FA}$ ) efficiencies for each of the eleven sediment samples analyzed from W8402A-14GC.

| Standard      | $\text{aiC}_{24}^1$   |                    | $\text{iC}_{20}\text{FA}^2$ |                    | $\text{aiC}_{21}\text{FA}^3$ |                    |
|---------------|-----------------------|--------------------|-----------------------------|--------------------|------------------------------|--------------------|
|               | easily-extracted<br>% | acid-released<br>% | easily-extracted<br>%       | acid-released<br>% | easily-extracted<br>%        | acid-released<br>% |
| Depth<br>(cm) |                       |                    |                             |                    |                              |                    |
| 1.5           | 70                    | 85                 | 65                          | 73                 | 65                           | 88                 |
| 7.5           | 72                    | 66                 | 62                          | 82                 | 62                           | 95                 |
| 16.5          | 81                    | 82                 | 14                          | 86                 | 14                           | 145 <sup>4</sup>   |
| 19.5          | 76                    | 78                 | 22 <sup>4</sup>             | 75                 | 44 <sup>4</sup>              | 102                |
| 22.5          | 85                    | 72                 | 63                          | 52                 | 63                           | 55                 |
| 25.5          | 70                    | 93                 | 69                          | 60                 | 69                           | 449 <sup>4</sup>   |
| 28.5          | 86                    | 88                 | 76                          | 71                 | 84                           | 95                 |
| 31.5          | 79                    | 76                 | 64                          | 69                 | 72                           | 107                |
| 34.5          | 85                    | 77                 | 71                          | 81                 | 75                           | 90                 |
| 37.5          | 82                    | 75                 | 73                          | 78                 | 78                           | 91                 |
| 44.5          | 89                    | 82                 | 75                          | 75                 | 84                           | 95                 |
| ave (n)       | 80 (11)               | 79 (11)            | 69 (9)                      | 73 (11)            | 72 (9)                       | 91 (9)             |
| s.d.          | $\pm 7$               | $\pm 6$            | $\pm 5$                     | $\pm 10$           | $\pm 8$                      | $\pm 15$           |

(1) alkane recovery standard, 3-methyl tricosane. (2) fatty acid recovery standard, 18-methyl nonadecanoic acid. (3) fatty acid methylation standard, 18-methyl eicosanoic acid. (4) suspect data point, not included in average.

recovery was obtained so the compound introduced as a standard or an interferent that elutes at the same time must have been present in the sediment samples.

Although the easily-extractable FAME's from depths 16.5 and 19.5cm gave anomalously low recovery values (1 and 22%, respectively), other evidence indicates their measured concentrations are accurate and no corrections have been made to the data. The alkane standard for these samples gave recoveries of 81 and 76% (16.5 and 19.5cm, respectively), indicating good recovery of this fraction and inferring successful extractions. Also lending credence to this explanation are the good recoveries of 86 and 75% (*i*C<sub>20</sub> fatty acid) obtained for the corresponding acid-released fatty acids. The apparent easily-extracted fatty acid information loss could have occurred due to incomplete methylation of the fatty acids as the methylation standard (*ai*C<sub>21</sub> fatty acid) indicates only 1% (16.5cm) and 45% (19.5cm) methylation, as compared to the 72±8% average methylation of the nine other easily-released fatty acid fractions (Table 2). The close agreement between recovery and methylation standards supports the incomplete methylation explanation; a fatty acid must be methylated in order to be detected and quantified by GC because a free carboxyl group will interact with the column. While it is possible that the fatty acid methyl ester information for samples 16.5 and 19.5cm underestimates the true concentrations of these compounds in the sediments, the lowest concentrations of long-chain alkenones also occur in these sample depths (Appendix A), and the alkenones are not affected by methylation. This is also the region of the TOC profile with the lowest concentrations. Therefore, the relatively lower FAME concentrations detected in these samples will be considered accurate, and no corrections based on recovery or methylation efficiency standards have been applied to any of the data to be discussed in this work.

Total organic carbon and CaCO<sub>3</sub> were determined on a LECO carbon analyzer using an adaptation of the wet oxidation technique of Weliky et.al. (1983). In brief, this method employs a phosphoric acid treatment to liberate the carbonate carbon followed by a concentrated dichromate/sulfuric acid

treatment to oxidize the remaining organic carbon. In both cases the carbon is measured as CO<sub>2</sub> by thermal conductivity detection. Repeated analyses of a MANOP site C bulk sediment standard indicate measurements are precise to  $\pm 6\%$  (Lyle, pers.comm.).

## MARINE, TERRESTRIAL, BACTERIAL AND MARINE/MIXED BIOMARKERS: DEFINITIONS AND DATA

A wide variety of extractable lipid information can be obtained from a low organic carbon, open ocean sediment as demonstrated by this study of core W8402A-14GC. This information greatly aids paleoenvironmental reconstructions. The lipid classes detected and quantified via gas chromatography include: (a) the *n*-alkanes, (b) the polyaromatic hydrocarbons, (c) the *n*-fatty acids analyzed as methyl esters (FAME's) and (d) the coeluting long-chain alkenones, (e) the  $\alpha$ -,  $\beta$ -, and  $\omega$ -hydroxy fatty acids analyzed as methyl esters, (f) the  $\alpha$ , $\omega$ -dicarboxylic acids analyzed as methyl esters, (g) the fatty alcohols analyzed as silyl ethers, and (h) the 4-methyl and 4-desmethyl sterols analyzed as silyl ethers. This study will focus on the long-chain alkenones, and the short- and long-chain fatty acid methyl esters; appendix A lists the concentrations of individual compounds detected in site C sediments. The downcore concentrations and a brief definition of each biomarker to be discussed in this section are listed in Table 3.

Data normalization. The data to be discussed throughout this thesis have been normalized to dry sediment weight and corrected for carbonate content (ng/g, carbonate-free). The choice of normalization to sediment weight on a carbonate-free basis has the greatest effect in the uppermost part of the core where the carbonate content drops off from nearly 90% to around 80% (Figure 6). Other choices for presentation of the data include reporting it without any normalization (ng) or normalizing the data to total organic carbon (ng/TOC). Reporting the data as concentrations has little meaning as it says nothing about sample size or the quality of the sediment sampled. Due to the wide variation in organic carbon content of sediments analyzed for lipids by all organic chemists, it would be appropriate to normalize to TOC. However, dilution effects produced by sedimentary calcium carbonate variation within the upper 50cm of this calcareous ooze makes the carbonate correction advisable. Due to the relative constancy of the sedimentation rate determined in the upper 50cm of W8402A 14-GC (Murray, 1987), conversion to material fluxes does not significantly change the

TABLE 3. BIOMARKER CONCENTRATIONS IN MANOP SITE C SEDIMENTS.

All concentrations are in  $\mu\text{g/g}$ , carbonate-corrected. The CPI and  $C_{\text{max}}$  are unitless.

| Depth<br>(cm) | Age<br>(kyr) | Marine <sup>1</sup> |                   | Marine/Mixed <sup>2</sup> |      | Bacterial <sup>3</sup> |      | Terrestrial <sup>4</sup> |      | CPI <sup>5</sup> |                 | C <sub>max</sub> <sup>6</sup> |      |
|---------------|--------------|---------------------|-------------------|---------------------------|------|------------------------|------|--------------------------|------|------------------|-----------------|-------------------------------|------|
|               |              | easy                | acid              | easy                      | acid | easy                   | acid | easy                     | acid | easy             | acid            | easy                          | acid |
| 1.5           | 1.19         | 1.59                | 18.66             | 5.60                      | 1.21 | 1.77                   | 4.75 | 3.23                     | 3.50 | 5.06             | C <sub>26</sub> | C <sub>26</sub>               |      |
| 7.5           | 4.44         | 0.54                | 2.27              | 3.13                      | 0.35 | 0.87                   | 2.89 | 1.92                     | 2.58 | 8.62             | C <sub>26</sub> | C <sub>26</sub>               |      |
| 16.5          | 9.78         | 0.81                | 0.50              | 3.34                      | 0.18 | 0.98                   | 1.62 | 2.77                     | 3.71 | 5.34             | C <sub>26</sub> | C <sub>26</sub>               |      |
| 19.5          | 11.54        | 0.84                | 1.01              | 2.08                      | 0.25 | 0.51                   | 1.35 | 1.98                     | 3.71 | 4.63             | C <sub>26</sub> | C <sub>26</sub>               |      |
| 22.5          | 13.31        | 1.71                | 1.74              | 4.80                      | 0.32 | 2.14                   | 4.03 | 3.54                     | 3.05 | 4.22             | C <sub>26</sub> | C <sub>26</sub>               |      |
| 25.5          | 15.09        | 1.49                | 1.90              | 3.13                      | 0.37 | 1.16                   | 3.45 | 2.37                     | 3.14 | 5.26             | C <sub>26</sub> | C <sub>26</sub>               |      |
| 28.5          | 16.86        | 3.73                | 2.23              | 5.86                      | 0.38 | 1.64                   | 6.39 | 4.08                     | 3.65 | 5.13             | C <sub>26</sub> | C <sub>26</sub>               |      |
| 31.5          | 18.64        | 7.11                | 1.91              | 9.18                      | 0.26 | 3.00                   | 9.23 | 7.02                     | 4.06 | 6.25             | C <sub>26</sub> | C <sub>26</sub>               |      |
| 34.5          | 20.40        | 8.10                | 1.97              | 8.07                      | 0.31 | 2.52                   | 8.65 | 6.70                     | 4.16 | 5.92             | C <sub>26</sub> | C <sub>26</sub>               |      |
| 37.5          | 22.13        | 9.24                | 1.53              | 7.06                      | 0.28 | 2.20                   | 7.12 | 6.32                     | 3.96 | 6.21             | C <sub>26</sub> | C <sub>26</sub>               |      |
| 44.5          | 25.72        | 5.34                | 1.46              | 5.48                      | 0.20 | 1.40                   | 4.38 | 4.11                     | 3.72 | 5.87             | C <sub>26</sub> | C <sub>26</sub>               |      |
| ave.          |              | 3.68                | 1.65 <sup>7</sup> | 5.24                      | 0.37 | 1.65                   | 4.89 | 4.00                     | 3.57 | 5.39             |                 |                               |      |
| s.d.          |              | 3.23                | 0.55              | 2.24                      | 0.28 | 0.76                   | 2.66 | 1.88                     | 0.47 | 0.67             |                 |                               |      |

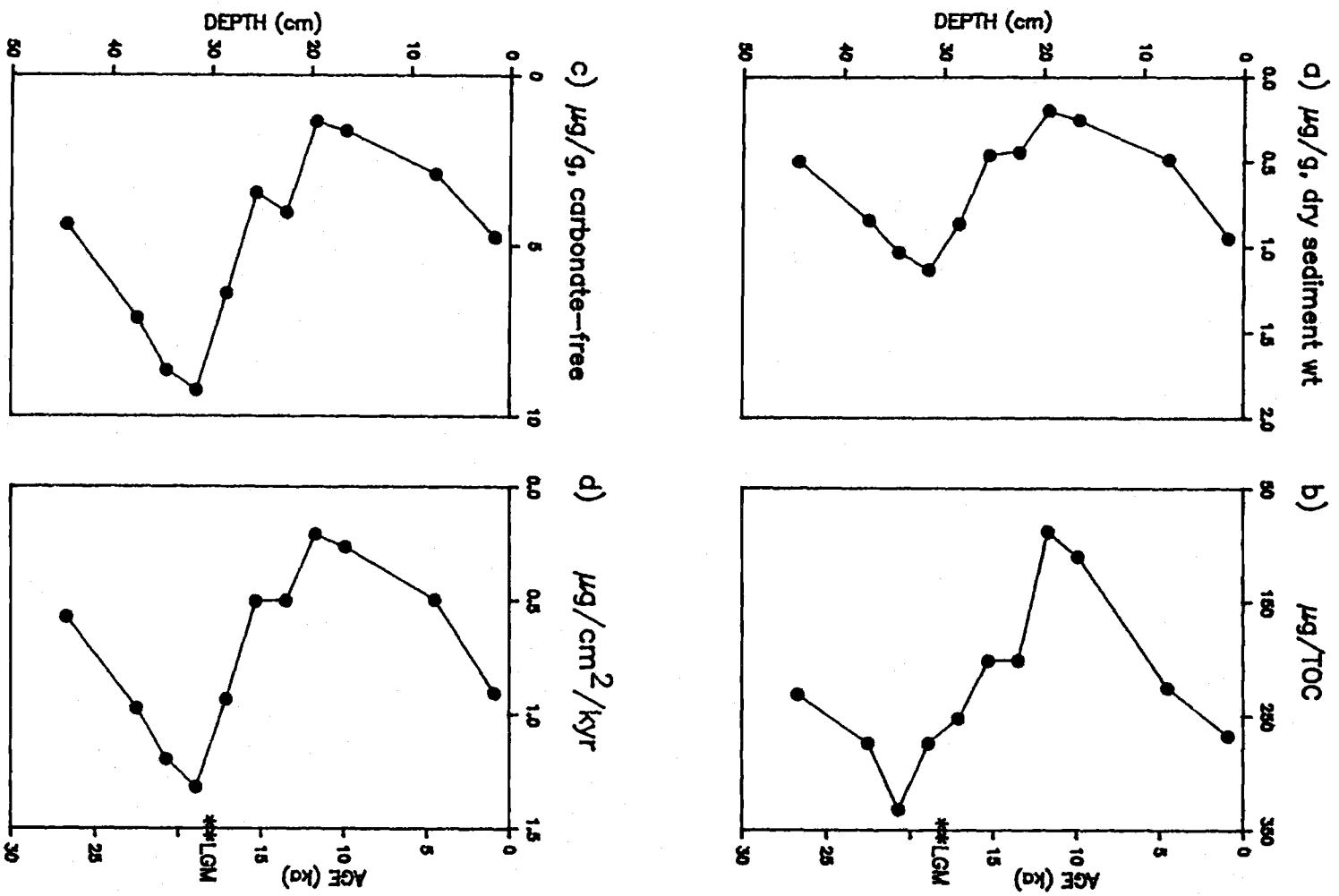
(1)  $\Sigma$ alkenones:  $C_{37}+C_{38}+C_{39}$ . (2)  $\Sigma$ FAME's:  $C_{14}+C_{16}+C_{18}$ . (3)  $\Sigma$ FAME's:  $C_{15}+C_{17}$ , n- and branched. (4)  $\Sigma$ FAME's:  $C_{20}+C_{21}+C_{22}+\dots+C_{30}$ .(5) CPI=carbon preference index =  $\frac{1}{2} \left\{ \left( \frac{\Sigma C_{20}-C_{28} \text{ evens}}{\Sigma C_{21}-C_{29} \text{ odds}} \right) + \left( \frac{\Sigma C_{22}-C_{30} \text{ evens}}{\Sigma C_{21}-C_{29} \text{ odds}} \right) \right\}$ . (7) n=10, 1.5cm sample not included in average because it is an extreme outlier. (6)  $C_{\text{max}}$  is the carbon chainlength of the most abundant long-chain FAME.

(8) n=10, 7.5cm sample not included in average because the concentrations of three of the FAME's included in this parameter were nonzero but too low to be properly measured and the CPI value is therefore questionable.

Figure 6. A representative downcore record from MANOP site C comparing various data normalizations: (a)ng/g dry sediment, (b)ng/TOC, (c)ng/g dry sediment, carbonate-corrected, and (d)accumulation rate in  $\mu\text{g}/\text{cm}^2/\text{kyr}$ . Accumulation rate was calculated using the equation  $A = C \cdot D \cdot S$  (Murray, 1987) where  $A$ ≡accumulation rate ( $\mu\text{g}/\text{cm}^2/\text{kyr}$ ),  $C$ ≡concentration ( $\mu\text{g}/\text{g}$  dry sediment weight),  $D$ ≡dry bulk density ( $\text{g}/\text{cm}^3$ ) and  $S$ ≡sedimentation rate ( $\text{cm}/\text{kyr}$ ).



Figure 6.



downcore profiles (Figure 6) so accumulation rates will not be utilized in the upcoming discussions.

Although there are cases when a single compound serves as a biomarker, as with dinosterol, a dinoflagellate biomarker (Boon et.al., 1979), a biomarker is most commonly comprised of a series of similar compounds with distinguishing characteristics. In this case, reducing the related data to a single parameter greatly simplifies data interpretation and discussion. The biomarkers to be discussed in this work are all in series or groups of three or more individual compounds. Therefore, for each biomarker the appropriate individual concentrations have been subdivided into the "marine", "terrestrial", "marine/mixed", and "bacterial" indicators as defined below.

Marine primary productivity biomarker. The Coccolithophoridae are a microscopic calcareous algae extant in all modern oceans (Haq, 1978). These primary producers bear calcium carbonate platelets or "coccoliths" that can contribute significantly to sediments (Bramlette, 1958) and are useful for dating and correlating ocean sediments (Haq, 1978). Until recently, the inorganic  $\text{CaCO}_3$  coccoliths were the only portion of these algae of interest to paleoceanographers but new discoveries have shown that unique long-chain, unsaturated alkenones synthesized by a coccolithophorid and some related algae (Volkman et.al., 1980b, 1981; Marlowe et.al., 1984) may provide important information about the temperature in which these organisms lived (Brassell et.al., 1986; Prahl and Wakeham, 1987).

Lipid surveys have documented long-chain alkenones in a well-known coccolithophid Emiliania huxleyi and four related but non-coccolith-producing members of the class Prymnesiophyceae. Other Coccolithophoridae surveyed to date lack these unusual lipids (Volkman et.al., 1980a,b; Marlowe et.al., 1984). The Prymnesiophyceae are an important component of the phytoplankton community. Thus, the long-chain alkenones are an excellent indicator of a specific type of marine organic carbon input to sediments. They can also be utilized to reconstruct the paleotemperature of the oceanic

euphotic zone when they are measured in the underlying ocean sediments (Brassell et.al, 1986; Prahl and Wakeham, 1987).

The fluidity of membrane lipids is directly affected by environmental temperature so plants and microbes have specially developed mechanisms to respond to changes in temperature (Harwood and Russell, 1984). The most widely employed mechanism is selective synthesis of lipids with differing degrees of unsaturation, i.e. at lower growth temperatures, lower melting-temperature (more unsaturated) lipids are observed. The alkenones, distinguished by their ketone functional group, are produced in chain lengths of 37, 38 and 39 carbons and can be di- or tri-unsaturated; tetra-unsaturated C<sub>37</sub> alkenones are also produced (Marlowe et.al., 1984a,b; Volkman, 1980b). Some structural differences occur with chain length as the C<sub>37</sub> is found only as methyl ketones, C<sub>38</sub> is found as methyl and ethyl ketones, and only C<sub>39</sub> ethyl ketones are found (Volkman et.al., 1980b). In culture, the total alkenone abundance in *E. huxleyi* accounts for 8±3% of the total cellular organic carbon, and this total alkenone concentration does not vary appreciably with growth temperature (Prahl et.al, 1988). This relatively large contribution to cellular organic carbon, the very long chain lengths, and general lipid structure supports a membrane function for the alkenones (Prahl et.al., 1988). However, in a strictly chemical sense, organic compound melting points are more strongly affected by *cis* unsaturation due to the kink caused by this stereoarrangement (Morrison and Boyd, 1964). The double bonds in C<sub>37:2</sub>, C<sub>37:3</sub> and C<sub>37:4</sub> have been demonstrated to be the *trans* isomer by careful synthesis (Rechka and Maxwell, in press) of tentative structures assigned previously by de Leeuw et.al.(1980) and Marlowe et.al.(1984a,b) and subsequent GC coinjection with the natural alkenones from *E. huxleyi*.

The original detection of the alkenones occurred not in algae but in sediments during routine work on Deep-Sea Drilling Project (DSDP) cores from the Walvis Ridge (Boon et.al., 1978) and were further identified through gas chromatography-mass spectrometry of a Black Sea coccolith ooze (de Leeuw et.al., 1980). Their modern and recent sedimentary distribution was rapidly expanded to include the Japan Trench (Brassell et.al., 1980), Kane Gap,

eastern equatorial Atlantic (Brassell et. al., 1986a,b), the Peru slope (Farrington et.al., in press), the equatorial Pacific (this study) as well as others (Brassell et.al., 1986b and references therein). Other long-chain alkenones have been detected in two Cretaceous black shales from the Blake-Bahama Basin, western North Atlantic, but these compounds differ in that chain-lengths of up to C<sub>42</sub> exist and only diunsaturated homologues were found (Farrimond et.al., 1986). These black shales are reportedly circa 95 and 105 Ma, substantially predating the first appearance datum of *E. huxleyi* at 268ka (Thierstein et.al., 1977); therefore the postulated source is an algal ancestor (Farrimond et.al., 1986) which could account for some of the structural differences. In addition, it is possible that depositional and preservational conditions have had an affect on the observed distributions.

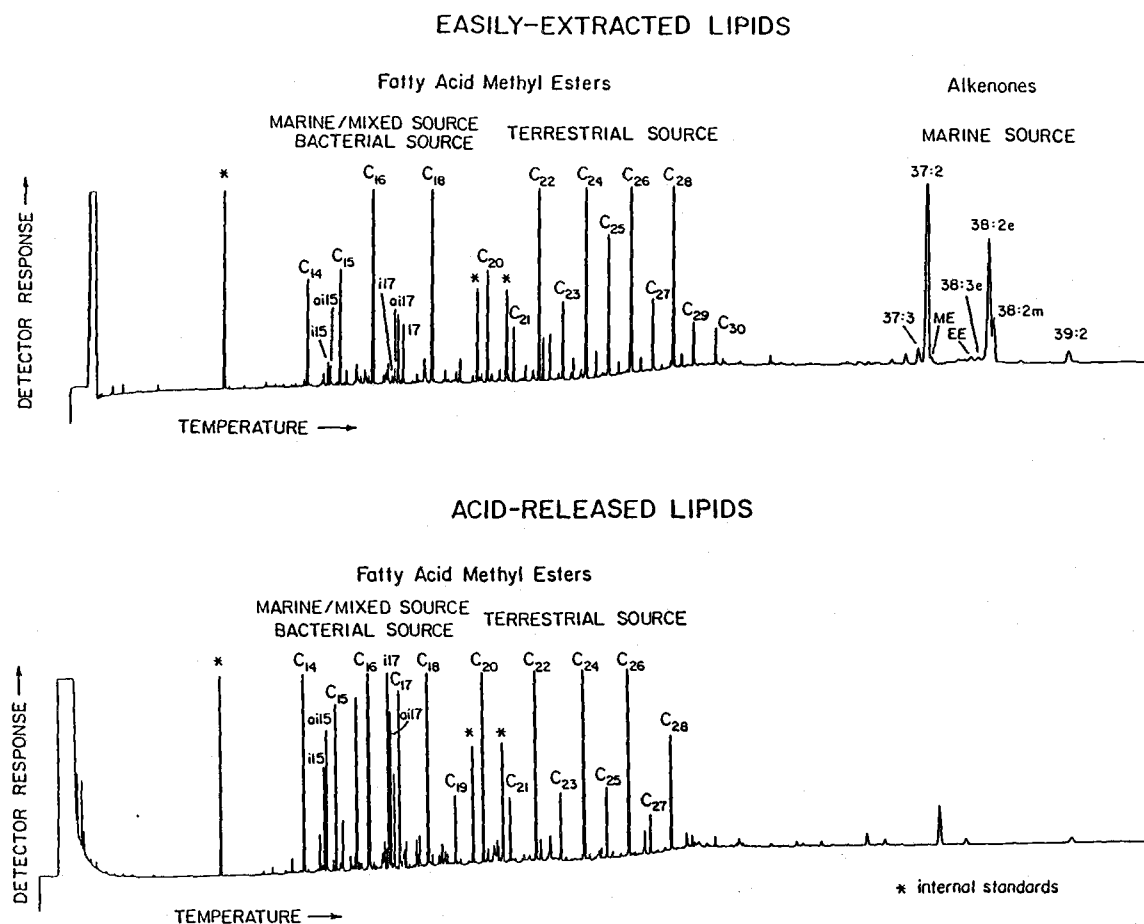
Site C alkenone data. The gas chromatogram (Figure 7) illustrates that the long-chain alkenone elution order is from shorter to longer chains and from more to less unsaturated homologues with increasing time. Individual concentrations measured in the site C sediments are on the order of ten to one hundred ng/g dry sediment, carbonate-free (Appendix A). In general, the C<sub>37</sub> alkenones are most abundant on an individual basis and the di-unsaturated homologs dominate over the tri-unsaturated. Not unexpectedly, no tetra-unsaturated long-chain alkenones were detected in this sediment because the surface water temperatures are too warm for this compound to be produced (Prahl et.al., 1988).

The marine indicator is defined as the sum of the concentrations of all long-chain alkenones, in this case a total of seven distinct and measureable compounds: C<sub>37:3</sub>, C<sub>37:2</sub>, C<sub>38:3</sub> ethyl ester, C<sub>38:3</sub> methyl ester, C<sub>38:2</sub> ethyl ester, C<sub>38:2</sub> methyl ester and C<sub>39:2</sub> (Figure 7, Table 3).

A significant difference is noted between the GC traces from the easily-extractable and acid-released fractions: the long-chain alkenones are completely recovered during the first extraction and are not present in the acid-released fraction (Figure 7). This feature is important for choosing the laboratory methods to be employed in future studies of this biomarker. It

Figure 7. Representative gas chromatograms of the long-chain alkenones (a) and the fatty acid methyl esters from the (a)easily-extractable and, (b)acid-released lipids detected in W8402A-14GC (MANOP site C sediments). Individual compound peaks are labelled by carbon chain length and structural characteristics where a≡anteiso and i≡iso branching. For the alkenones, m≡methyl ester, e≡ethyl ester, and :x indicates the number of double bonds in the chain. "\*" indicates internal standards hexamethylbenzene, iC<sub>21</sub>FAME and aiC<sub>21</sub>FAME.

Figure 7.



suggests that the alkenones exist in the sediments independently of the  $\text{CaCO}_3$  mineral which constitutes the bulk of this sediment, i.e. the alkenones are not chemically nor physically bound to the  $\text{CaCO}_3$ . In fact, most of the Prymnesiophyte algae known to produce long-chain alkenones do not produce coccoliths (Marlowe et.al., 1984). It may be that alkenone preservation is enhanced by the physical presence of calcite in the form of foraminiferal tests and coccoliths, but alkenones can occur in sediments without the protection of this physical entity. This may have special significance for sediments accumulating below the calcium compensation depth (CCD) which would be devoid of  $\text{CaCO}_3$  but could still contain valuable alkenone information (Volkman et.al., 1980b).

$U_{37}^k$ -index definition. The relative unsaturation of the long-chain alkenones from different climatic regimes varies widely; this led Brassell et.al. (1986a) to investigate a euphotic zone temperature-dependent alkenone unsaturation effect. The concentration variability of the alkenone homologues were quantified with the following unsaturation measure, called the " $U_{37}^k$ -index":

$$U_{37}^k = \{C_{37:2} - C_{37:4}\} / \{C_{37:2} + C_{37:3} + C_{37:4}\}$$

where  $C_{37}$  indicates the carbon chain length and :2, :3 and :4 indicate the degree of unsaturation, i.e. the number of double bonds in the chain (Brassell et.al, 1986a). The absence of  $C_{37:4}$  in most sediments simplifies the index to:

$$U_{37}^k = C_{37:2} / \{C_{37:2} + C_{37:3}\} \quad (\text{Brassell et.al., 1986a}).$$

In order to test the alkenone unsaturation temperature response, a 500kyr record of the  $U_{37}^k$ -index was determined in a core from the equatorial Atlantic. The record, spanning several glacial/interglacial cycles, was compared to an oxygen isotope stratigraphy measured from specific planktonic and benthic foraminifera from the same core (Brassell et.al., 1986a). Oxygen isotope records measured from the  $\text{CaCO}_3$  produced by foraminifera mainly reflect global ice volume changes with secondary effects

due to changes in sea-surface temperature and other phenomena such as vital effects (Mix, 1987). The temperature effects are greater for planktonic than benthonic foraminifera since deep-sea temperatures vary little, so Brassell et.al. (1986a) focused their attention on the correlation of the  $U^{k'}_{37}$ -index to  $\delta^{18}O$  data from a planktonic foraminifera (Globigerinoides sacculifer) and found them to be well-correlated ( $r=0.932$ ) through isotope stage 5 (127ka, Martinson et.al., 1987), with a general similarity ( $r=0.676$ ) between the records extending back to 500ka. From these results it was concluded that a common element, Milankovitch-type climate-forcing orbital cycles, had caused the two records (Brassell et.al., 1986a). However, only limited laboratory data were available to compare the sedimentary record to  $U^{k'}_{37}$ -index values produced by E. huxleyi at different growth temperatures.

Subsequent laboratory studies involving cultures of E. huxleyi grown at five temperatures ranging from 8 to 25°C have directly established the relationship of alkenone unsaturation ( $U^{k'}_{37}$ -index) and growth temperature (T):

$$U^{k'}_{37} = 0.034T + 0.039; \quad r=0.99 \quad (\text{Prah} \text{ et.al., 1988}).$$

This equation is based on four to seven replicate measurements from each of the cultures grown at various temperatures except the 8°C culture where  $n=1$ , for a total  $n=22$ .  $U^{k'}_{37}$ -index field data from suspended particulate materials and sediment trap samples with accompanying known surface mixed layer temperatures collected from several oceanic regimes largely follow this transfer equation, demonstrating its applicability to field samples (Prah and Wakeham, 1987).

Alkenone preservation. Several factors may influence the alkenone record. Analytical precision allows paleotemperature prediction to within  $\pm 0.5^\circ\text{C}$  (i.e.  $U^{k'}_{37}$ -index accuracy is  $\pm 0.02$ ; Prah and Wakeham, 1987) but this does not take into account preservation effects occurring en route to and/or within the sediments or vital effects resulting in different alkenone/growth



temperature relationships from that found in the modern E. huxleyi culture, which could cause the margin of paleotemperature error to increase.

The alkenone unsaturation systematically changes with the growth temperature of E. huxleyi (Prahl and Wakeham, 1987) and it is hoped that this relationship is not altered en route to sedimentary preservation. Feeding experiments with the copepod Calanus helgolandicus provided a diet of E. huxleyi showed that alkenones were present in the faecal pellets at concentrations reduced by only a small percentage from the levels present in the coccolithophorid diet (Volkman et.al, 1980b). Also, no alkenones were detected in the copepod lipids, apparently due to the inability of the copepod to assimilate the alkenones, resulting in passage through the gut unaltered (Volkman et.al., 1980a; Corner et.al., 1986).

It is doubtful that the alkenones are transported to and preserved in sediments at 100% efficiency, considering that much less than 0.1% of surface TOC production is ultimately preserved in sediments (Müller and Suess, 1979), and alkenones represent  $\approx 8\%$  of TOC in E. huxleyi (Prahl and Wakeham, 1987). A single site C sediment trap lipid analysis indicates that the alkenones may be degraded faster than total organic carbon (Prahl et.al., 1988). The total alkenone concentration decreased from  $300\mu\text{g/gTOC}$  in the sediment trap to  $115\mu\text{g/gTOC}$  in the sediments (Prahl and Muehlhausen, 1988). However, the relative alkenone unsaturation at this location is preserved as evidenced by the good agreement between the  $U^{k'}_{37}$ -index predicted temperatures from the sediment trap and the uppermost sediment sample,  $27.0\pm 0.5^\circ\text{C}$  and  $26.3\pm 0.5^\circ\text{C}$ , respectively (Prahl et.al., 1988; Figure 9). This provides some field evidence that the  $U^{k'}_{37}$ -index is unaltered during the process of sedimentation from the water column. As long as the alkenones are not preserved differentially by chain length or unsaturation, the relative abundances will not change and the paleotemperature record will be accurately preserved.

Indications exist that the tetra-unsaturated alkenones are more labile because they are detected in the algal cell extracts but not in sediment samples (Brassell et.al., 1986a). As already mentioned, only the di- and tri-

unsaturated alkenone concentrations are included in the  $U^{k'}_{37}$ -index for this reason (Brassell et.al., 1986a; Prahl and Wakeham, 1987). It is unknown whether hydrogenation across the double bond is causing conversion to the more saturated homologues or if the  $C_{37:4}$  molecule is being otherwise degraded. The lack of mono-unsaturated long-chain alkenones in sediments provides evidence against interhomologue conversion (Brassell et.al., 1986a). Abiological oxidation across the double bond could result in hydroxy-ketones due to the addition of  $H_2O$  (Morrison and Boyd, 1973); to date no hydroxy-ketones have been reported from sediments and the absence of hydroxyl functions in *E. huxleyi* lipid extracts has been noted (Volkman et.al., 190b). Biochemical hydrogenation of unsaturated fatty acids is very rare, and only bacteria found in the rumens of cows and sheep are known to be capable of conversion to a fully saturated molecule (Harwood and Russell, 1984). Thus it seems highly unlikely that polyunsaturated alkenones are being converted to less unsaturated homologues.

Although the alkenone thermometer will benefit from ongoing investigation to further validate its applicability, results thus far support its soundness as a reliable paleotemperature measure. Certainly it does offer an independent method to compare to the traditional microfossil-assemblage paleotemperature method utilized by CLIMAP (1978, 1981). Analytically, the  $U^{k'}_{37}$ -index predicted paleotemperature is precise to  $\pm 0.5^\circ C$  (Prahl and Wakeham, 1987), and taking into consideration the greater variability caused by real-world affects, is at least comparable to and possibly better than the  $\pm 1.6^\circ C$  (CLIMAP, 1976) achieved with micropaleontological studies.

Other alkenone parameters. Two recently-defined, long-chain unsaturated lipid parameters (Prahl et.al., 1988) can also be utilized to characterize an alkenone record. The first,  $K_{37}/K_{38}$ , utilizes a relative measure of the carbon chain length of the alkenones. In addition to the previously mentioned saturation effects, the fluidity of a lipid can be altered by changing the carbon chain length; longer chains display higher melting temperatures (Harwood and Russell, 1984). Therefore, if the alkenones are integral components of algal membranes as has been suggested (Volkman et.al.,

1981; Prahl et.al., 1988), the length of the alkenones produced may be dependent on growth temperature for biochemical reasons. The second parameter,  $EE/K_{37}$ , ratios the concentration of another unique long-chain compound, a  $C_{36}$  fatty acid ethyl ester (EE), to the sum of the  $C_{37}$  alkenones. Both parameters have been monitored over the 8 to 25°C temperature range for *E. huxleyi* in culture (Prahl et.al., 1988; Table 4).

$K_{37}/K_{38}$ . The alkenone carbon chain length variation with growth temperature is quantifiable with  $K_{37}/K_{38}$ , a ratio defined as the total concentration of all  $C_{37}$  alkenones divided by the total concentration of all  $C_{38}$  alkenones (Prahl et.al., 1988). Cultures of *E. huxleyi* show a relative increase in concentrations of the shorter (37 carbons) alkenones over the longer (38 carbons) alkenones at higher growth temperatures (Table 4; Prahl, et.al., 1988). Thus, in *E. huxleyi* the parameter  $K_{37}/K_{38}$  varies positively with growth temperature from 8 to 20°C (Figure 8), contrary to the negative relationship expected if the chain length were being varied by the algae in response to growth temperatures (Harwood and Russell, 1984). The response of plants and microbes to changes in growth temperature can be mediated by a combination of lipid modifications including unsaturation and chain length adjustments (Harwood and Russell, 1984). Given that *E. huxleyi* unsaturation changes in response to growth temperature are dramatically linear and in the direction predicted by membrane fluidity needs (Prahl and Wakeham, 1987), it might be expected that lipid chain length would respond to temperature in a like manner. However, this is not the case as the  $K_{37}/K_{38}$  varies in the opposite direction of that expected and is not linear but rather shows a decrease from the 20°C culture to the 25°C culture (Figure 8). Laboratory results suggest that carbon chain length responds more slowly to growth temperature changes than does unsaturation. In contrast to the  $U^{k'}_{37}$ -index, the  $K_{37}/K_{38}$  alkenone parameter showed no change in a four-day experiment involving a sudden growth temperature change from 20 to 15°C (Prahl et.al., 1988). Also,  $K_{37}/K_{38}$  is much more variable than the  $U^{k'}_{37}$ -index in cells acclimated at a given temperature ( $\pm 3\%$  to  $\pm 15\%$  vs.  $\pm 2\%$  to  $\pm 8\%$ ; Prahl et.al., 1988). Clearly the role of alkenone chain length in *E. huxleyi* is complex and not well-understood at this time.

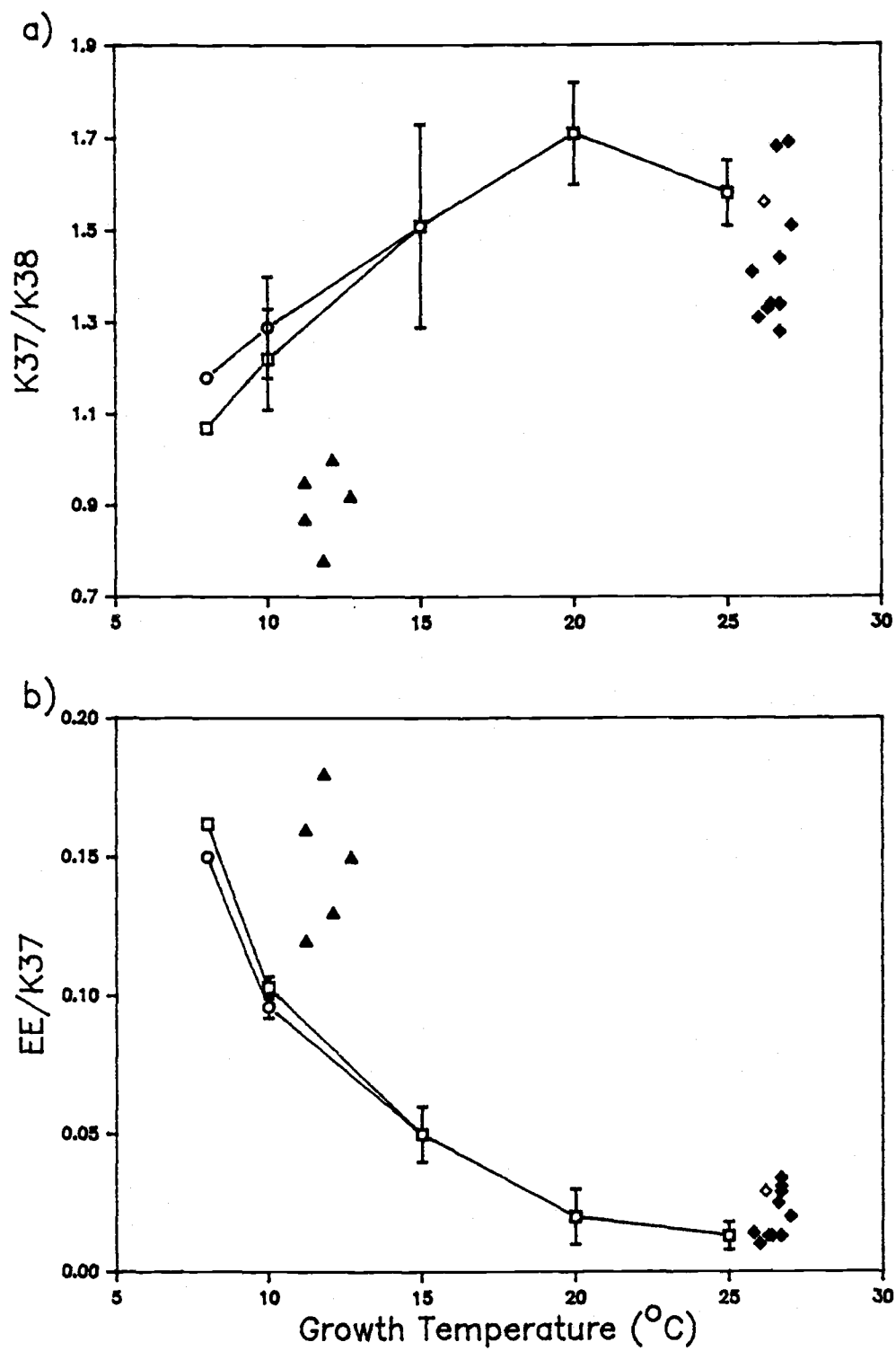
Table 4. Long-chain lipid parameters determined from *E. huxleyi* grown in the laboratory (from Prahl et.al., 1988).

| Growth<br>T, °C | n | $U_{37}^{k'1}$  | $K_{37}/K_{38}^2$ | $EE/K_{37}^3$     | $\Sigma, \text{pg/cell}^4$ |
|-----------------|---|-----------------|-------------------|-------------------|----------------------------|
| 8               | 1 | 0.29            | 1.18              | 0.15              | -                          |
| 10              | 4 | $0.31 \pm 0.02$ | $1.34 \pm 0.04$   | $0.10 \pm 0.006$  | $1.31 \pm 0.03$            |
| 15              | 5 | $0.56 \pm 0.02$ | $1.51 \pm 0.22$   | $0.048 \pm 0.013$ | $1.42 \pm 0.13$            |
| 20              | 8 | $0.73 \pm 0.02$ | $1.71 \pm 0.11$   | $0.018 \pm 0.007$ | $0.87 \pm 0.10$            |
| 25              | 4 | $0.86 \pm 0.02$ | $1.58 \pm 0.07$   | $0.012 \pm 0.006$ | $1.52 \pm 0.24$            |

(1)  $U_{37}^{k'} = C_{37:2} / (C_{37:2} + C_{37:3})$ . (2) Measure of alkenone chain length where  $K_{37}$  and  $K_{38}$  are the sum of all  $C_{37}$  and  $C_{38}$  alkenones, respectively. (3) Measure of relative contribution of long-chain lipid classes where EE denotes the diunsaturated  $C_{36}$  fatty acid ethyl ester. (4) total concentration of alkenones  $C_{37}$ ,  $C_{38}$  and  $C_{39}$ .

Figure 8. Long-chain alkenone parameters (a) $K_{37}/K_{38}$  and (b) $EE/K_{37}$  measured in cultures of *E. huxleyi* at various growth temperatures (square). Values measured from MANOP site C (closed diamond) and Washington coastal sediments (triangle) as well as a site C sediment trap (open diamond) are superimposed (figure from Prahl et.al., 1988).

Figure 8.



The  $K_{37}/K_{38}$  parameter has been determined for the eleven sediment samples from site C and can be compared to the values measured in E. huxleyi cultures (Figure 9). Because the  $U^{k'}_{37}$ -index predicted paleotemperature has ranged from 25.8 to 27.1°C over the last 26kyr (Table 5), the best agreement would be expected with data from the 25°C culture. The average sedimentary  $K_{37}/K_{38}$  value,  $1.43 \pm 0.14$ , does overlap the range of those found for the plant grown at 25°C ( $K_{37}/K_{38} = 1.58 \pm 0.07$ ; Table 4), and a single site C sediment trap  $K_{37}/K_{38}$  value (1.56) lies within this range (Figure 9). Examining the sedimentary  $K_{37}/K_{38}$  time series, the samples from 1.2, 4.4 and 11.5ka do agree with the 25°C culture, but other  $K_{37}/K_{38}$  values, especially from the older samples, fall slightly below this range (Figure 9). This deviation may be due to alteration of the original signal caused by changes in the environment of deposition. A strong correlation to  $\Sigma$ alkenones or TOC could indicate that the  $K_{37}/K_{38}$  record is linked to input levels or degradational effects, however, only weak correlations ( $r=0.42$  and  $r=0.43$ , respectively) are observed (Figure 10a,b). Based on the small temperature range (1.3°C) observed in these sediments over the last 26kyr, little variation in the  $K_{37}/K_{38}$  would be expected. Given that the  $K_{37}/K_{38}$  variation in E. huxleyi grown at a given temperature is around 10% (Table 4) and the standard deviation about the average sedimentary  $K_{37}/K_{38}$  value is also 10%, the  $K_{37}/K_{38}$  margin of error is estimated as  $\pm 0.14$  in the site C samples. Thus, it could also be argued that the observed time-series does not deviate significantly from the range of  $K_{37}/K_{38}$  values expected from controlled laboratory research.

EE/K<sub>37</sub>. Although they have yet to receive the attention afforded the long-chain, unsaturated alkenones, other long-chain unsaturated lipids have been detected in association with the alkenones (Volkman et.al., 1980; Marlowe et.al., 1984; Prahl et.al. 1988). Specifically, those produced by E. huxleyi are methyl and ethyl esters of a di-unsaturated C<sub>36</sub> fatty acid (Prahl et.al., 1988). Parameterization of these unusual fatty acids allows for their integration into an overall long-chain lipid analysis and provides an estimate of the quality of biomarker preservation. Due to chromatographic resolution, only the C<sub>36</sub> fatty acid ethyl ester (EE) can be quantified with

Table 5. Long-chain lipid parameters measured in MANOP site C sediments.

| Depth,cm | Age,kyr <sup>1</sup> | U <sup>k'</sup> <sub>37</sub> <sup>2</sup> | T,°C <sup>3</sup> | K <sub>37</sub> /K <sub>38</sub> <sup>4</sup> | EE/K <sub>37</sub> <sup>5</sup> | Σ,μg/g <sup>6</sup> |
|----------|----------------------|--|-------------------|---|---------------------------------|---------------------|
| 1.5      | 1.2                  | 0.96                                       | 27.0              | 1.69  | 0.020                           | 1.59                |
| 7.5      | 4.4                  | 0.96                                       | 27.1              | 1.51  | ----- <sup>7</sup>              | 0.54                |
| 16.5     | 9.8                  | 0.95                                       | 26.7              | 1.28  | 0.031                           | 0.81                |
| 19.5     | 11.5                 | 0.94                                       | 26.6              | 1.69  | 0.025                           | 0.84                |
| 22.5     | 13.3                 | 0.95                                       | 26.7              | 1.44  | 0.034                           | 1.71                |
| 25.5     | 15.1                 | 0.95                                       | 26.7              | 1.35  | 0.029                           | 1.49                |
| 28.5     | 16.9                 | 0.94                                       | 26.6              | 1.35  | 0.015                           | 3.73                |
| 31.5     | 18.6                 | 0.94                                       | 26.4              | 1.34  | 0.013                           | 7.11                |
| 34.5     | 20.4                 | 0.92                                       | 25.8              | 1.31  | 0.010                           | 8.10                |
| 37.5     | 22.1                 | 0.92                                       | 25.8              | 1.42  | 0.014                           | 9.24                |
| 44.5     | 25.7                 | 0.93                                       | 26.3              | 1.33  | 0.013                           | 5.34                |
| ave:     |                      | 0.94                                       | 26.5              | 1.43  | 0.020                           | 3.68                |
| s.d.:    |                      | ±0.01                                      | ±0.4              | ±0.14   | ±0.009                          | ±3.23               |

(1) Interpolated from data in Murray, 1987. (2)  $U_{37}^{k'} = C_{37:2} / \{C_{37:2} + C_{37:3}\}$ .  
(3) Paleotemperature calculated from relationship  $U_{37}^{k'} = 0.034T + 0.039$ ,  
Prahl et.al., 1988. (4) Measure of alkenone chain length where K<sub>37</sub> and K<sub>38</sub>  
are the sum of all C<sub>37</sub> and C<sub>38</sub> alkenones, respectively. (5) Measure of  
relative contribution of long-chain lipid classes where EE denotes the  
diunsaturated C<sub>36</sub> fatty acid ethyl ester. (6) Sum of the concentrations of all  
C<sub>37</sub>, C<sub>38</sub> and C<sub>39</sub> alkenones, normalized to dry sediment weight on a  
carbonate-free basis. (7) Nonzero but immeasurable; EE concentration too low  
to be properly integrated.



Figure 9. Time-series of (a)  $K_{37}/K_{38}$  and (b)  $EE/K_{37}$  measured in site C sediments. Also plotted are a single site C sediment trap value (inverted triangle) and the range of values measured in *E. huxleyi* grown at 25°C (shaded area) from data in Prahl et.al., (1988). The 7.5cm sample has been omitted from (b) because the EE concentration was nonzero but too low to be properly computed.

Figure 9.

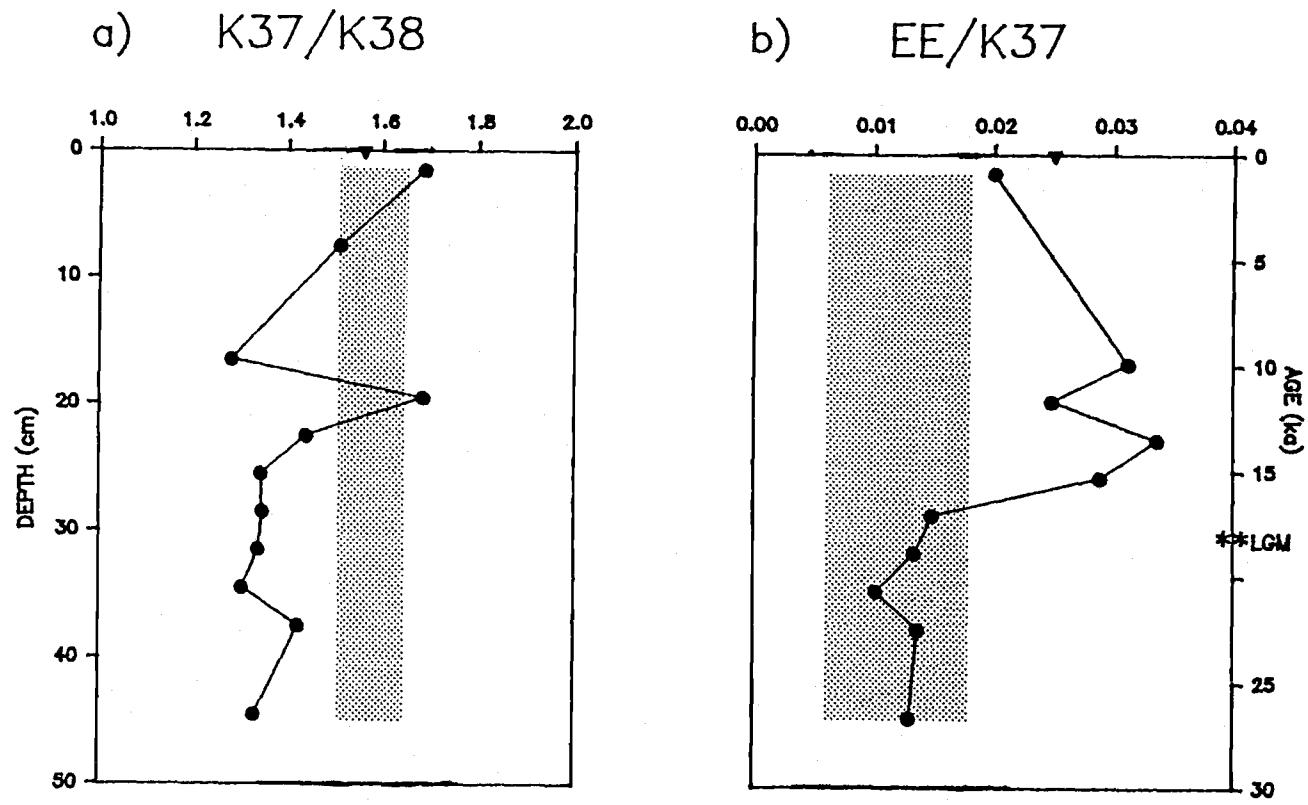
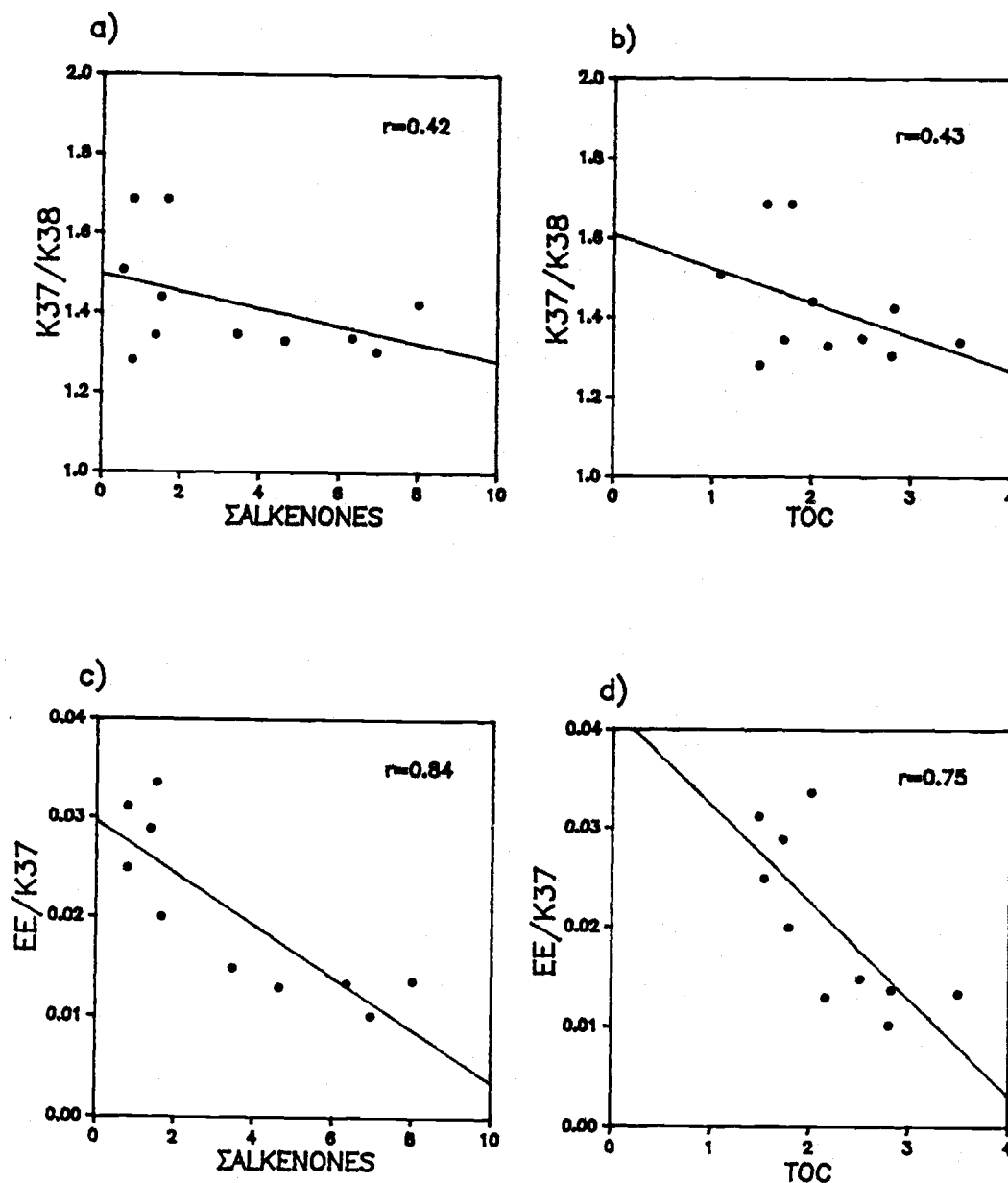


Figure 10. Regression analyses of the alkenone parameters: (a)  $K_{37}/K_{38}$  against the sum of all long-chain alkenones ( $\Sigma$ alkenones), (b)  $K_{37}/K_{38}$  against carbonate-free total organic carbon, (c)  $EE/K_{37}$  against the sum of all long-chain alkenones ( $\Sigma$ alkenones), and, (d)  $EE/K_{37}$  against carbonate-free total organic carbon.



certainty, so, a ratio of EE to the total  $C_{37}$  alkenones ( $K_{37}$ ) has been defined to compare the response of the different long-chain lipid classes (fatty acid vs. alkenone) to growth temperature (Prahl et.al., 1988).

From laboratory studies of E. huxleyi, the ester decreases relative to the alkenone with increasing growth temperature in a nonlinear relationship, i.e.  $EE/K_{37}$  varies inversely with growth temperature (Figure 8; Prahl et.al., 1988). Again comparing the site C sediment values (average paleotemperature =  $26.5^{\circ}\text{C}$ ) to values measured in cells grown at  $25^{\circ}\text{C}$ , ( $EE/K_{37} = 0.012 \pm 0.006$ ; Table 4) good agreement is observed only for some of the samples, in this case the five lower core samples (Figure 9).

Again, this may be due to the very small temperature range in the sediments ( $25.8\text{--}27.1^{\circ}\text{C}$ ) compared to that surveyed in E. huxleyi ( $8\text{--}25^{\circ}\text{C}$ ). But in the laboratory, the  $EE/K_{37}$  of E. huxleyi displays excellent temperature sensitivity, adjusting within four days to a  $5^{\circ}\text{C}$  temperature change (Prahl et.al., 1988). The parameter  $EE/K_{37}$  may be affected by differential preservation depending on input levels and the environment of deposition. This is suggested by the good correlations resulting from regression analyses (Figure 10c,d) against  $\Sigma$ alkenones ( $r = 0.83$ ) and carbonate-free TOC ( $r = 0.75$ ). Possibly these correlations are caused by differential preservation of the lipid classes (ester vs. alkenone) resulting in a distorted record. If so, the data suggest that the older samples are better preserved than those nearer the surface.

The MANOP site C alkenone parameter data can be compared to the other existing  $K_{37}/K_{38}$  and  $EE/K_{37}$  data, which come from sediments off the coast of Washington state (Prahl et.al., 1988). The Washington coastal waters are much cooler than MANOP site C, with an average  $U^{k'}_{37}$ -index predicted paleotemperature of  $11.8^{\circ}\text{C}$ . As can be seen in Figure 8, these data also cluster near the E. huxleyi values although not as closely as do the site C data. Based on the available data from two oceanic settings (Washington coast and central equatorial Pacific, MANOP site C), the site C sediment

$K_{37}/K_{38}$  and  $EE/K_{37}$  values more closely agree with those produced by E. huxleyi in the laboratory.

However, MANOP site C is not an ideal location from which to obtain sediment samples for investigating the general integrity of alkenone data sets. The  $U^{k'}_{37}$ -index has been calibrated from E. huxleyi cultures grown at a maximum of 25°C and site C surface temperatures are all higher. The  $U^{k'}_{37}$ -index ranges from 0 to 1 and the values measured in site C sediments are around 0.95, at the upper limit of applicability. Also, so little glacial/interglacial temperature variation occurs at the equatorial oceans that the variation is scarcely larger than the margin of error for some of these parameters.

Terrestrial organic carbon inputs to marine sediments. Intuitively, one would not expect to find significant terrestrial contributions to the organic carbon record at a remote ocean site such as site C. However, organic matter bearing biochemical signatures of land plants and representing a variety of lipid classes have been detected in aerosol samples collected from all the world's oceans. Early reports include organic material with an European or African continental origin collected some 5000km across the Atlantic Ocean at Barbados (Delany et.al., 1967). The discovery came as a surprise to the authors who state the study site was chosen because no terrestrially-derived material was expected in the aerosol samples. Later investigations showed that Saharan Desert dust storms are the source of this material (Simoneit, 1977). Another early aerosol study conducted in the eastern equatorial Pacific Ocean found undefined organic material associated with high proportions of terrestrially-derived quartz as far west as 110°W, roughly 3000km from South America (Prospero and Bonatti, 1969). These latter authors concluded that although eolian transport to open ocean sediments had been detected, the quantities were insufficient to be considered important relative to non-eolian inputs.

Some more recent studies have centered on specific lipid families such as the n-alkanes found in aerosols collected over the Atlantic, Pacific and Indian

Oceans (Duce and Gagosian, 1982; Simoneit, 1977). The Sea-Air Exchange Program (SEAREX) has resulted in an aerosol-lipid data base for selected locations in the Pacific Ocean (Gagosian et.al., 1982; Zafiriou et.al., 1985; Schneider and Gagosian, 1985; Gagosian and Peltzer, 1986; Gagosian et.al., 1987). These studies have highlighted the relative importance of atmospheric input of several lipid classes (*n*-alkanes, fatty alcohols, and fatty acids as long-chain wax esters and as salts) to ocean sediments with one report giving special emphasis to the fatty acid salts which represent up to 50% of total lipids in some aerosols (Gagosian and Peltzer, 1986).

Terrestrial biomarker. Turning our attention to the MANOP site C sediments, a distinct series of lipids, the *n*-fatty acids analyzed as their methyl esters (FAME's), can be observed in the GC traces (Figure 7). The long-chain (C<sub>20</sub> through C<sub>30</sub>) FAME's displaying a strong even-to-odd carbon predominance are well-accepted terrestrial plant biomarkers as they are uniquely found as components of the epicuticular waxes of higher plants (Kollatukudy et.al., 1976). Other terrestrially-derived fatty acid series have been detected in aerosol samples from the tropical Pacific Ocean (Zafiriou et.al., 1985), the south Pacific Ocean (Gagosian et.al., 1987), off the coast of Peru (Schneider and Gagosian, 1985), the Atlantic Ocean (Simoneit, 1977), and the Indian Ocean (Simoneit and Eglinton, 1977).

Individual concentrations of the alkenones are on the order of ten to one hundred ng/g dry sediment on a carbonate-free basis (Appendix A). In contrast to the alkenones, the FAME's are present as both easily-extractable and acid-released lipids. Overall, comparable *n*-fatty acid methyl ester concentrations are measured from the two procedurally-defined fractions, easily-extractable and acid-released, but they do differ somewhat as a greater concentration of C<sub>29</sub> and C<sub>30</sub> FAME's are detected from the easily-extractable lipids (Appendix A).

In order to quantify the terrestrial biomarker, the individual concentrations of all *n*-fatty acid methyl esters ranging from C<sub>20</sub> to C<sub>30</sub> have been summed for each individual sample (Table 3). Averaging the terrestrial

indicator measured in the eleven samples gives  $4890 \pm 2660 \text{ ng/g}$  and  $4000 \pm 1880 \text{ ng/g}$  dry sediment (carbonate-free basis) in the easily-extractable and acid-released lipids, respectively.

The terrestrial biomarker data obtained from the two different extraction procedures is believed to originate from the same source due to the great similarities in the biomarker patterns and abundances as will be more fully discussed in the section on terrestrial source regions. However, the occurrence of terrestrial FAME's in both the easily-extractable and acid-released fractions may indicate a difference in the mode of transport to the sediments and/or preservation therein. The nature of these differences may be some kind of biochemical bonding or a looser association with the carbonate mineral; it is impossible to ascertain the true nature of these differences based on the available data. Therefore, it is recommended that future studies targeted at the terrestrial *n*-fatty acids consider at least some acidic analyses to spotcheck for differences or similarities between these procedurally-defined lipid fractions.

Bacterial and marine/mixed inputs. The final biomarkers to be presented are the short-chain ( $<C_{19}$ ) *n*-fatty acids, also analyzed as their methyl esters. The MANOP site C sediments contain FAME's ranging from  $C_{14}$  to  $C_{18}$  in concentrations similar to that measured for the longer-chain, terrestrially-derived FAME's (Figure 7; appendix A). Two biomarker series are present within this family of lipids: the  $C_{15}$  and  $C_{17}$  branched- and straight-chain FAME's produced mainly by bacteria, and the even-carbon-numbered FAME's ( $C_{14}$ ,  $C_{16}$  and  $C_{18}$ ) originating from a mixture of marine algal, bacterial and potentially terrestrial sources.

Bacterial biomarker.  $C_{15}$  and  $C_{17}$  branched-chain fatty acids were first reported in sediments from the Green River shale, two Gulf of Mexico sediments and a back-reef sediment from Belize (British Honduras) (Leo and Parker, 1966). These fatty acids are now routinely reported in sediment organic geochemical studies from diverse sources such as the Middle America Trench off southern Mexico (Brassell et.al., 1981) and Lake Biwa, Japan

(Kawamura and Ishiwatari, 1985). Based on the high abundance of short, branched-chain fatty acids measured in many cultures of bacteria (Kaneda, 1963, 1967), the first sedimentary reports credited them to a bacterial origin (Leo and Parker, 1966; Cooper and Blumer, 1968). This interpretation is now generally accepted (Goossens et.al., 1986). Minor amounts of branched-chain fatty acids have also been detected in fungi, plants, mammals (Goossens et.al., 1986 and references therein), molluscs, marine phytoplankton and a yeast isolated from a marine sediment (Perry et.al, 1979 and references therein). However, these secondary sources contribute only small amounts and are not significant relative to the bacterial production occurring within the water and sedimentary columns (Goossens et.al., 1986; Perry et.al., 1979; Cranwell, 1974).

Recent studies have stressed the importance of bacterial activity on sinking particles, overall water column biogeochemical cycles (Cho and Azam, 1988), and as contributors to sedimentary TOC (Goossens et.al, 1986). Direct counts of bacteria in Venezuelan Basin sediments gave totals of  $10^7$  to  $10^8$  cells per gram dry sediment weight (Harvey et.al, 1984). Most bacteria are not photosynthesizers and do not contribute to terrestrial or marine primary productivity. They are heterotrophs and do consume and alter the organic carbon produced by photosynthetic organisms. Their presence in the water and sedimentary columns is indicative of degradative processes.

The odd-carbon-numbered, short-chain fatty acids produced by bacteria will be considered together as an indicator of the presence of bacteria and bacterial processes. The bacterial indicator will be enumerated by a summation of the  $n$ -,  $i$ - and  $ai$ - $C_{15}$  and the  $n$ -,  $i$ - and  $ai$ - $C_{17}$  FAME's ( $n$  = straight-chain,  $i$  = iso-branched, and  $ai$  = anteiso branched).

Marine/mixed indicator. The short, even-carbon-numbered fatty acids found in sediments have been considered to be of marine algal origin (De Baar et.al., 1983; Sargent et.al., 1976) but have also been detected in gram-positive and gram-negative bacteria (Goossens et.al, 1986) and Desulfovibrio desulfuricans, a ubiquitous anaerobic bacteria (Davis, 1968). Other possible sources of these FAME's include the fungi, whose major fatty acids are  $C_{16}$



and C<sub>18</sub> (Weete, 1976). Cutin, a terrigenous plant wax, also contains C<sub>16</sub> and C<sub>18</sub> fatty acids but the majority are  $\omega$ -hydroxy fatty acids (Kolattukudy et.al, 1976).

Due to the open ocean location, marine algal sources probably dominate the C<sub>14</sub>, C<sub>16</sub> and C<sub>18</sub> FAME's measured in MANOP site C sediments. However, as outlined above, the lack of source specificity of these FAME's necessitates a looser interpretation than for other biomarkers found in these sediments. This biomarker will be termed the "marine/mixed source indicator" and will be enumerated by the sum of the C<sub>14</sub>, C<sub>16</sub> and C<sub>18</sub> *n*-FAME's.

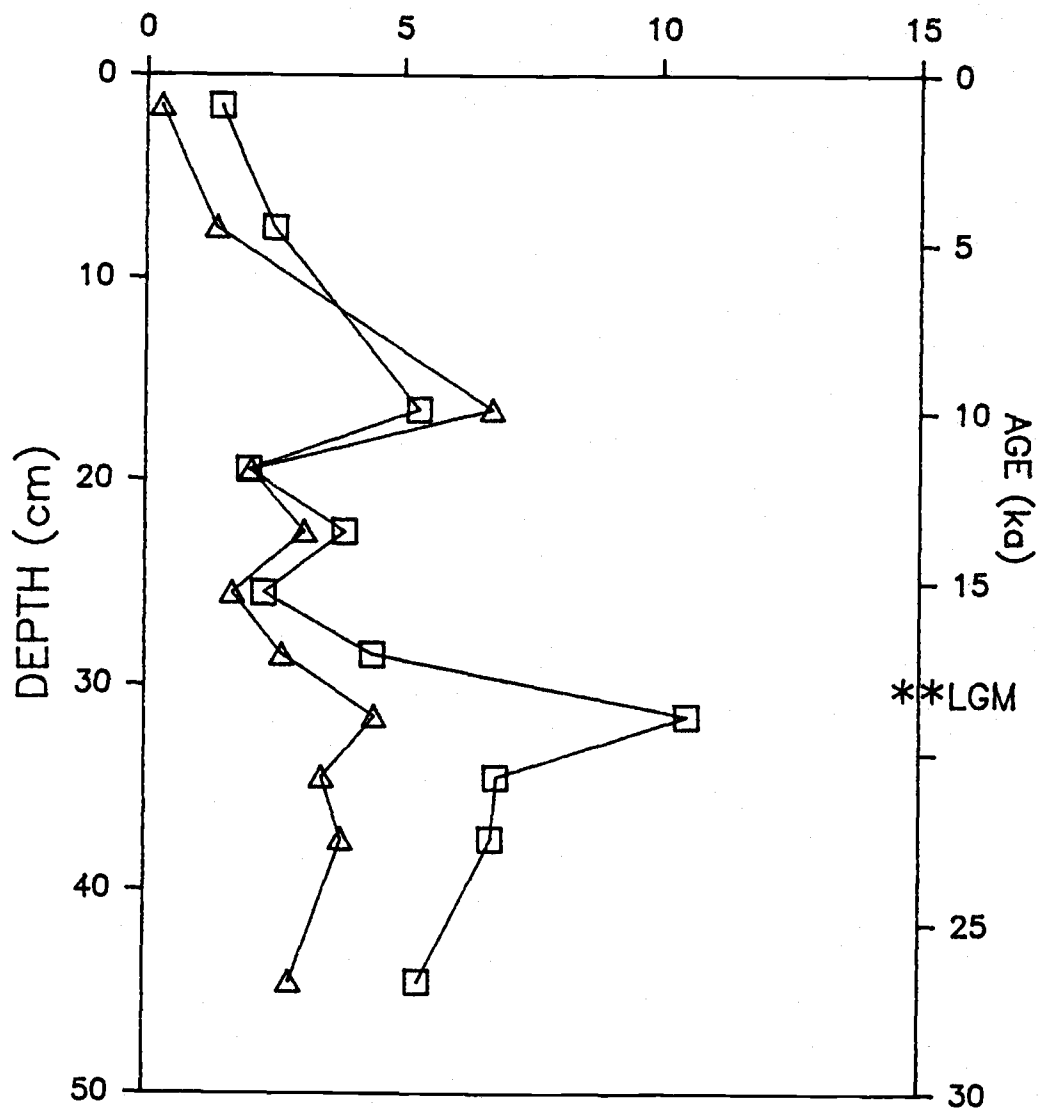
The bacterial and marine/mixed indicator data from site C will be overviewed together. Individual compound concentrations range from around one hundred ng/g dry sediment, carbonate-corrected for the branched C<sub>15</sub> and C<sub>17</sub> FAME's to a high of 11,600 ng/g dry sediment, carbonate-corrected for C<sub>18</sub> in the surface sample (appendix A). The marine/mixed biomarker concentration averages  $1650 \pm 550$  and  $5,240 \pm 2240$  ng/g dry sediment (carbonate-free) for the easily-extracted and acid-released fractions, respectively (Table 3). The bacterial indicator averages  $370 \pm 280$  and  $1,650 \pm 760$  ng/g (carbonate-free) in the easily-extractable and acid-released lipids, respectively (Table 3).

It should be noted that in all except the uppermost sample, the concentrations measured in the acid-released lipids are considerably greater than those measured in the easily-extractable lipids for both of these short-chain FAME biomarkers, leading to an acid-released/easily-extractable ratio greater than one (Figure 11). Also, the C<sub>15</sub> and C<sub>17</sub> branched-chain FAME's are most abundant relative to the *n*C<sub>15</sub> and *n*C<sub>17</sub> FAME's in the acid-released fraction. As is the case for the long-chain FAME's, the acidic extraction released significant information and future lipid studies should include this procedure or something similar to obtain a full suite of information for this lipid class. This also holds true for other lipids such as the  $\beta$ -hydroxy fatty acids, a uniquely bacterial biomarker, which are detected only after breaking

an amide linkage by acid hydrolysis of sediment samples (Figure 5; Goossens et.al., 1986).

At the outset of this work, the downcore TOC profile was presented (Figure 4) and two distinct peaks (1.2 and 18.6ka) were noted. The primary goal was to examine the sources of the organic carbon and determine whether these TOC maxima indicate periods of increased primary production of organic carbon, increased terrestrial inputs, or were caused by preservational and depositional effects. Now, armed with a look at the data and knowledge of the biomarkers to be utilized, we are ready to examine and attempt to decipher the TOC record and look for clues about paleoenvironmental conditions.

Figure 11. Ratio of acid-released to easily-extractable short FAME's: marine/mixed indicator (triangle) and bacterial indicator (square) vs. depth and age.



## SOURCES AND SIGNIFICANCE OF THE NEAR-SURFACE TOC PEAK

Let us examine the composition, sources and long-term fate of the near-surface TOC peak. Does it reflect increased primary productivity? If not from primary production, what is the derivation of this organic carbon? Will this relatively young TOC peak survive in situ degradational effects within the aerobic portion of the sediment column? Are there any biomarkers that can be used to answer these questions?

Examining the biomarker time-series presented in Figure 12, two records exhibit a significant increase coincident with the near-surface TOC peak. The easily-extractable bacterial and easily-extractable marine/mixed indicators display decidedly unimodal downcore distributions with a strong near-surface (1-2cm) concentration maximum (Figure 12.b). The remaining biomarker records display similar but lesser increases in the near-surface sample (Figure 12.c,e,f). The upper 7cm of this core have been determined to be the sedimentary mixed-layer within which benthic organisms burrow and mix the sediments (Emerson et.al., 1987). This suggests that organic carbon in this region is transitory in nature because of susceptibility to removal by respiration. According to one estimate, 20-40% of the sedimentary mixed-layer organic carbon is degradable in the abyssal ocean (Emerson et.al., 1987). If the mixed-layer TOC in site C sediments were reduced by this amount, there would essentially be no near-surface maximum.

Short-chain lipids commonly display near-surface maxima and are thought to be more degradable than are longer ( $>C_{19}$ ) lipids (Kawamura and Ishiwatari, 1984a; Matsuda and Koyama, 1977). In addition to shorter chain lipids being relatively degradable, it has been observed that unbound lipids (here termed easily-extractable) are more degradable than are bound or tightly bound lipids (here termed acid-released) (Kawamura and Ishiwatari, 1984b; Van Vleet and Quinn, 1979). As the strongest relative near-surface maxima are observed in the easily-extractable, short-chain FAME's from site C, it is believed that the mixed-layer TOC peak will not be ultimately preserved in this sediment.

Figure 12. Downcore concentration records from MANOP site C of (a)total organic carbon, (b)the easily-extractable marine/mixed indicator (triangle) and the easily-extractable bacterial indicator (diamond), (c)the acid-released marine/mixed indicator (inverted triangle) and the acid-released bacterial indicator (square), (d)the  $U^{k'}_{37}$ -index predicted paleotemperature, (e)the marine indicator, and (f)the easily-extractable terrestrial indicator (open square) and the acid-released terrestrial indicator (open triangle). Agescale for W8402A-14GC developed by Murray (1987); last glacial maximum (LGM) indicated by \*\*.

Figure 12.

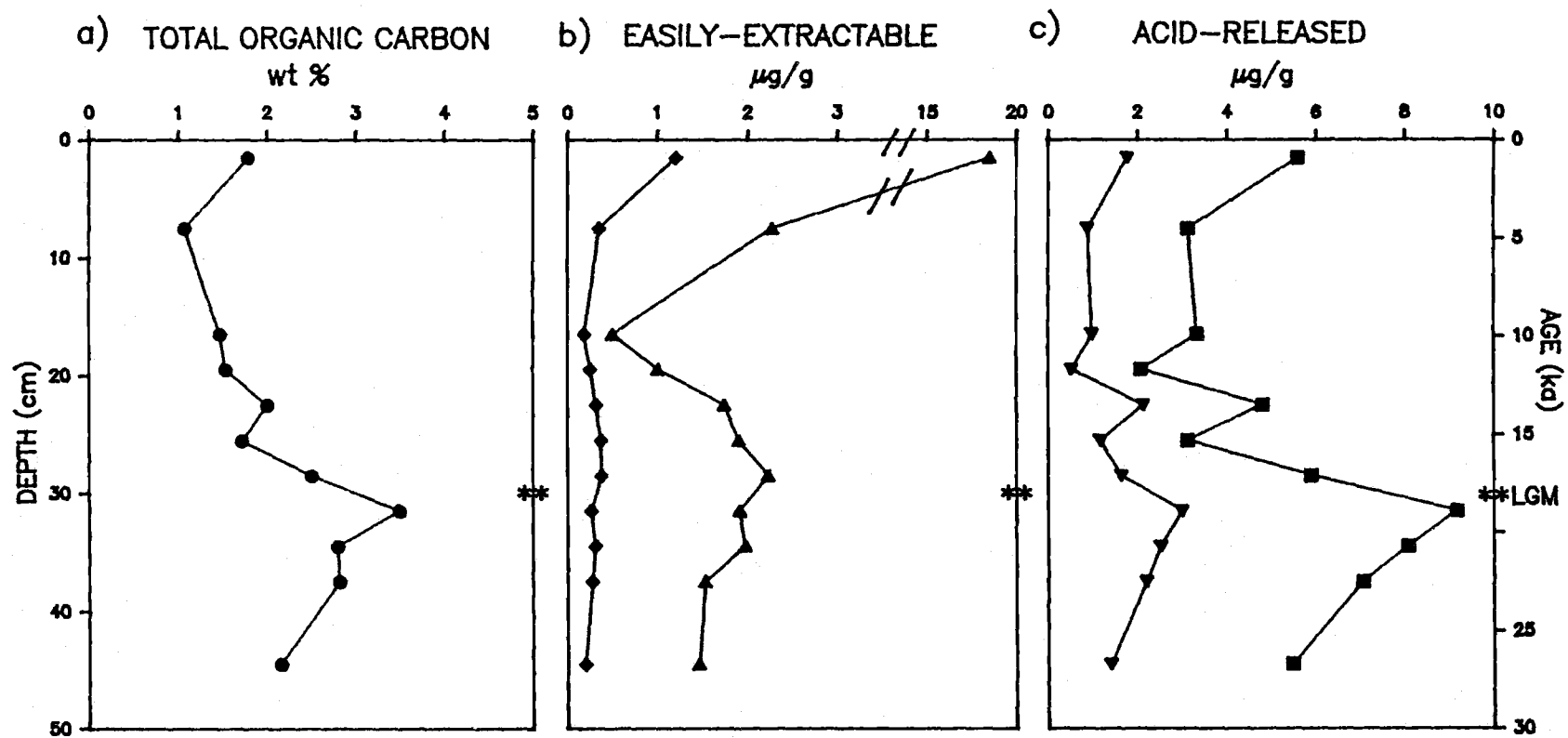
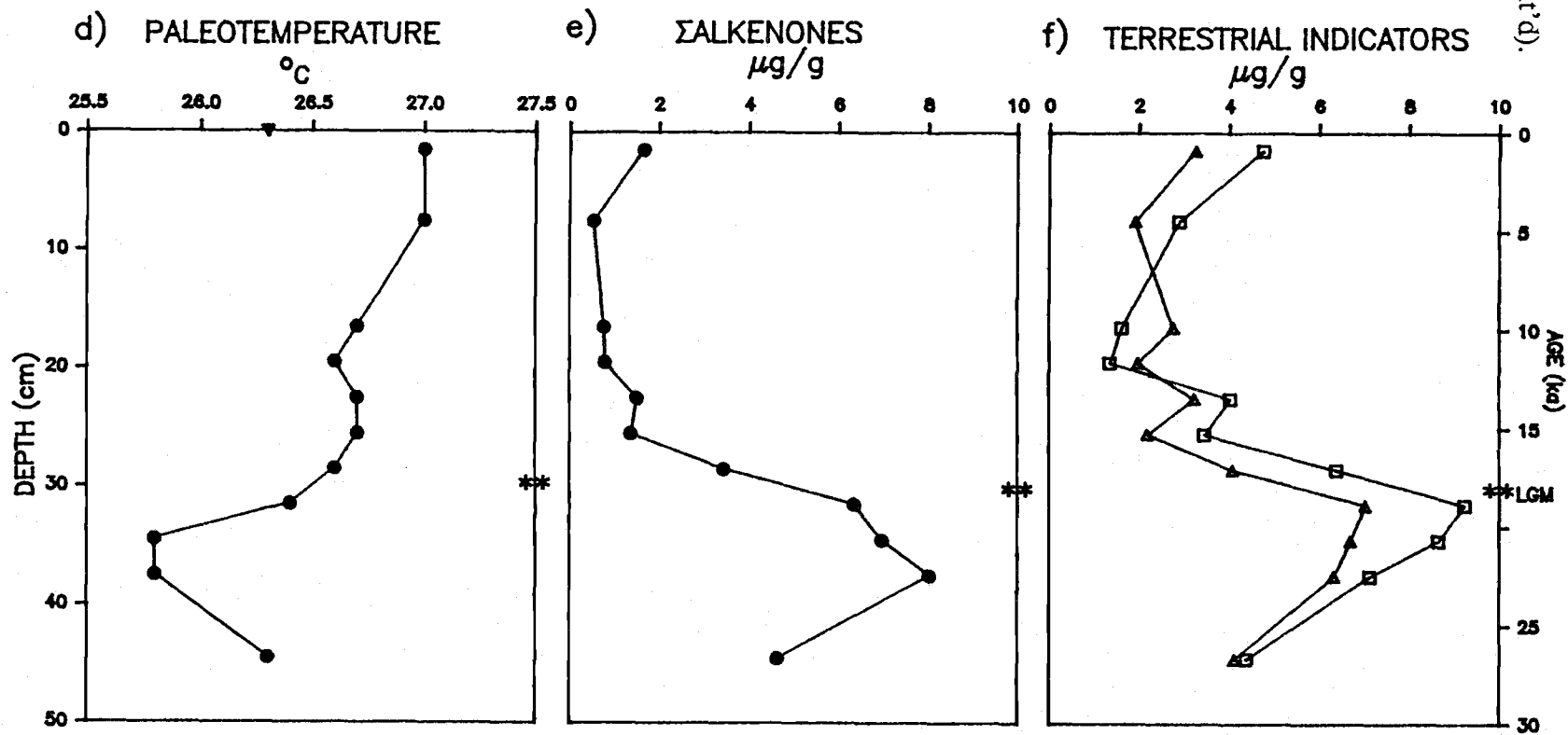


Figure 12 (cont'd).



Examining the bacterial and marine/mixed indicator downcore records (Figure 12.b,c; Table 3), it is immediately evident that the profiles from the easily-extractable lipids are highly similar, as are the two profiles obtained from the acid-released lipids. Conversely, when the bacterial indicator time-series from the two lipid classes are compared they are quite different, as are the marine/mixed indicator profiles. The acid-released bacterial and marine/mixed indicators display a pattern similar to terrestrial and marine indicators, i.e. a marked maximum coincident with the latest glacial maximum and a lesser near-surface peak (Figure 12). Thus, the LGM maximum observed in the acid-released bacterial and acid-released marine/mixed indicators will be considered together with the other biomarkers in the following discussion about the sources and stability of the LGM-aged TOC peak.

In conclusion, the near-surface TOC peak is transitory and will not be preserved within the sedimentary column on a long-term basis. This interpretation has been based on the near-surface (1-2cm) location of this maximum within the 7cm mixed-layer, the demonstration that the lipid fraction of the organic carbon is comprised largely of relatively degradable short-chain fatty acids, and is recovered almost exclusively from the easily-extractable lipids. In situ degradation is being accomplished by sediment-dwelling bacteria as evidenced by the near-surface peak in the bacterial indicator record. Thus, this near-surface TOC maximum should be considered a transient in terms of geologic time and is an example of sedimentary organic carbon degradational processes.



## INCREASED UPWELLING ASSOCIATED WITH THE LAST GLACIAL MAXIMUM

This section discusses the  $U^{k'}_{37}$ -index predicted paleotemperature record, the  $\Sigma$ alkenone record, the opal record, and inferred increased equatorial upwelling and their relationships with the TOC maximum observed at the last glacial maximum (LGM).

The  $U^{k'}_{37}$ -index predicted paleotemperature record at Site C. The  $U^{k'}_{37}$ -index predicted paleotemperature record for site C (Figure 12.d) was calculated from the equation:

$$T = [U^{k'}_{37} - 0.039] \div 0.034 \quad (\text{Prah} \text{ et. al., 1988}).$$

Over the last 26kyr, site C  $U^{k'}_{37}$ -index predicted paleotemperatures average 26.5°C and range from 25.8 to 27.1°C, a spread of 1.3 degrees (Table 5). Strong evidence exists that  $U^{k'}_{37}$ -index values predict the surface-mixed-layer temperatures in which the alkenone-producing algae grow (Prah1 and Wakeham, 1987).

Although a larger temperature range may be expected from a time section spanning the LGM, Broecker and Peng (1982) examined planktonic and benthic foraminiferal  $\delta^{18}\text{O}$  records and concluded that on average over the global oceans, the glacial temperatures could have been at most 2.3°C colder than today. This globally averaged glacial/interglacial temperature range can be expected to have the greatest expression near the polar regions --CLIMAP (1981), predicts that North Atlantic glacial sea-surface temperatures were up to 15°C colder than today-- and the least at the equator so that the 1.3°C range observed at site C is quite reasonable.

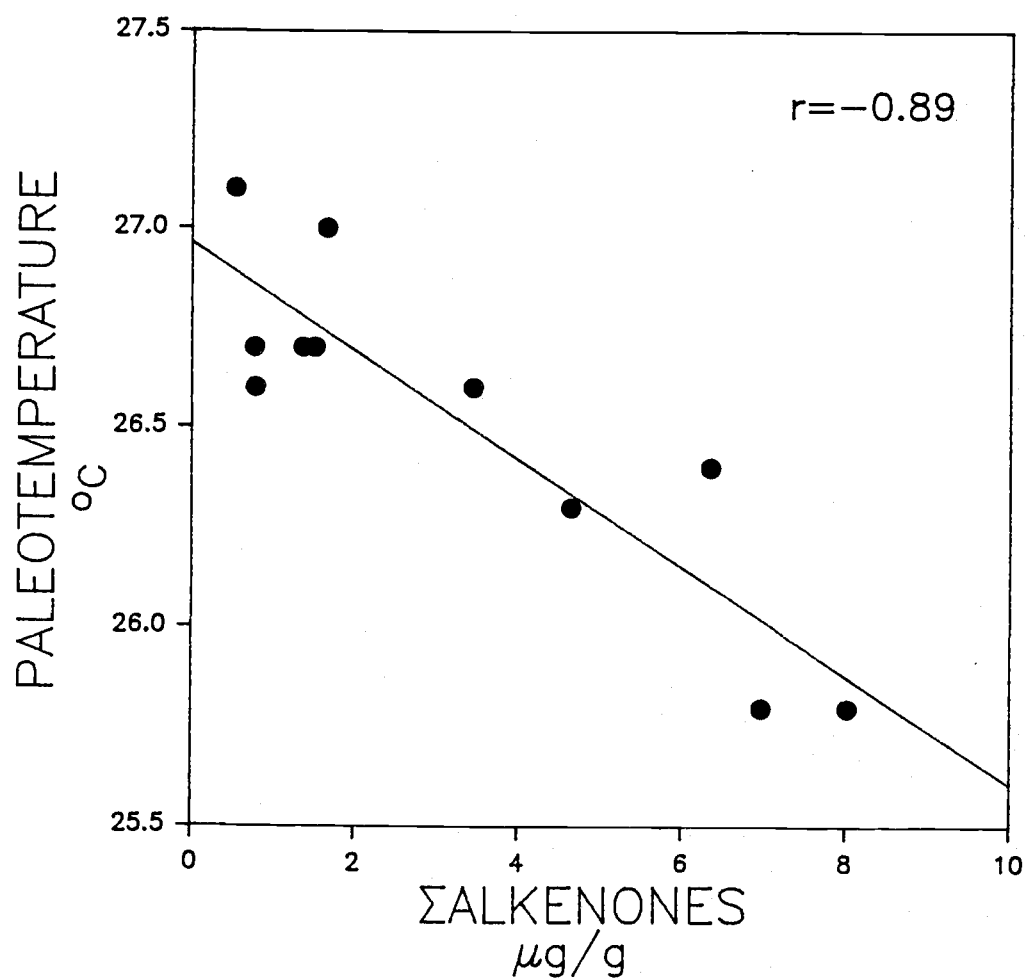
Glacial and interglacial sea surface temperatures (SST's) have also been estimated by factor analysis and transfer functions based on microfossil assemblages from recent and glacial-aged ocean sediments (Imbrie and Kipp, 1971). This method results in a glacial/interglacial SST range of 2°C around MANOP site C for February and August (CLIMAP, 1981). The  $U^{k'}_{37}$ -index

predicted 18ka temperature for site C, 26.4°C, falls within the CLIMAP 18ka temperature predictions of 23 and 27°C for August and February, respectively, for this vicinity (CLIMAP 1976, 1981). Transfer functions of radiolarian assemblages from a nearby core, RC11-210 (2°N, 140°W; Figure 17), give a mean SST of 26.4°C±0.8 when six August and six February predictions from the period 6-29ka are averaged together (total n=12; Pisias and Rea, 1988). Excellent agreement with other paleotemperature predictions provides support for the accuracy of the  $U^{k'}_{37}$ -index predicted paleotemperature record.

The coldest paleotemperatures do not coincide with the LGM as might be expected (Figure 12.d). The coldest sea-surface temperature estimate occurs at 22.1 and 20.4ka, predating the accepted 18ka for the LGM. Interestingly, the marine indicator also peaks at 22.1 and 20.4ka (Figure 12.e). This may indicate that the  $U^{k'}_{37}$ -index (and therefore the paleotemperature record) is influenced by the total alkenone concentration, an indicator of marine productivity. It is important to the integrity of  $U^{k'}_{37}$ -index predicted paleotemperature records that the index be independent of productivity and preservation. In culture, alkenone production and temperature are independent, as *E. huxleyi* produces a remarkably constant total alkenone concentration per cell ( $1.20 \pm 0.28$ pg) over a wide range of growth temperatures (8-25°C; Prahl et.al., 1988).

In site C sediments, regression analysis of the eleven 0-26ka  $U^{k'}_{37}$ -index predicted paleotemperatures against the corresponding  $\Sigma$ alkenones shows a strong correlation ( $r=-0.89$ , Figure 13). This negative correlation could result from preferential preservation of the  $C_{37:2}$  over the  $C_{37:3}$  in times of lower overall alkenone concentrations, leading to falsely higher  $U^{k'}_{37}$ -index temperature predictions. However, it is also possible that this is a false interpretation of cause and effect. The improbability of desaturation via hydrogenation has already been emphasized. In a tropical environment such as MANOP site C where only a small amount of  $C_{37:3}$  is produced relative to  $C_{37:2}$  (Figure 14), differential preservation between the di- and tri-unsaturated alkenones would have a greater affect on  $U^{k'}_{37}$ -index temperature estimates than in colder environments. Alkenone analysis of a one-year

Figure 13. Regression analysis of  $U^{k'}_{37}$ -index predicted paleotemperatures against  $\Sigma$ alkenones.

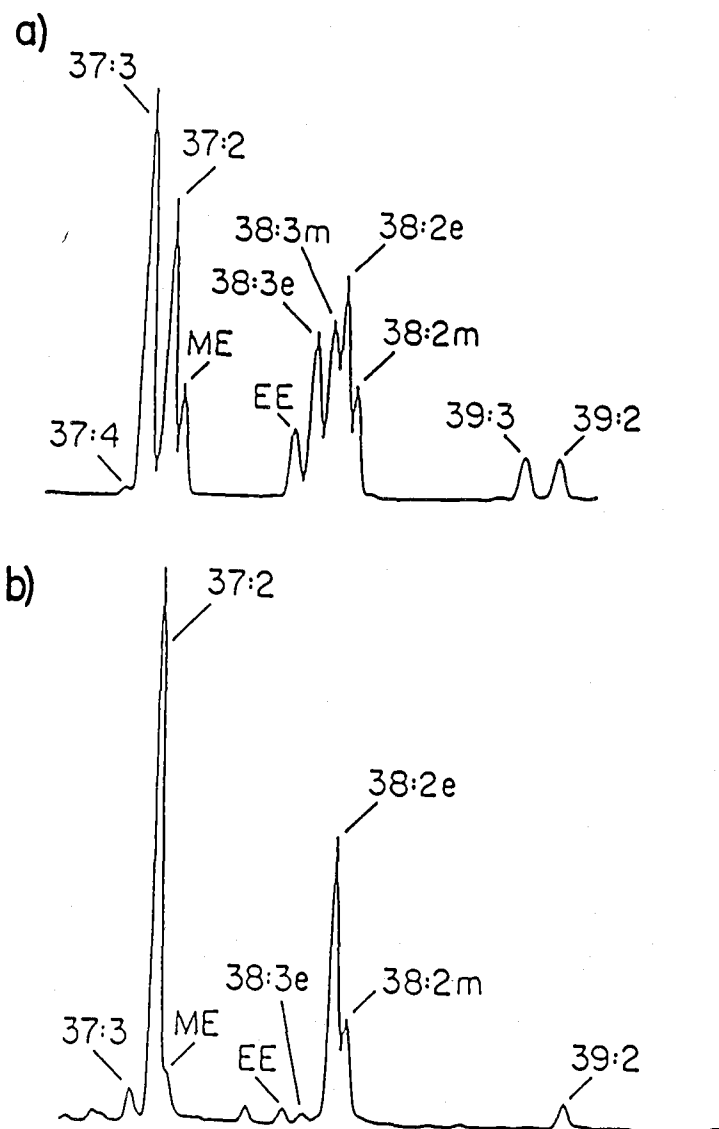


site C sediment trap sample gives a  $U^{k'}_{37}$ -index predicted temperature of 26.3°C, and the 1-2cm sediment sample temperature estimate is 27.0°C. Given that the precision of these temperature estimates is at best  $\pm 0.5^\circ\text{C}$  (Prahl and Wakeham, 1987), the ranges of these two analyses overlap, indicating that the alkenones are not differentially degraded based on degree of unsaturation.

One could also interpret the paleotemperature/ $\Sigma$ alkenone correlation to indicate that temperature is affecting alkenone production, rather than the reverse cause and effect relationship just discussed. A strengthening of equatorial upwelling could cause a change in upper-mixed-layer water temperature and also nutrient content, thereby enhancing alkenone and overall organic carbon production. It is common oceanographic knowledge that newly upwelled water is generally colder and more nutrient-rich than surface water.

In order to evaluate the possibility of increased upwelling at site C during the LGM, we need to seek and evaluate other indicators of upwelling. Equatorial upwelling is driven by divergent surface winds (Pickard and Emery, 1982), so a wind-strength indicator would be useful. Based on cross-spectral analysis of grain size data and radiolarian indicators, increased wind intensity as indicated by increased grain size does result in increased divergence within the equatorial zone of the Pacific (Pisias and Rea, 1988). Increased winds could also be recorded by the organic carbon terrestrial indicator presented in this study. A larger flux of terrestrial material would be delivered to the ocean if windstrength increased. Because arid lands are more erodable, an expansion in continental desert areas would provide a greater source leading to an increase in the dust load or concentration of particles carried by the wind (Prospero and Nees, 1977). Siliceous and calcareous phytoplankton groups respond differently to nutrient concentration variations so their indicator records may reflect changes in nutrient supply. The remainder of this discussion will focus on the organic geochemical terrestrial and marine indicator records in an effort to explain the LGM-aged TOC peak and the older  $U^{k'}_{37}$ -index predicted paleotemperature minimum centered around 21ka.

Figure 14. Representative gas chromatograms comparing the relative concentrations of the long-chain alkenones from (a) Washington state coastal sediments and (b) MANOP site C sediments (Washington coast sediment data from Prahl et.al, 1988).



Prior to embarking on a temporal discussion, the significance of the up to 5kyr offset between the coldest paleotemperature and the TOC maximum at the LGM should be mentioned. The  $U^{k'}_{37}$ -index predicted paleotemperatures are analytically accurate to  $\pm 0.5^\circ\text{C}$ , with an additional small but uncertain greater variability due to real-world effects. The alkenone concentrations have an estimated error of  $\pm 7\%$  based on replicate gas chromatographs of a given sample (Muehlhausen, unreported data). The LGM has been located to within  $\pm 2\text{ka}$  in W8402A-14GC (Murray, 1987; Lyle, pers.comm.). Thus, the observed differences in timing of these events push the limits of analytical accuracy but are intriguing enough to warrant discussion and further investigation.

Proposed phytoplankton succession. Around the LGM, the TOC and  $\Sigma$ alkenones maxima are offset with the onset of increased alkenone concentration preceeding the TOC maximum by nearly 5kyr (Figure 12a,e). The coldest  $U^{k'}_{37}$ -index predicted paleotemperatures also occur 2 to 5kyr before the 18ka LGM, suggesting that enhanced upwelling occurred as early as 22ka. The high fertility of this region results from upwelled nutrients so a link between the upwelling and marine productivity records is very plausible.

Before interpreting the  $\Sigma$ alkenones time-series, it is necessary to establish what this parameter records with respect to past organic carbon inputs. Can the  $\Sigma$ alkenones be used to estimate the marine organic carbon input as a whole or does this parameter reflect only a portion of the marine productivity? If so, which portion? Based on early laboratory findings that *E. huxleyi* produces long-chain alkenones, it was suggested that the total sedimentary concentration of alkenones may be a specific measure of coccolithophorid production (Volkman et.al. 1980a,b). Subsequent discovery of alkenones in related but noncoccolithophorid Prymnesiophyte algae led to the recommendation that they be applied as a more general Prymnesiophyte algal productivity indicator (Marlowe et.al., 1984a,b).

If the Prymnesiophytes significantly dominate the marine productivity at a given location, the  $\Sigma$ alkenones could be utilized to estimate overall marine

inputs. In site C sediments, the  $\Sigma$ alkenones profile resembles the TOC profile (Figure 15) and regression analysis of  $\Sigma$ alkenones vs. TOC results in a strong positive correlation ( $r=0.89$ , Figure 16). Assuming that TOC reflects paleoproductivity, it could be argued from this correlation that  $\Sigma$ alkenones also record paleoproductivity in Holocene and late Pleistocene sediments from site C. However, the alkenones seem to experience a much wider variation than the overall TOC record in the interval (Figure 15). Also, the siliceous phytoplankton (diatoms) comprise over 50% of the opal flux measured in sediment traps and opal comprises 5 to 15% of sediment weight in the upper 50cm (Murray, 1987), indicating that other phytoplankton are important at MANOP site C. Therefore, the  $\Sigma$ alkenones record in site C sediments will be applied as a productivity measure of a specific group of phytoplankton, the alkenone-producing Prymnesiophytes.

Applying the  $\Sigma$ alkenones as a Prymnesiophyte productivity tracer, it appears that this phytoplankton subgroup peaked 4000 years before total productivity as measured by the TOC record. As can be observed in Figure 15, the Prymnesiophyte indicator concentrations peaked at 22ka with elevated but lower levels at 18ka. This suggests that one or more other organic carbon sources account for increased contributions at 18ka to cause a TOC peak at this time. These sources could be other marine phytoplankton or terrestrial carbon inputs.

An opal record has been constructed from silicon (Si) content in W8402A-14GC measured by X-ray fluorescence and corrected for detrital Si based on extraction studies of surface sediments (Murray, 1987; Lyle et.al., 1988). Proceeding upsection, the opal record (Figure 15) shows a marked increase beginning at the LGM (30cm) with a further increase at 10ka (17cm). The porewater silica profile (Jahnke et.al., 1982) has been interpreted to signify that the upper 15 to 20 cm of the opal record is still subject to possible dissolution by porewater but the accumulation increase occurring at the LGM is real (Murray, 1987). Assuming that opal concentration records siliceous phytoplankton productivity and  $\Sigma$ alkenones records Prymnesiophyte algal productivity, it can be postulated that a phytoplankton group succession

Figure 15. Comparison of time-series from MANOP site C sediments: (a)TOC, a general productivity indicator, (b) $\Sigma$ alkenones, the Prymnesiophyte indicator, and (c)opal, a siliceous phytoplankton indicator. Opal data from Lyle et.al. (1988), and pers. comm.. The data in (a) and (b) have been corrected for carbonate content.



Figure 15.

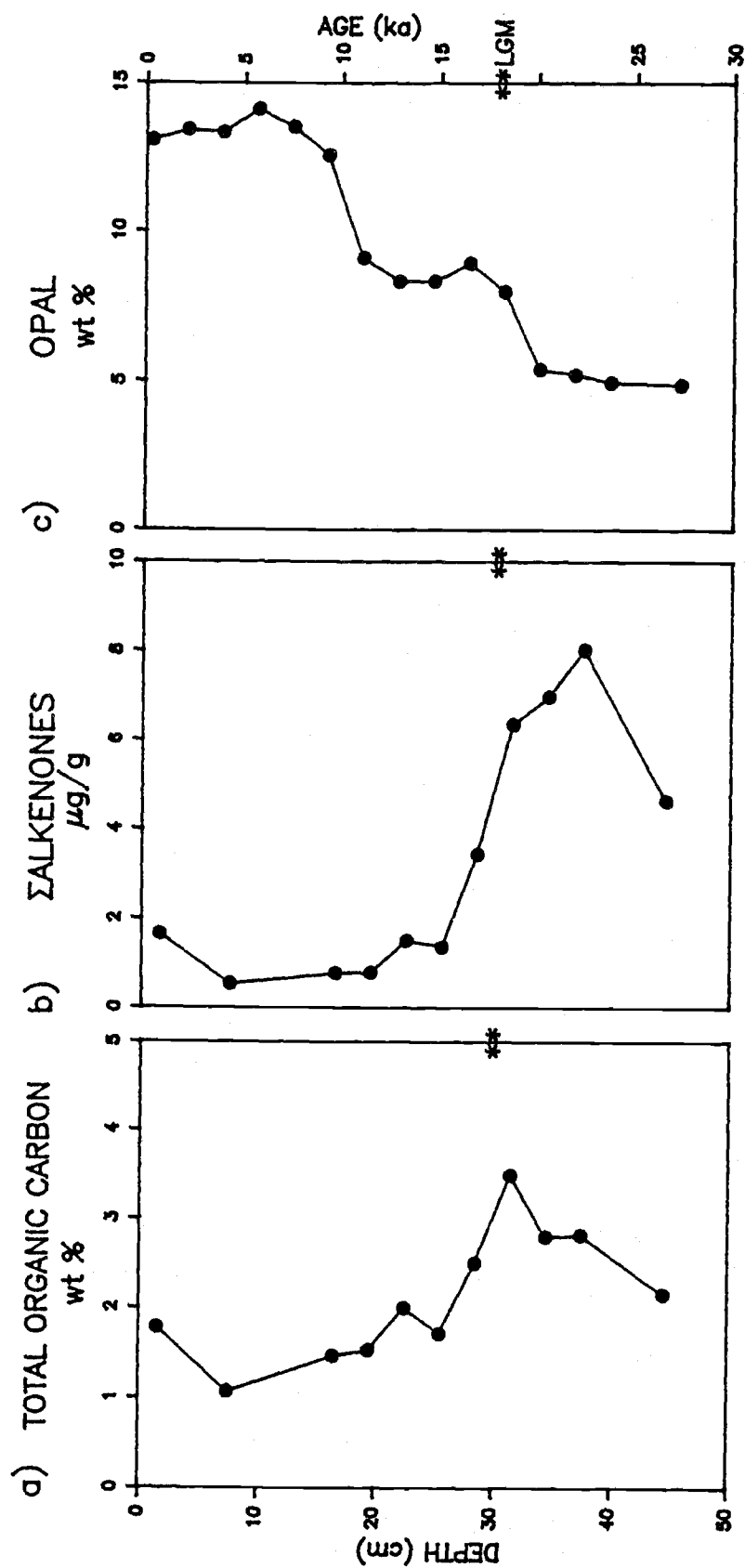
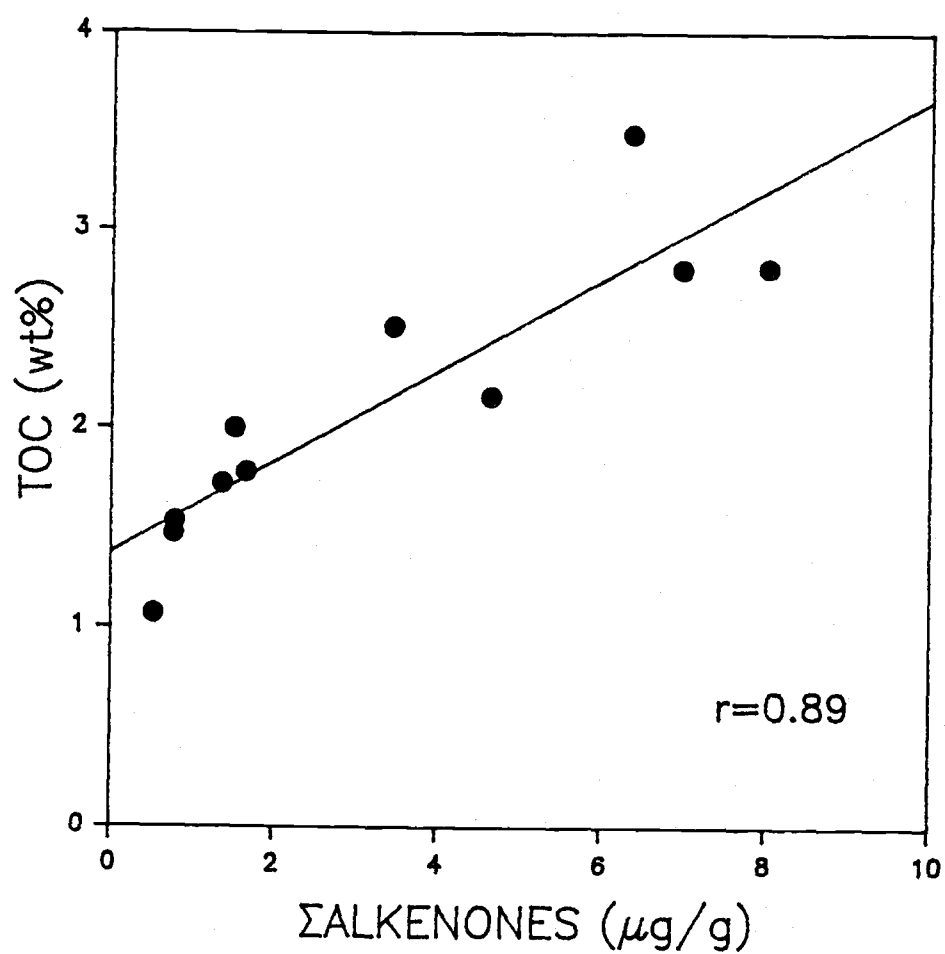


Figure 16. Regression analysis of TOC (weight percent, carbonate-free) vs.  $\Sigma$ alkenones (ng/g, carbonate-free).



occurred from a Prymnesiophyte algae-dominated period at 22 to 18ka followed by increasing importance of siliceous phytoplankton beginning around 19ka, continuing to modern times.

This postulated phytoplankton succession can be compared to two similar reports from different time-scales. A 0-300ka study of opal, calcite and TOC records from an eastern equatorial Pacific core (V19-28; Figure 17a) indicates oscillation between two different phytoplankton communities, one producing mainly opal and the other being calcite-rich (Lyle et.al, 1988). When considered alone, neither the  $\text{CaCO}_3$  nor the opal record could account for the TOC record. However, when the two records were examined together, it became apparent that some TOC maxima were associated with opal, some with  $\text{CaCO}_3$ , and some by a combination of these indicators of the phytoplankton groups; only then could all of the TOC variations over the 300ka period could be explained (Lyle et.al., 1988). On a much shorter time-scale, this same phenomenon has been proposed to explain sediment trap data collected in waters overlying MANOP site S (11°N, 140°W, Figure 17a; Dymond and Collier, 1988). Analyses probing the origin of a productivity pulse during El Niño show little change in calcareous rain rate concurrent with an 8-fold increase in siliceous rain rate. The authors believe that the current structure caused doming of nutrient-rich water into the euphotic zone, and the diatoms responded more strongly to the available nutrients than did the coccolithophorids. The ability of diatoms to better utilize higher concentrations of nutrients in the presence of non-limiting silica is well-known (Valiela, 1984).

In summary, the proposed historical events of marine productivity are as follows: responding to enhanced nutrient levels delivered by intensified upwelling, Prymnesiophyte productivity peaked at 22-20ka. Siliceous phytoplankton began to increase around 19ka and have remained at relatively high levels into the present.

## PALEOPRODUCTIVITY

Can we quantify the productivity increase associated with the LGM? What was happening on land? Does the terrestrial indicator record support increased winds to drive increased upwelling at the time of the LGM? How do increased terrestrial inputs affect the TOC record?

Total organic carbon. When it can be shown that significant alteration by degradational effects has not affected a TOC record, TOC time-series can be applied to estimate relative increases and decreases in marine paleoproductivity (Lyle, 1988). More elaborate models linking primary productivity and sedimentation rates to the organic carbon content of sediments have resulted in empirical equations used to successfully predict paleoproductivity from organic carbon records (Müller and Suess, 1979). However, not everyone agrees with these techniques; some researchers argue that degradational effects alter organic carbon inputs to such an extent that the TOC record cannot be relied on to predict paleoproductivity (e.g. Emerson 1985). In answer to these criticisms, a model deepwater oxygen record was developed from  $\delta C_{13}$  data to estimate the corrosiveness of bottom waters over the last 300kyr at an eastern equatorial Pacific Ocean core site (V19-28; 2°S, 85°W, Figure 17.a; Lyle et.al., 1988). If the TOC record and bottom water oxygen content were well-correlated, then it would demonstrate that the TOC record had been a product of preservation rather than primary production. However, the two records lacked coherence, and the TOC records from V19-28, W8402A-14GC, and VN-1-49GC (7°N, 93°W, Figure 17.a) were applied to study paleoproductivity over the last 300kyr in the equatorial Pacific Ocean (Lyle et.al., 1988; Lyle, 1988). Thus, TOC has been shown to record changes in paleoproductivity in the area including MANOP site C at least in a semiquantitative fashion.

The detailed TOC for the upper 45cm of sediment core W8402A-14GC, MANOP site C exhibits a marked maximum at 18.6ka, with elevated values observed at 22 to 20ka as well as a near-surface peak (Figure 12.a). A "background" level was estimated for TOC by averaging the TOC measured

from samples 7.5, 16.5, 19.5, 22.5 and 25.5cm (4.4 to 15.1ka). These samples were chosen because they have the lowest TOC content in the upper 45cm of the core and display little intersample variation. The relative increase over background can then be calculated from the TOC increases, giving a 2-fold increase at 18.6ka, and a 1.5-fold increase at 22 to 20ka. The productivity increases can be attributed to an increased nutrient supply delivered by intensified equatorial upwelling. The near-surface TOC peak increases 1.6 times over background but is believed to be ephemeral in nature as has been discussed. Therefore, assuming that the TOC record is a reliable paleoproductivity measure, these increases over background give a rough, relative estimate of productivity increases around the time of the LGM. These estimates should be considered upper limits because preservation is known to be enhanced during periods of increased primary production (Meyers et.al., 1984)

Prymnesiophyte productivity. Returning to the detailed  $\Sigma$ alkenones record for the last 26ka (Figure 12.e), the highest values are observed around 18.6 to 22ka and to a lesser extent at the near-surface; a "background" calculation analogous to that used for TOC (average of samples 7.5 through 25.5cm, inclusive) allows relative quantification of these alkenone maxima. From this estimate, the near-surface peak (1.5cm) is 2.4 times greater than background and the three samples (31.5, 34.5, 37.5cm) centered at 20.4 ka are on average 6 times enriched over interglacial levels. The lesser near-surface increase in alkenone concentration lies within the upper 7cm mixed-layer (Emerson et.al., 1987) which is believed to be undergoing *in situ* degradation and is probably ephemeral in nature.

Terrestrial paleoinput. Examining the terrestrial indicator time-series (Figure 12.f), increased terrestrial contribution began at 22.1ka, with high levels continuing through the LGM and on into the 16.9ka sample. Applying the "background" calculation to the terrestrial indicator, the five samples aged from 4.4 to 15ka average  $2.67 \pm 1.16$  and  $2.42 \pm 0.56 \mu\text{g/g}$  (carbonate-free) for the easily-extractable and acid-released lipids, respectively. The greatest terrestrial indicator values occur at 18.6ka and are 3.5 and 2.9 times

extractable and acid-released, respectively) greater than their respective background values. The onset of terrestrial inputs does occur prior to the LGM but the maximum terrestrial input coincides with the TOC peak at the LGM.

Based on the discussion thus far, it may have been expected for the wind-transported terrestrial indicator maximum to coincide with the conjectured maximum upwelling prior to the LGM. However, terrestrial inputs are controlled by the availability of material to transport as well as the strength of the delivery system. Mineralogic studies uncouple these factors by using eolian grain size to measure the intensity of atmospheric circulation and eolian flux to measure the aridity of the source region (Rea et. al., 1985).

Source changes of the terrestrial biomarker can be recognized by two parameters: CPI and  $C_{max}$ . The carbon preference index (CPI),

$$CPI = \frac{1}{2} \left\{ \frac{(\Sigma C_{20}-C_{28} \text{ evens} / \Sigma C_{21}-C_{29} \text{ odds}) + (\Sigma C_{22}-\Sigma C_{30} \text{ evens} / \Sigma C_{21}-C_{29} \text{ odds})}{1} \right\}$$

provides a numerical measure of the relative abundance of the even-carbon-numbered fatty acids to the odd-carbon-numbered fatty acids (Kvenvolden, 1966). Values greater than one indicate that the even-carbon-numbered fatty acids are more abundant than odd-carbon-numbered fatty acids. Differences in the CPI in a given location and sediment type could be caused by changes in original input or by changes in the environment of deposition leading to preservational affects (Kvenvolden, 1966). Site C CPI values are very similar in the two fractions, with values averaging  $3.57 \pm 0.47$  for the easily-extractable lipids and  $5.39 \pm 0.67$  for the acid-released lipids (Table 3).

The  $C_{max}$  is defined as the carbon chainlength at which the maximum concentration occurs. In site C sediments, the  $C_{max}$  remains unchanged at  $C_{26}$  for all sample ages from both lipid fractions (Table 3). Gagosian et.al. (1987) used differences in major component chain length to distinguish among source regions for monthly aerosol samples collected in New Zealand. If such

an interannual variation exists at site C, it goes unresolved as only an overall average for the 1500kyr sample can be measured. The consistent  $C_{26}$  maximum at site C indicates that either the specific source locale has not changed temporally, or that the different major source regions had vegetation producing similar biomarker records.

$C_{max}$  values suggest that the character of the terrestrial source region did not change over the surveyed time period. The CPI data is not as clear. It is not possible to effectively uncouple the source aridity vs. windstrength issue based on these biomarker parameters because in this case they are not as definitive as the mineralogic parameters used for this purpose. Unfortunately mineralogic eolian data from nearby core RC11-210 (Figure 17.a) is not reliable in the time interval of the present study (Chuey et.al., 1987).

The available data can be interpreted to indicate that increased windstrength did occur prior to the LGM, but maximum aridity of the source region did not develop until the LGM when the greatest terrestrial indicator input occurred. On a much longer timescale (0-750kyr), mineralogic evidence from Deep-Sea Drilling Project hole 503B (4°N, 96°W; Figure 17.a) in the eastern equatorial Pacific indicates that maximum eolian accumulations are younger than glacial maxima as defined by oxygen isotope stages (Janecek and Rea, 1985).

The terrestrial biomarker from both lipid fractions (easily-extractable and acid-released) displays a bimodal time-series (Figure 12.e) with a lesser maximum at the near-surface (1.2ka) in addition to the already discussed maximum occurring at around the LGM. This near-surface maximum falls within the sediment mixed-layer and may be subject to continued degradation such that it is not ultimately preserved. However, terrestrial organic matter that has survived long-range eolian transport may be less susceptible to *in situ* degradation than marine organic carbon (Gagosian and Peltzer, 1986). Thus, it is possible that a greater proportion of land-derived organic carbon will be preserved than more degradable components such as the easily-extractable short-chain fatty acids.

Bacterial and marine/mixed indicators. The dissimilarity of these biomarkers from the two lipid fractions, easily-extractable and acid-released (Figure 12.b,c), suggests that these compounds are significantly affected by the low pH (3 to 4) reached during the carbonate dissolution and may actually exist in nature in a different form. Biosynthesis of fatty acids is limited to a maximum of 18 carbons in a given chain so C<sub>16</sub> and C<sub>18</sub> fatty acids are used as building blocks in the formation of larger biochemicals (Harwood and Russell, 1984). Cutin, a terrigenous plant wax, is one example where C<sub>16</sub> and C<sub>18</sub> w-hydroxy fatty acids are present as components of longer compounds (Kolattukudy et.al., 1976). The profile of the acid-released marine/mixed biomarker closely resembles that of the terrestrial indicator. The acid-released marine/mixed indicator increases 2.8 times over background levels at the time of the LGM, a value very similar to those estimated for the terrestrial indicator. Taken together, these facts lead to the interpretation that the marine/mixed biomarker detected in the acid-released fraction has a distinctly "mixed" source, largely derived from terrestrial material.

The  $\beta$ -hydroxy acids of bacterial origin are detected only after acid treatment because the low pH disrupts a pH-sensitive amide linkage (Goossens et.al., 1985). However, no similar evidence exists for the branched, short-chain fatty acids included here in the bacterial indicator. Because branched C<sub>15</sub> and C<sub>17</sub> fatty acids have been detected from bacterial cultures (Kaneda, 1963; 1967), it is interpreted that the acid-released bacterial indicator in W8402A-14GC does originate from bacterial remains, left as relicts of the time when this portion of the sediment column represented the sediment mixed-layer. Given that increased amounts of organic carbon were reaching the sediments around the time of the LGM, it is plausible to expect a bacterial population living within the sediment mixed-layer similar to that found in the modern near-surface TOC peak.



## THE IMPACT OF TERRESTRIAL ORGANIC CARBON INPUTS ON MARINE SEDIMENTARY RECORDS

In the previous section, evidence was presented that the TOC record from MANOP site C is largely a measure of paleoproductivity. However, inferences from the terrestrial biomarkers found at each depth suggest that a significant fraction of the TOC may be terrestrial in origin. This section highlights possible source regions and transport pathways of terrestrial inputs to MANOP site C, estimates the relative terrestrial contribution to site C sediments over the last 26ka, and discusses the impact of terrestrial carbon inputs on the use of TOC records to estimate paleoproductivity.

Terrestrial source regions and transport paths. The long distances between major land masses and Site C, located about 4400km WSW of Central America, 7000km W of South America, roughly 15,000km ESE of Asia and 9000km NE of Australia (Figure 17.a), make it safe to assume that eolian transport accounts for all terrestrial carbon inputs. The precise source location of the land-derived material reaching site C is problematic due to the paucity of aerosol samples from within this region. It seems the farther one goes from continents, the less there is known about the impact of continental material on a region.

Site C underlies the southeast tradewinds (Figure 17.c) so a source located to the east (i.e. the Americas) is a logical possibility. An increase of Central American aridity coupled with weakening SE tradewinds led to a greater input of continental material from the Central and North Americas to the southeast Pacific during isotope stage 5 (Dauphin, 1983). A similar but more recent occurrence within the timeframe of the present study is not mentioned but if 18ka conditions were similar to stage 5 conditions, eolian input from the east and northeast to site C during the LGM could have resulted. Gagosian and Peltzer (1986) name Central American regions as a minor, seasonal source of lipids collected at Enewetak Atoll (Figure 17.a) in the southwest North Pacific on the basis of meteorologic data and fatty alcohol distribution. Alternatively, interpretation of mineral aerosol samples

Figure 17. Maps of the Pacific Ocean showing (a) location of MANOP site C and other cores mentioned in this discussion and the surrounding land masses, (b) oceanic surface currents around site C (figure after Pisias and Rea, 1988), and (c) modern prevailing winds (figure from Pickard and Emery, 1982).

Figure 17.

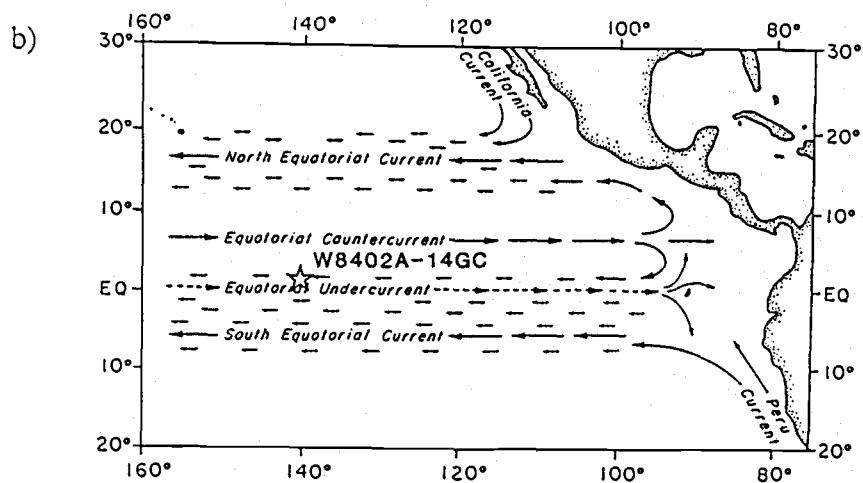
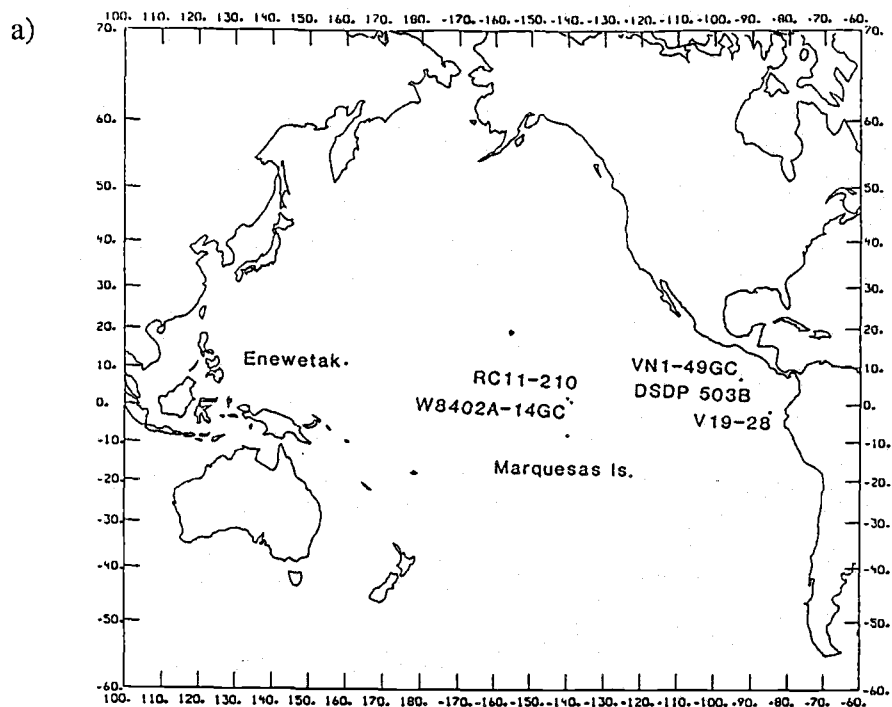
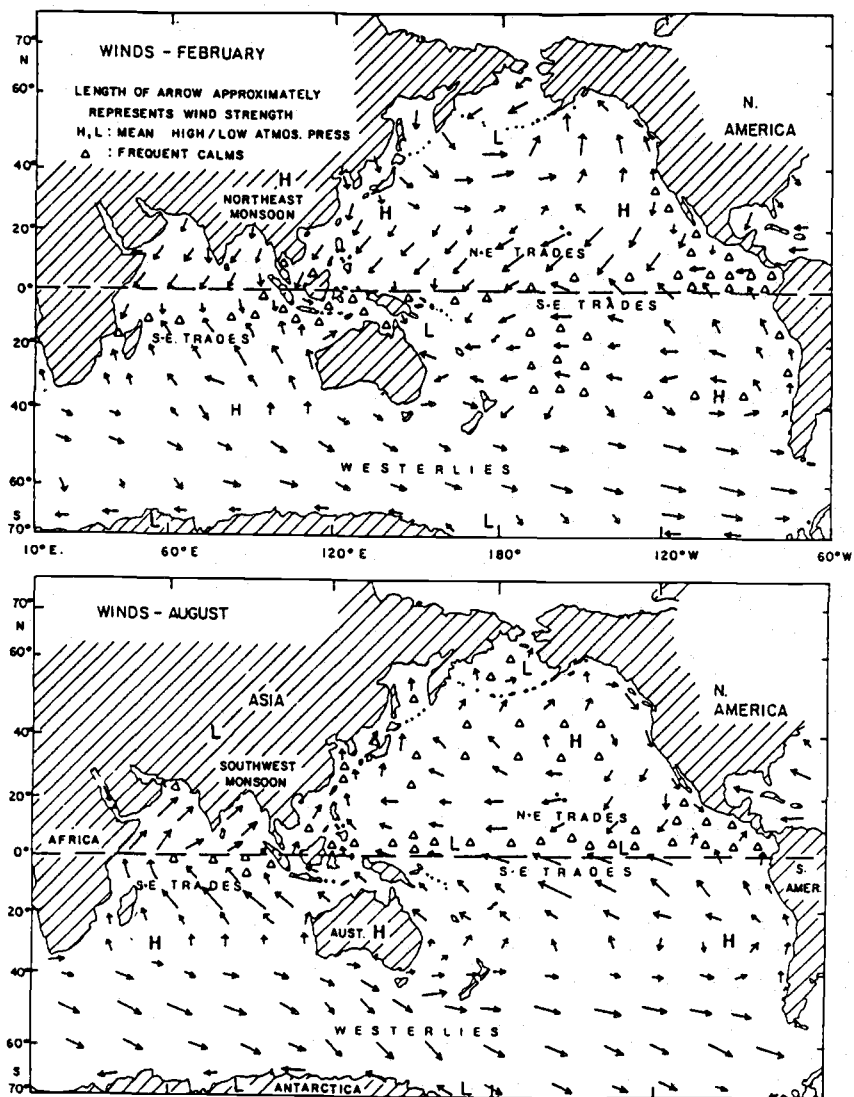


Figure 17 (cont'd).

c)



from six north Pacific SEAREX sites including Enewetak Island suggests the majority of land-derived material delivered to the Pacific ocean between 0 and 30°N and west of 155°W is loess from Asiatic deserts (Uematsu et.al., 1983; Duce et.al. 1980). Sediment surface and downcore mineralogic data identify the transport path from Asia to the North Pacific as lying between 25 and 40°N, with an equatorward shift during the LGM at 18ka (Dauphin, 1983). As far east as 140°W, quartz grain size continues to decrease, implying that Asiatic material is carried still farther east (Dauphin, 1983) so delivery to the site C longitude is possible but the latitudes are not a good match. If the southeast Pacific has wind patterns similar to the strong westerlies credited for carrying Asiatic dust as far east as 140° W, even Australia is a possible source region (Chuey et.al., 1987).

In addition to location, the size and quality (aridity) of possible ice-age source regions must also be considered. Presumably, drier terrestrial areas erode more easily than do heavily vegetated areas. Sarnthein (1978) places the fullest extent of worldwide subtropical deserts at 18ka. A computerized 18ka-climate simulation predicts arid conditions in northern South America, equatorial Africa and southeast Asia (Manabe and Hahn, 1977). A review of three glacial climate computer models shows discrepancies in location of American continental deserts but the models all predict less rain in much of southeast Asia (Heath, 1979). Scouring of plant surfaces by wind-blown particles may lead to direct emission of waxy substances (Gagosian et.al., 1982); if this process is significant then the aridity of a continental source region may not be as crucial for providing a source of land-derived plant material to the atmospheric transport system.

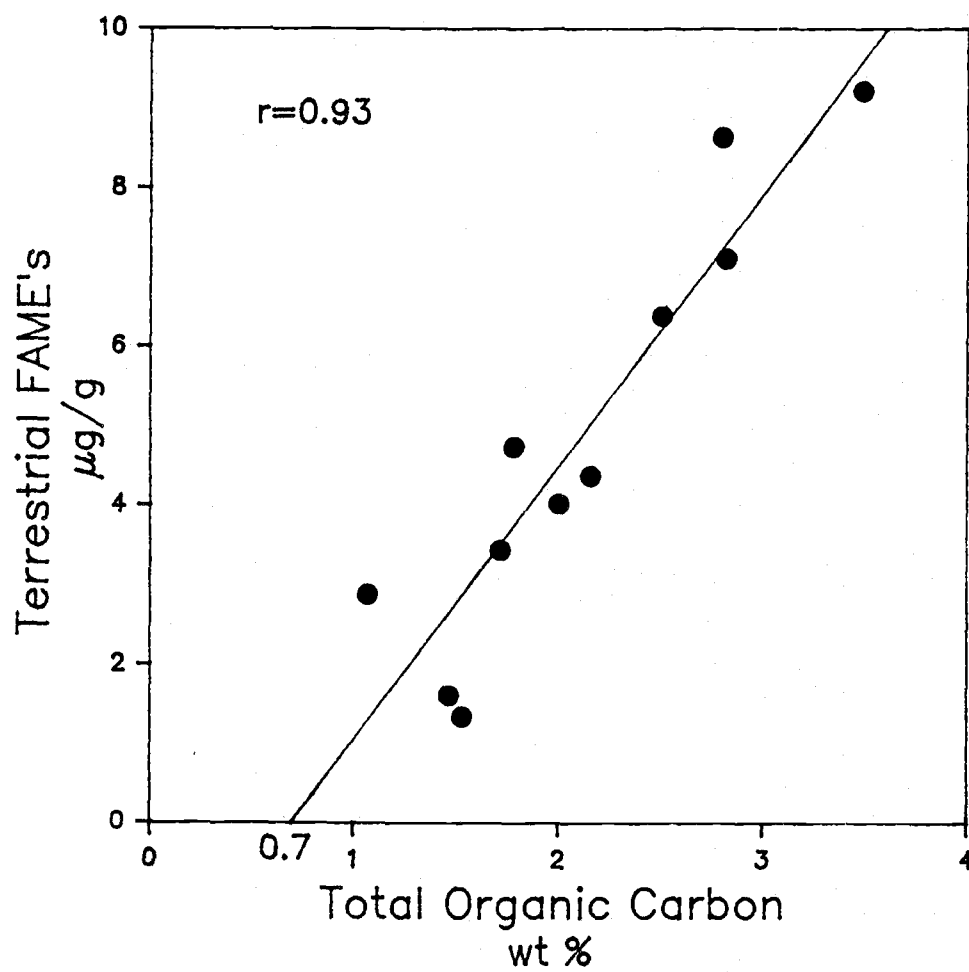
In conclusion, nearly any continent surrounding the Pacific Ocean could be the source of terrestrially-derived material detected in the sediments of W8402A-14GC. The nonvariability of the  $C_{max}$  and CPI (Table 3) detected in site C sediments do not indicate a change in the source region over the last 0-26kyr, but these data do not allow identification of the source. This inconclusive conclusion largely agrees with the possibilities outlined by Chuey et.al. (1987), who studied mineralogic eolian input from RC11-210

(Figure 17.a), and gave plausible reasons to consider northern South America, Asia, or Australia as possible source regions. However, they cite pollen studies from the northern Andes and eastern equatorial Pacific DSDP results to arrive at the conclusion that northern South America was relatively humid during glacial intervals and therefore violates the aridity factor that enriches a continental source, whereas the computer-model (Manabe and Hahn, 1977) cited above predicts arid conditions in northern South America at the LGM. Because regional pollen records can be expected to be more accurate than global computer models, northern South America is not as likely to be the terrestrial source region at the LGM as originally proposed. Based on the spotty data, Asia is inferred as the most likely source.

Estimation of terrestrial organic carbon inputs. Two methods will be presented to estimate the relative contribution of terrestrial organic carbon to site C sediments. The first is derived from the correlation of the terrestrial biomarker with TOC in site C sediments. The second uses lipid aerosol data collected at Enewetak Atoll (Zafiriou et.al., 1985).

The TOC and terrestrial indicator time series from site C sediments are very similar (Figure 12.a,f) and linear regression results in a correlation coefficient of 0.93 ( $n=11$ , Figure 18). Because the x-intercept of this line is nonnegative, i.e. the terrestrial indicator goes to zero before TOC becomes equal to zero, it can be argued that the TOC value at this point, (0.70 weight percent, carbonate-free), is the only portion of TOC contributed by marine sources. Beyond this point, any increases in TOC are due only to additions of terrestrial organic carbon while marine organic carbon inputs are fixed at some relatively low level. This interpretation assumes that the relative amount of the terrestrial biomarker in eolian carbon does not vary, that is,  $\Sigma\text{FAME}/\text{TOC}_{\text{eolian}}$  is constant. This implies that the source region is very stable temporally. It further assumes that the slope of the regression line (3.4) represents the ratio  $\Sigma\text{FAME}/\text{TOC}_{\text{eolian}}$  which can be thought of as the composition of eolian inputs.

Figure 18. Linear regression of the easily-extractable terrestrial indicator ( $\Sigma$ FAME's) against total organic carbon (both are carbonate-free).



Then, given the regression line

$$\Sigma \text{Terrestrial FAMES's} = 3.4 * \text{TOC} - 2.4$$

which is of the form  $y=mx+b$ , the magnitude of the terrestrial input can be calculated if TOC is known. This could be very useful because it is much easier to measure TOC than it is to measure  $\Sigma \text{FAME's}$ . After completing enough  $\Sigma \text{FAME}$  analyses to establish the precise relationship between  $\Sigma \text{FAME's}$  and TOC for a given location, a much larger number of terrestrial inputs could be computed from the TOC values.

Innumerable previous investigations have suggested that the vast majority of deep-sea TOC came from marine sources, and there are several lines of evidence which disprove a fixed-marine-input, terrestrially-driven TOC model. (1) The model assumes that the long-chain FAME's represent terrestrial organic carbon; however, fatty acids are but one of many biochemicals produced by terrestrial plants and possibly transported to oceanic sediments. Because of their source-specificity, they are useful to establish that terrestrial organic carbon does reach ocean sediments and to estimate relative input changes over time, but they cannot be used in a strictly mathematical sense to represent the entire terrestrial input just as the  $\Sigma$ alkenones cannot be used to trace all of the marine carbon inputs. (2) The CPI and  $C_{\text{max}}$  temporal records can be interpreted to indicate that the character of the source region did not change but that does not preclude the possibility of similar but different source regions. Given the world-wide effects of interglacial/glacial cycles, it is likely that the terrestrial source regions for site C terrestrial organic carbon inputs did change during the last 0-26kyr. Indeed, it has been demonstrated from eolian lipid work that Enewetak Atoll (Figure 17.a) experiences an interannual variation in terrestrial organic carbon sources from two sources on opposite sides of the Pacific ocean (Gagosian et.al., 1987). (3) The temporal variation of the Prymnesiophyte indicator and opal records in site C sediments demonstrate that marine inputs do change and are not fixed.



The strong correlation between the TOC and terrestrial biomarker indicates that the oceans, atmosphere and continents are an interactive system. All sectors of this system were affected by and responded to global climate changes associated with a period of time known as the last glacial maximum. It is not within the scope of this thesis to discuss Milankovitch-type global climate forcing and so the ultimate cause of these changes will not be discussed here. The observed responses from different sectors are quite similar because they are linked by global conditions such as the intensity of atmospheric circulation.

The second terrestrial contribution estimate utilizes aerosol lipid data. The existing aerosol data most proximal to site C was collected by the Sea-Air Exchange Program at Enewetak Atoll, Marshall Islands (11°20'N, 162°20'E), located in the west-central tropical Pacific Ocean (Figure 17.a). Using data collected on a total of ten days during April, May, July and August of 1979, five different models were proposed to estimate the annual rainfall fluxes of selected organic components at Enewetak Atoll (Zafiriou et.al., 1985). These five models, based on a variety of assumptions and data extrapolations, led to estimated total terrestrial fatty acid fluxes ranging from 160 to 1500  $\mu\text{g}/\text{m}^2/\text{yr}$ . For three of these models, sufficient data was available to determine the corresponding total organic carbon flux. Therefore, these models, "mean concentration", "constant scavenging ratio fluxes", and "volume effect adjustment", have been applied to give an estimate of the relative terrestrial contribution to organic carbon at site C (Prah1 and Muehlhausen, 1988).

Salient features of the Zafiriou et.al. (1985) models can be summarized as follows. The first, "mean concentration", assumes that the fatty acid concentration measured in rainy season samples represents the mean concentration of all aerosol samples regardless of season. This model probably overestimates the fatty acid flux because little deposition occurs without rainfall (Zafiriou et.al., 1985). The second, "constant scavenging ratio fluxes", adjusts the rainy season data for seasonal concentration variation but assumes the fatty acids to be "scavenged" or deposited at the same relative

concentration under all conditions, whether rainy or dry. The third and most realistic model, "volume effect adjustment", attempts to adjust for increased organic carbon deposition during rainy conditions, the so-called "volume effects" noted from a correlation between rain volume and fatty acid concentration measured in the aerosol samples (Zafiriou et.al., 1985).

To construct a temporal record of relative terrestrial carbon inputs at site C, the aerosol and sedimentary data must be in comparable forms. Beginning with the aerosol data, the first calculation normalizes the  $\Sigma$ terrestrial FAME to total organic carbon and obtains the values 471, 554, and 1288  $\mu\text{g } \Sigma$ terrestrial FAME/g TOC for the aforementioned models, respectively (Prah1 and Muehlhausen, 1988). Then, assuming that the aerosol lipid to TOC ratios measured at Enewetak are the same as those delivered to site C over the last 26kyr, these model aerosol input estimates can be related to the sedimentary terrestrial organic carbon content. Dividing each of the values above (471, 554 and 1288  $\mu\text{g FAME/TOC}$ ) by the  $\Sigma$ terrestrial FAME ( $\mu\text{g/TOC}$ ) measured downcore at site C results in a percentage terrestrial contribution to TOC (Table 6).

Overall, the values vary widely, ranging from 7 to 70% terrestrial carbon content. The highest estimated value, 70% terrestrial organic carbon, is almost certainly an overestimate. If terrestrial organic carbon inputs were this high they would dominate the TOC record to such an extent that marine input variations such as the 6-fold increase in the  $\Sigma$ alkenones observed at the LGM would be obliterated. Still, these calculations are a reasonable attempt at estimating the relative terrestrial contribution to site C sediments.

The results from the third model will be utilized because it includes corrections which best approximate a year-round data period. Plotting them against depth/age gives a 0-26ka time-series of estimated terrestrial organic carbon as a percentage of the TOC (Figure 19). The time-series resembles the terrestrial biomarker profile as expected since it is calculated from this data set, with values ranging from 7% to a maximum of 26% and averaging  $17.5 \pm 5.5\%$ .

Table 6. Estimation of relative terrestrial organic carbon input to MANOP site C sediments.

| Depth<br>(cm) | Age <sup>1</sup><br>(Ka) | Model A <sup>2</sup> | Model B <sup>2</sup> | Model C <sup>2</sup> |
|---------------|--------------------------|----------------------|----------------------|----------------------|
| 1.5           | 1.2                      | 57                   | 48                   | 21                   |
| 7.5           | 4.4                      | 48                   | 41                   | 17                   |
| 16.5          | 9.8                      | 23                   | 20                   | 9                    |
| 19.5          | 11.5                     | 19                   | 16                   | 7                    |
| 22.5          | 13.3                     | 43                   | 36                   | 16                   |
| 25.5          | 15.1                     | 43                   | 36                   | 16                   |
| 28.5          | 16.9                     | 54                   | 45                   | 20                   |
| 31.5          | 18.6                     | 58                   | 49                   | 21                   |
| 34.5          | 20.4                     | 70                   | 60                   | 26                   |
| 37.5          | 22.1                     | 58                   | 49                   | 21                   |
| 44.5          | 25.7                     | 49                   | 42                   | 18                   |

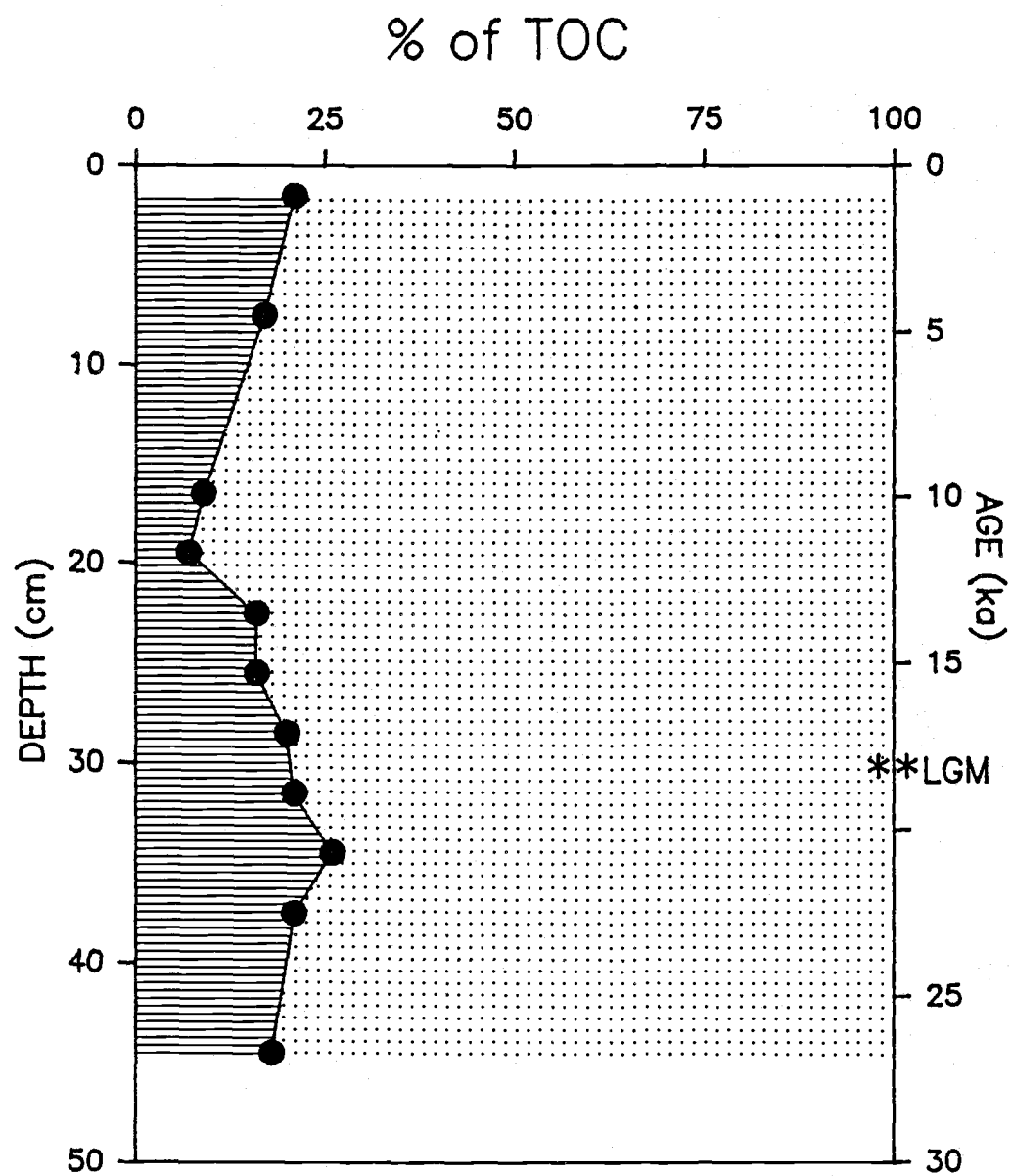
(1) Interpolated from data in Murray, 1987. (2) Estimations based on models (A) mean concentration, (B) constant scavenging, and (C) volume effects from Zaririou et.al., (1985); models summarized in text.

Many of the criticisms of the first method apply to this one. It is unknown whether Enewetak and site C share the same terrestrial carbon source, and therefore unknown if it is reasonable to use this aerosol data in site C estimates. The assumption that modern aerosol data can be applied over the last 26kyr is questionable although the microfossil transfer functions are based on a similar assumption (Imbrie and Kipp, 1971). Unlike the terrestrial estimate model first presented, this second method does allow for a greater and variable marine contribution which is more realistic based on the variability demonstrated by the marine biomarkers presented here.

Relative marine contribution to TOC. In the site C sediments, two sources of organic carbon exist, marine and terrestrial. Given that these two sources must total 100%, we can make a simple difference calculation to arrive at the relative marine contribution to total organic carbon using the average terrestrial contributions estimated from the Enewetak aerosol data. This gives an estimated marine contribution ranging from 74% to 93% (Figure 19). The most remarkable feature of this plot is that never in the last 26ka has the sedimentary organic carbon at site C been composed entirely of marine carbon. This leads to the question: how does up to 20% relative terrestrial organic carbon in open ocean sediments affect using TOC to reconstruct paleoproductivity records?

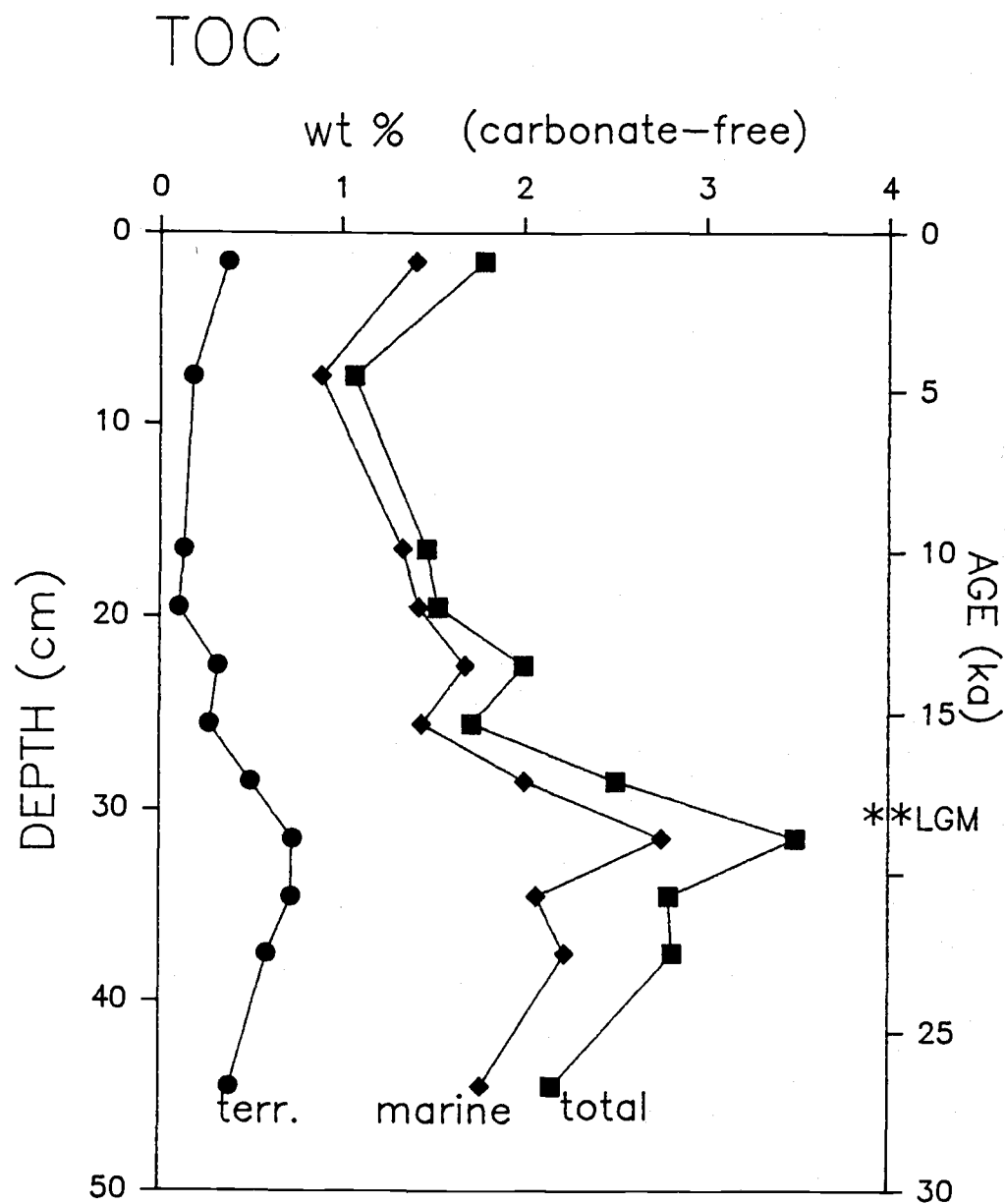
Impact on sedimentary organic carbon records. At least two significant points have been made from these estimates. First, terrestrial organic carbon inputs can be very important, contributing approximately 10 to 20% of TOC even at the remotest oceanic locales. This point has been asserted before (Gagosian et.al., 1987; Zafiriou et.al., 1985;) but numerical estimates of terrestrial organic carbon in the sedimentary record have been lacking. Nor has a temporal study of terrestrial carbon inputs to sediments been done on a geologic time-scale before. It will be interesting to compare these results with those of future studies to ascertain if the observations presented here are an unusual case or are common to other oceanic regions. The latter is suspected.

Figure 19. Terrestrial (striped area) and marine (dotted area) organic carbon inputs to MANOP site C sediments estimated from Zafiriou et.al. (1985) aerosol data.



Second, terrestrial organic carbon inputs should be considered prior to using TOC to estimate paleoproductivity because the application of TOC records to predict paleoproductivity assumes sedimentary TOC to be completely of marine origin, and it has been suggested that it may not have a 100% marine origin. In order to establish the sources of organic carbon, solvent-extractable lipids must be examined for terrestrial biomarkers to enable at least a "spot check" for terrestrially-derived organic carbon and ideally an estimate of the terrestrial contribution to TOC would be undertaken for all samples. In this study, the terrestrial contribution is relatively low, and the other biomarkers display different relative abundances and/or different abundance maxima downcore in the presence of a terrestrial component; therefore any observed variations in site C TOC may be largely attributable to variations in paleoproductivity. Figure 20 illustrates that the marine component dominates the TOC profile in site C sediments, and the terrestrial component does not interfere with applying TOC as an indicator of bulk marine productivity. More biomarker estimations of the relative terrestrial contribution to marine TOC records are necessary to determine whether these results hold true in other oceanic regimes.

Figure 20. Estimated terrestrial (circle) and marine (diamond) inputs as their absolute contributions to TOC (square). Terrestrial input estimate based on aerosol data (Zafifiou et.al., 1985) and marine input found by difference from TOC (carbonate-corrected).



## CONCLUSIONS

At 22-20ka, global glacial conditions caused increased surface winds which in turn led to an intensified upwelling of colder, nutrient-rich water and subsequent increased marine productivity along the equatorial divergence. Terrestrial inputs began to increase due to increased winds but did not peak until the slower expansion of continental deserts peaked around 19ka. The acid-released bacterial and marine/mixed indicators are consistent with the historical interpretation based on the prymnesiophyte and terrestrial indicators. All of these organic carbon sources are recorded as a TOC maximum coincident with the LGM.

Terrestrial organic carbon inputs to the central equatorial Pacific are estimated at roughly 10 to 20%, significant enough to warrant inclusion in future sedimentary organic carbon studies but not enough to negate using TOC to predict marine productivity.

The more recent near-surface TOC peak is an example of in situ degradational processes and will not be preserved on a geologic time-scale.

Molecular biomarkers have provided new and useful insight into the paleoceanography of this region. Similar studies spanning other time periods and from other oceanic regions will improve paleoenvironmental analyses world-wide.

Suggestions for future studies.  $U^{k'}_{37}$ -index paleotemperature record reconstructions could be improved with a number of laboratory studies. First, other major coccolithophorid species need to be surveyed for their lipid content. A north-south coccolithophorid survey along 155°W identified E. huxleyi at all latitudes but other species (e.g. Gephyrocapsa oceanica, Umbellosphaera irregularis, U. tenuis, Rhabdosphaera clavigera, Florisphaera profunda and Thorosphaera flabellata) were found to contribute up to 50% of the standing stock at lower latitudes (Okada and Honjo, 1973) and could therefore be important contributors to the alkenone record if indeed they



produce alkenones. Those species found to contain alkenones could be cultured at a range of growth temperatures and the response of alkenone unsaturation monitored. Lipid surveys of related but non-coccolith-producing algal species will augment existing data on the distribution and temperature dependence of alkenone production, extend the applicability of the  $U^{k'}_{37}$ -index paleotemperature method, and aid chemotaxonomic efforts.

The effects of growth temperatures exceeding 25°C on alkenone unsaturation have yet to be examined under laboratory conditions (Prahl and Wakeham, 1987). As SST's greater than 25°C are commonly observed in the tropical ocean, further laboratory studies at higher temperatures are necessary to extend the calibrated range of the  $U^{k'}_{37}$  index-temperature relationship.

Available data indicates that the  $U^{k'}_{37}$ -index predicted temperatures reflect surface mixed-layer conditions (Prahl and Wakeham, 1987) but more field data are needed to substantiate precisely where in the water column Prymnesiophyte algae produce the alkenones. If the plants are not recording sea-surface temperatures, what are they recording? Samples of the euphotic zone water column need to be collected for a combined phytoplankton survey and alkenone determination. Sediment trap time-series on a monthly or seasonal basis are needed to determine when during the year the Prymnesiophytes contribute the greatest flux to the sediment record. How do seasonal population changes affect the time-averaged temperature signal detected in the sediment record? Is the paleotemperature record weighted toward colder temperatures associated with periods of increased upwelling?

More sedimentary long-chain lipid data detailing the  $K_{37}/K_{38}$  and  $EE/K_{37}$  parameters are needed for comparison to current data. Calculation of these parameters from existing alkenone data sets and inclusion of these parameters in future alkenone studies will extend this intriguing data set and allow some of the current uncertainties to be clarified. Also, laboratory studies designed to elucidate the physiological role of the  $C_{36}$  fatty acid esters and to confirm the suggested membrane role of the alkenones (Prahl et.al., 1988) will clarify the reasons algal biochemical synthesis responds to

growth temperature. Synthetic, radiolabelled alkenones (Rechka and Maxwell, in press) may be useful in these studies.

A downcore continuation at MANOP site C through other glacial/interglacial cycles is essential to allow comparison to this 0-26ka study and to help varify the initial observations presented here. In addition, examination of other cores are recommended for future work. In respect to  $U^{k'}_{37}$ -index paleotemperature predictions, it would be especially interesting to chose cores from areas where CLIMAP has predicted larger glacial/interglacial SST change such as the North Sea or the Sea of Japan. Samples older than 300ka from nearby core RC11-210 (Figure 17.a) display greater SST amplitude than do younger samples (Pisias and Rea, 1988), so it would be interesting to determine the  $U^{k'}_{37}$ -index paleotemperature predictions for some of these samples and compare them to the microfossil paleotemperature record.

The quantity and source location(s) of terrestrial organic carbon and mineralogic inputs to equatorial Pacific sediments should be better constrained. I suggest collection of aerosol samples over one year with concurrent monitoring of wind velocity and other meterologic data at a nearby remote ocean site such as the Marquesas Islands (Figure 17.a). The results from such a study would clarify the uncertainties which currently handicap organic geochemical (this study), and minerologic (Chuey et.al., 1987) studies of this area. It would also be worthwhile to evaluate the mineralogic wind indicators in W8402A-14GC and compare them to the biomarkers, especially because the mineralogic data from the upper 50ka in RC11-210 is questionable (Chuey et.al., 1987).

## BIBLIOGRAPHY

- Boon, J.J., van der Meer, F.W., Schuyl, P.J.W., de Leeuw, J.W., Schenck, P.A., and Burlingame, A.L. (1978). Organic geochemical analyses of core samples from site 362, Walvis ridge, DSDP leg 40. In: Bolli, H.M, Ryan, W.B.R. et.al., Init. Rep. DSDP, 40:627-637, Washington, U.S. Govt. Printing Office.
- Boon, J.J., Rijpstra, W.I.C., deLange, F. and deLeeuw, J.W. (1979). Black Sea sterol- a molecular fossil of dinoflagellate blooms. *Nature*, 277:125-127.
- Bramlette, M.N. (1958). Significance of coccolithophorids in calcium-carbonate deposition. *Bull. Geol. Soc. Am.* 69:121-126.
- Brassell, S.C., Comet, P.A., Eglinton, G., Isaacson, P.J, McEvoy, J., Maxwell, J.R., Thomson, I.D., Tibetts, P.J., and Volkman, J.K. (1980). Preliminary lipid analyses of sections 440A-7-6, 440B-3-5, 440B-8-4, 440B-62-2, and 436-11-4: LEGS 56 and 57, In: Scientific Party., Init. Rep. DSDP, 66:1367-1390, Washington, U.S. Govt. Printing Office.
- Brassell, S.C., Eglinton, G., and Maxwell, J.R. (1981). Preliminary lipid analyses of two quaternary sediments from the Middle America Trench, Southern Mexico Transect, Deep Sea Drilling Project LEG 66. In: Watkins, J.S., Moore, J.C., et.al., Init. Rep. DSDP, 66:557-580, Washington, U.S. Govt. Printing Office.
- Brassell, S.C., Eglinton, G., Marlowe, I.T., Pflaumann, U., and Sarnthein, M. (1986a). Molecular stratigraphy: a new tool for climatic assessment. *Nature*, 320:129-133.
- Brassell, S.C., Brereton, R.G., Eglinton, G., Grimalt, J., Liebezeit G., Marlowe, I.T., Pflaumann, U. and Sarnthein, M. (1986b). Palaeoclimatic signals recognized by chemometric treatment of molecular stratigraphic data. *Org. Geochem.*, 10:661-669.
- Broecker, W.S. and Peng, T-H. (1982). Tracers in the Sea. Lamont-Doherty Geological Observatory, Columbia University, New York, 691pp.
- Chavez, F.P. and Barber, R.T. (1987). An estimate of new production in the equatorial Pacific. *Deep-Sea Res.*, 34:1229-1243.
- Chavez, F.P. (1987). The area of enhanced new production in the equatorial Pacific and its relation to global new production. *EOS, Trans. Amer. Geophys. Union*, 68:1692.
- Cho, B.C. and Azam, F. (1988). Major role of bacteria in biogeochemical fluxes in the ocean's interior. *Nature*, 332:441-443.
- Chuey, J.M., Rea, D.K., and Pisias, N.G. (1987). Late Pleistocene Paleoclimatology of the Central Equatorial Pacific: a quantitative record of eolian and carbonate deposition. *Quat. Res.*, 28:323-339.

- CLIMAP (1976). The surface of the ice-age earth. *Science*, 191:1131-1137.
- CLIMAP (1981). Seasonal Reconstructions of the Earth's Surface at the Last Glacial Maxima. Geol. Soc. of America, map and chart series, MC-36:3A, 3B, 4A, 4B, Boulder, Colorado.
- Cooper, W.J. and Blumer, M. (1968). Linear, iso and anteiso fatty acids in Recent sediments of the North Atlantic. *Deep-Sea Res.*, 15:535-540.
- Corner, E.D.S., O'Hara, S.C.M., Neal, A.C., and Eglinton, G. (1986). Copepod faecal pellets and the vertical flux of biolipids. In: The Biological Chemistry of Marine Copepods, E.D.S. Corner and S.C.M. O'Hara, (eds.), Oxford Science Publications, pp. 260-321.
- Cranwell, P.A. (1974). Monocarboxylic acids in lake sediments: Indicators, derived from terrestrial and aquatic biota, of paleoenvironmental trophic levels. *Chem. Geol.*, 14:1-14.
- Dauphin, J.P. (1983). Eolian Quartz Granulometry as a Paleowind Indicator in the Northeast Equatorial Atlantic, North Pacific and Southeast Equatorial Pacific. Ph.D. dissertation, University of Rhode Island, Kingston.
- Davis, J.B. (1968). Paraffinic hydrocarbons in the sulfate-reducing bacterium Desulfovibrio desulfuricans. *Chem. Geol.*, 3:155-160.
- De Barr, H.J.W., Farrington, J.W. and Wakeham, S.G. (1983). Vertical flux of fatty acids in the North Atlantic Ocean. *J. Mar. Res.*, 41:19-41.
- Degens, E.T. (1969) Biogeochemistry of stable carbon isotopes. In: Organic Geochemistry, G. Eglinton and E.T.J. Murphy, (eds.), Springer Verlag, Berlin, pp. 304-329.
- Delany, A.C., Delany, A.C., Parkin, D.W., Griffin, J.J., Goldberg, E.D., and Reimann, B.E.F. (1967). Airborne dust collected at Barbados. *Geochim. Cosmochim. Acta*, 31:885-909.
- Duce, R.A. (1986). The impact of atmospheric nitrogen, phosphorus and iron species on marine biological productivity. In: The Role of Air-sea Exchange in Geochemical Cycling, P. Bual-Menard (ed), D.Reidel, Boston, pp.497-529.
- Duce, R.A., and Gagosian, R.B. (1982). The input of atmospheric  $n$ -C<sub>10</sub> to  $n$ -C<sub>30</sub> alkanes to the ocean. *J. Geophys. Res.*, 87:7192-7200.
- Duce, R.A., Unni C.K., Ray, B.J., Prospero J.M., and Merrill, J.T. (1980). Long-range atmospheric transport of soil dust from Asia to the tropical North Pacific: Temporal variability. *Science*, 209:1522-1524.
- Dymond, J. (1985). Particulate barium fluxes in the oceans: an indicator of new productivity. *EOS, Trans. Amer. Geophys. Union*, 66:1275.

- Dymond, J. and Collier, R. (1988). Biogenic particle fluxes in the equatorial Pacific: Evidence for both high and low productivity during the 1982-83 El Nino. *Global Biogeochem. Cycles*, 2:129-137.
- Emerson, S. (1985). Organic carbon preservation in marine sediments. In: The Carbon Cycle and Atmospheric CO<sub>2</sub>: Natural Variations Archean to Present, E.T. Sundquist and W.S. Broecker, (eds.), Washington, D.C., pp.78-87.
- Emerson, S., Stump, C. Grootes, P.M., Stuiver, M., Farwell, G.W. and Schmidt, F.H. (1987). Estimates of degradable organic carbon in deep-sea surface sediments from <sup>14</sup>C concentrations. *Nature*, 329:51-53.
- Farrimond, D. Eglinton, G. and Brassell, S.C. (1986). Alkenones in Cretaceous black shales, Blake-Bahama Basin, western North Atlantic. In: Advances in Organic Geochemistry 1985. *Org. Geochem.*, 10:897-903.
- Farrington, J.W., Davis, A.C., Sulanowski, J., McCaffrey, M.A., McCarthy, M., Clifford, C.H., Dickinson, P. and Volkman, J.K. (in press). Biogeochemistry of lipids in surface sediments of the Peru upwelling area at 15°S. Advances in Organic Geochemistry, 1987, Pergamon Press, Oxford.
- Froelich, P.N., Klinkhammer, G.P., Bender, M.L., Luedtke, N.A., Heath, G.R., Cullen, D., Dauphin, P., Hammond, D., Hartman B., and Maynard, V. (1979). Early oxidation of organic matter in pelagic sediments of the eastern equatorial Atlantic: suboxic diagenesis. *Geochem. Cosmochim. Acta*, 43:1075-1090.
- Gagosian, R.B., and Peltzer, E.T. (1987). The importance of atmospheric input of terrestrial organic matter to deep sea sediments. *Org. Geochem.*, 10:661-669.
- Gagosian, R.B., and Peltzer, E.T. (1986). The importance of atmospheric input of terrestrial organic matter to deep sea sediments. In: Advances in Organic Geochemistry, 1985, *Org. Geochem.*, 10:661-669.
- Gagosian, R.B., Zafiriou, O.C., Peltzer, E.T. and Aford J.B. (1982). Lipids in aerosols from the tropical North Pacific: Temporal variability. *J. Geophys. Res.*, 87:11,133-11,144.
- Garrels, R.M. and Perry E.A. Jr. (1974). Cycling of carbon, sulfur and oxygen through geologic time. In: The Sea, V.5, Goldberg, E.D., ed., John Wiley and Sons, New York, pp. 303-336.
- Goossens, H., Irene, W., Rijpstra, C. DÜren, R.R., De Leeuw, J.W. and Schenck, P.A. (1986). Bacterial contribution to sedimentary organic matter; a comparative study of lipid moieties in bacteria and Recent sediments. In: Advances in Organic Geochemistry, 1985, *Org. Geochem.*, 10:683-696.
- Haq, B.U. (1978). Calcareous nannoplankton. In: Introduction to Marine Micropaleontology, B.U. Haq and A. Boersma, (eds.), Elsevier, New York, pp. 79-107.

- Harvey, H.R., Richardson, M.D. and Patton J.S. (1984). Lipid composition and vertical distribution of bacteria in aerobic sediments of the Venezuela Basin. *Deep-Sea Res.* 31:403-413.
- Harwood, J.L. and Russell, N.J. (1984). Lipids in Plant and Microbes, George Allen and Unwin, London, 162pp.
- Heath, G.R. (1979). Simulations of a glacial paleoclimate by three different atmospheric general circulation models. *Paleogeography, Paleoclimatology, Paleoecology*, 26:291-303.
- Hunt, J.M. (1979). Petroleum Geochemistry and Geology. W.H. Freeman and Co., San Francisco, 617pp.
- Imbrie, J. and Kipp, N.G. (1971). A new micropaleontological method for paleoclimatology: application to a Late Pleistocene Caribbean core. In: The Late Cenozoic Glacial Ages, K.K. Turekian, (ed.), Yale University, New Haven, pp. 71-181.
- Jahnke, R.A., Emerson, S.R. and Murray, J.W. (1982). A model of oxygen reduction, denitrification, and organic matter mineralization in marine sediments. *Limnol. Oceanogr.*, 27:610-623.
- Janecek, T.R. and Rea, R.K. (1985). Quaternary fluctuations in the northern hemisphere trade winds and westerlies. *Quat. Res.*, 24:150-163.
- Jasper, J. (1988). Organic Geochemical Approach to Problems of Glacial-Interglacial Climate Variability in the Late Quaternary Gulf of Mexico. Ph.D. dissertation, Woods Hole Oceanographic Institution, Massachusetts.
- Kaneda, T. (1963). Biosynthesis of branched-chain fatty acids. I. Isolation and identification of fatty acids from Bacillus subtilis (ATCC 7059). *J. Biol. Chem.*, 238:1222-1228.
- Kaneda, T. (1967). Fatty acids in the genus Bacillus. I. Iso- and anteiso-fatty acids as characteristic constituents of lipids in 10 species. *J. Bacteriol.*, 93:894-903.
- Kawamura, K. and Ishiwatari, R. (1984a). Fatty acid geochemistry of 200m sediment core taken from Lake Biwa. Early diagenesis and paleoenvironmental information. *Geochim. Cosmochim. Acta.* 48:251-266.
- Kawamura, K. and Ishiwatari, R. (1984b). Tightly bound aliphatic acids in Lake Biwa sediments: Their origin and stability. *Org. Geochem.* 7:121-126.
- Kawamura, K. and Ishiwatari, R. (1985). Distribution of lipid-class compounds in bottom sediments of freshwater lakes with different trophic status, in Japan. *Chem. Geol.*, 51:123-133.

- Kolattukudy, P.E., Crouteau, R. and Buckner, J.S. (1976). Biochemistry of plant waxes. In: Chemistry and Biochemistry of Natural Waxes, P.E. Kolattukudy, (ed.), Elsevier, New York, pp. 289-347.
- Kvenvolden, K.A. (1966). Molecular distributions of normal fatty acids and paraffins in some Lower Cretaceous sediments. *Nature*, 209:573-577.
- de Leeuw, J.W., van der Meer, F.W., Rijpstra, W.I.C., and Schenck, P.A. (1980). On the occurrence and structural identification of long chain unsaturated ketones and hydrocarbons in sediments. In: Adv. Org. Geochem. 1979, A.G. Douglas and J.R. Maxwell, (eds.), Pergamon Press, Oxford, pp. 211-217.
- Leo, R.F., Parker, P.L., (1966). Branched-chain fatty acids in sediments. *Science*, 152:649-650.
- Lyle, M. (1988). Climatic forcing of organic carbon burial in the equatorial Atlantic and Pacific oceans. *Nature*, 335:529-532.
- Lyle, M., Murray, D.W., Finney, B.P., Dymond, J., Robbins, J.M. and Brooksforce, K. (1988). The record of late Pleistocene biogenic sedimentation in the eastern tropical Pacific ocean. *Paleoceanography*, 3:39-59.
- Manabe, S. and Hahn, D. (1977). Simulation of the tropical climate of an Ice Age. *J. Geophys. Res.*, 82:3389-3911.
- Marlowe, I.T.; Green, J.C.; Neal, A.C.; Brassell, S.C.; Eglinton, G.; and Course, P.A. (1984a). Long chain alkenones in the Prymnesiophyceae. Distribution of alkenones and other lipids and their taxonomic significance. *Br. J. Phycol.*, 19:203-216.
- Marlowe, I.T., Brassell, S.C., Eglinton, G., and Green, J.C. (1984b). Long chain unsaturated ketones and esters in living algae and marine sediments. *Org. Geochem.*, 6:135-141.
- Martinson, D.G., Pisias, N.G., Hays, J.D., Imbrie, J. Moore, T.C.Jr., Shackleton, N.J. (1987). Age dating and the orbital theory of the ice ages: Development of a high-resolution 0 to 300,000-year chronostratigraphy. *Quat. Res.*, 27:1-29.
- Matsuda, G. and Koyama, T. (1977). Early diagenesis of fatty acids in lacustrine sediments-I. Identification and distribution of fatty acids in recent sediment from a freshwater lake. *Geochim. Cosmochim. Acta*, 41:777-783.
- McCorkle, D.C. (1987). Stable Carbon Isotopes in Deep Sea Pore Waters: Modern Geochemistry and Paleoceanographic Applications. Ph.D. dissertation, University of Washington, Seattle.

- McIntyre, A., Be, A.W.H., and Roche, M.B. (1970). Modern Pacific coccolithophorida: a paleontological thermometer. Trans. New York Academy of Sciences, pp.720-731.
- Meyers, P.A., Leenheer, M.J., Kawka, O.E. and Trull, T.W. (1984). Enhanced preservation of marine-derived organic matter in Cenomanian black shales from the southern Angola Basin. *Nature*, 312:356-359.
- Mix, A.C. (1987). The oxygen-isotope record of glaciation. In: North America and Adjacent Oceans During the Last Deglaciation, W.F. Ruddiman and H.E. Wright, Jr., (eds.), Boulder, CO, Geol. Soc. Amer., The Geology of North America, Vol. K-3:111-135.
- Morrison, R.T., and Boyd, R.N. (1973). Organic Chemistry, Allyn and Bacon, Inc., Boston, p.1058.
- Müller, P.J., Erlenkeuser, H., and von Grafenstein, R. (1983). Glacial-interglacial cycles in oceanic productivity inferred from organic carbon contents in eastern North Atlantic sediment cores. In: Coastal Upwelling, its sediment record. Part B: sedimentary records of ancient coastal upwelling. Thiede, J. and Suess, E., (eds.), Plenum Press, New York, pp. 365-398.
- Müller P.J. and Suess, E. (1979). Productivity, sedimentation rate and sedimentary organic matter in the oceans-I. Organic carbon preservation. *Deep-Sea Res.* 26:1347-1362.
- Murray, D.W. (1987). Spatial and Temporal Variations in Sediment Accumulation in the Central Tropical Pacific. Ph.D. dissertation, Oregon State University, Corvallis.
- Newell, R.E., Kidson, J.W., Vincent D.G. and Boer, G.J. (1972). The General Circulation of the Tropical Atmosphere and Interactions with Extratropical Latitudes. MIT Press, Cambridge. Vol. I.
- Okada, G. and Honjo, S. (1973). The distribution of oceanic coccolithophorids in the Pacific. *Deep-Sea Res.*, 26:355-374.
- Perry, G.J., Volkman, J.K., Johns, R.B., and Bavor, H.J. Jr. (1979). Fatty acids of bacterial origin in contemporary marine sediments. *Geochim. Cosmochim. Acta*, 43:1715-1725.
- Pickard, G.L. and Emery, W.J. (1982). Descriptive Physical Oceanography: an Introduction, Pergamon Press, Oxford, 249pp.
- Pisias, N.G. and Rea, D.K. (1988). Late Pleistocene paleoclimatology of the central equatorial Pacific: Sea surface response to the southeast trade winds. *Paleoceanog.*, 3:21-37.



- Prahl, F.G. and Muehlhausen, L.M. (1989). Lipid biomarkers as geochemical tools for paleoceanographic study. In: Productivity of the Ocean: Present and Past. W. Berger, (ed.), John Wiley and Sons, pp. 271-298.
- Prahl, F.G., Muehlhausen, L.M., and Zahnle, D. (1988). A well-preserved geochemical record for long-chain, unsaturated ketones. *Geochim. Cosmochim. Acta*, 52:2303-2310.
- Prahl, F.G. and Wakeham S.G. (1987). Calibration of unsaturation patterns in long-chain ketone compositions for paleotemperature assessment. *Nature*, 330:367-369.
- Prospero, J.M. and Bonatti, E. (1969). Continental dust in the atmosphere of the eastern equatorial Pacific. *J. Geophys. Res.*, 74:3362-3371.
- Prospero, J.M. and Nees R.T. (1977). Dust concentrations in the atmosphere of the equatorial North Atlantic: Possible relationships to the Sahalian droughts. *Science*, 196:1196-1198.
- Rea, D.K., Leinen, M. and Janecek, T.R. (1985). Geologic approach to the long-term history of atmospheric circulation. *Science*, 227:721-725.
- Rechka, J.A., and Maxwell, J.R. (in press). Characterisation of alkenone temperature indicators in sediments and organisms. Advances in Organic Geochemistry, 1987, Pergamon Press, Oxford.
- Sargent, J.R., Lee, R.F., and Nevenzel, J.C. (1976). Marine Waxes. In: Chemistry and Biochemistry of Natural Waxes. Kolattukudy, P.E., (ed.), Elsevier, New York, pp.49-91.
- Sarnthein, M. (1978). Sand deserts during glacial maximum and climatic optimum. *Nature*, 272:43-46.
- Sarnthein, M., Winn, K., Duplessy, J-C., and Fontugne, M.R. (1988). Global variations of surface ocean productivity in low and mid latitudes: Influence on CO<sub>2</sub> reservoirs of the deep ocean and atmosphere during the last 21,000 years. *Paleoceanog.*, 3:361-399.
- Schlenk, H. and Gellerman, J.L. (1960). Esterification of fatty acids with diazomethane on a small scale. *Anal. Chem.*, 32:1412-1414.
- Schneider, J.K. and Gagosian, R.B. (1985). Particle size distribution of lipids in aerosols off the coast of Peru. *J. Geophys. Res.*, 90:7889-7898.
- Simoneit, B.R.T. (1977). Organic matter in eolian dusts over the Atlantic Ocean. *Mar. Chem.*, 5:443-464.
- Simoneit, B.R.T. and Eglinton, G. (1977). Organic matter of eolian dust and its input to marine sediments. In: Advances in Organic Geochemistry, 1975, R. Campos and J. Goni, (eds.), ENADIMSA, Madrid, pp.415-430.

- Thierstein, H.R., Geitzenauer, K.R., Molino, B. and Shackleton, N.J. (1977). Global synchronicity of late Quaternary coccolith datum levels: validation by oxygen isotopes. *Geology*, 5:400-404.
- Tissot, B.P. and Welte, D.H. (1978). Petroleum Formation and Occurrence. Springer Verlag, New York, 538pp.
- Uematsu, M., Duce, R., Prospero, J., Chen, L., Merrill, J., and McDonald, R. (1983). The transport of mineral aerosol from Asia over the North Pacific Ocean. *J. Geophys. Res.*, 88:5343-5352.
- Valiela, I. (1984). Marine Ecological Processes. Springer Verlag, New York, 546pp.
- Van Vleet, E.S. and Quinn, J.G. (1979). Diagenesis of marine lipids in ocean sediments. *Deep-Sea Res.*, 26:1225-1236.
- Volkman, J.K., Smith, D.J., Eglinton, G., Forsberg T.E.V. and Corner E.D.S. (1981). Sterol and fatty acid composition of four marine haptophycean algae. *J. Mar. Biol. Ass. U.K.*, 61:509-527.
- Volkman J.K., Eglinton G., Corner E.D.S. and Sargent J.R. (1980a). Novel unsaturated straight chain C<sub>37</sub>-C<sub>39</sub> methyl and ethyl ketones in marine sediments and a coccolithophore *Emiliana huxleyi*. In: Advances in Organic Geochemistry 1979, A.G. Douglas and J.R. Maxwell, (eds.), Pergamon Press, pp. 219-227.
- Volkman, J.K., Corner, E.D.S. and Eglinton, G. (1980b). Transformations of biolipids in the marine food web and in underlying bottom sediments. In: Colloq. int. CNRS no. 293, R. Daumas, (ed.), Editions CNRS, Paris, pp. 185-197.
- Wakeham, S.G., Lee, C., Farrington, J.W. and Gagosian, R.B. (1984). Biogeochemistry of particulate organic matter in the oceans: results from sediment trap experiments. *Deep-Sea Res.*, 31:509-528.
- Weete, J.B., (1976). Algal and fungal waxes. In: Chemistry and Biochemistry of Natural Waxes, P.E. Kolattukudy, (ed.), Elsevier, Amsterdam, pp. 349-418.
- Weliky K., Suess E., Ungerer C.A., Müller P.J. and Fischer K. (1983). Problems with accurate carbon measurements in marine sediments and particulate matter in seawater: a new approach. *Limnol. Oceanogr.*, 28:1252-1259.
- Zafiriou, O.C.; Gagosian, R.B.; Peltzer, E.T.; Alford, J.B.; and Loder, T. (1985). Air-to-sea fluxes of lipids at Enewetak Atoll. *J. Geophys. Res.*, 90(D1): 2409-2423.

APPENDIX A: INDIVIDUAL COMPOUND CONCENTRATIONS ( $\mu\text{g/g}$  dry sediment weight, not carbonate-corrected)

EASILY EXTRACTABLE LIPIDS, fatty acid methyl esters

| DEPTH (cm)           | 1.5             | 7.5             | 16.5            | 19.5            | 22.5            | 25.5            | 28.5            | 31.5            | 34.5            | 37.5            | 44.5            |
|----------------------|-----------------|-----------------|-----------------|-----------------|-----------------|-----------------|-----------------|-----------------|-----------------|-----------------|-----------------|
|                      | $\mu\text{g/g}$ | $\mu\text{g/g}$ | $\mu\text{g/g}$ | $\mu\text{g/g}$ | $\mu\text{g/g}$ | $\mu\text{g/g}$ | $\mu\text{g/g}$ | $\mu\text{g/g}$ | $\mu\text{g/g}$ | $\mu\text{g/g}$ | $\mu\text{g/g}$ |
| C <sub>14</sub>      | 0.112           | 0.012           | 0.007           | 0.012           | 0.007           | 0.014           | 0.019           | 0.012           | 0.015           | 0.014           | 0.015           |
| iC <sub>15</sub>     | 0.034           | 0.004           | 0.003           | 0.003           | 0.003           | 0.004           | 0.004           | 0.002           | 0.003           | 0.003           | 0.002           |
| aiC <sub>15</sub>    | 0.030           | 0.004           | 0.002           | 0.003           | 0.000           | 0.003           | 0.004           | 0.003           | 0.003           | 0.003           | 0.002           |
| C <sub>15</sub>      | 0.053           | 0.021           | 0.016           | 0.017           | 0.019           | 0.023           | 0.024           | 0.015           | 0.019           | 0.017           | 0.014           |
| iC <sub>16</sub>     | 0.017           | 0.004           | 0.000           | 0.001           | 0.000           | 0.002           | 0.002           | 0.002           | 0.002           | 0.002           | 0.000           |
| C <sub>16</sub>      | 1.292           | 0.197           | 0.056           | 0.093           | 0.113           | 0.153           | 0.177           | 0.140           | 0.151           | 0.111           | 0.108           |
| iC <sub>17</sub>     | 0.019           | 0.004           | 0.002           | 0.003           | 0.000           | 0.002           | 0.002           | 0.002           | 0.002           | 0.000           | 0.000           |
| aiC <sub>17</sub>    | 0.028           | 0.007           | 0.003           | 0.005           | 0.003           | 0.004           | 0.003           | 0.002           | 0.003           | 0.002           | 0.000           |
| ??                   | 0.038           | 0.036           | 0.003           | 0.000           | 0.035           | 0.069           | 0.027           | 0.039           | 0.058           | 0.033           | 0.042           |
| C <sub>17</sub>      | 0.076           | 0.019           | 0.003           | 0.006           | 0.010           | 0.012           | 0.013           | 0.011           | 0.012           | 0.012           | 0.008           |
| C <sub>18</sub>      | 2.306           | 0.173           | 0.015           | 0.041           | 0.071           | 0.086           | 0.101           | 0.101           | 0.092           | 0.076           | 0.071           |
| C <sub>19</sub>      | 0.021           | 0.010           | 0.000           | 0.003           | 0.006           | 0.006           | 0.005           | 0.005           | 0.004           | 0.003           | 0.003           |
| iC <sub>20</sub> *   | 0.035           | 0.029           | 0.007           | 0.014           | 0.028           | 0.031           | 0.025           | 0.022           | 0.025           | 0.025           | 0.025           |
| C <sub>20</sub>      | 0.067           | 0.028           | 0.007           | 0.007           | 0.018           | 0.020           | 0.032           | 0.045           | 0.030           | 0.022           | 0.014           |
| aiC <sub>21</sub> ** | 0.071           | 0.172           | 0.197           | 0.027           | 0.039           | 0.034           | 0.035           | 0.034           | 0.032           | 0.031           | 0.031           |
| C <sub>21</sub>      | 0.029           | 0.024           | 0.003           | 0.004           | 0.015           | 0.015           | 0.017           | 0.028           | 0.021           | 0.019           | 0.010           |
| C <sub>22</sub>      | 0.078           | 0.054           | 0.010           | 0.017           | 0.042           | 0.042           | 0.064           | 0.081           | 0.067           | 0.055           | 0.035           |
| C <sub>23</sub>      | 0.034           | 0.026           | 0.006           | 0.007           | 0.020           | 0.019           | 0.031           | 0.041           | 0.034           | 0.028           | 0.016           |
| C <sub>24</sub>      | 0.177           | 0.074           | 0.039           | 0.032           | 0.073           | 0.064           | 0.138           | 0.206           | 0.178           | 0.148           | 0.082           |
| C <sub>25</sub>      | 0.054           | 0.032           | 0.013           | 0.012           | 0.028           | 0.026           | 0.052           | 0.071           | 0.058           | 0.048           | 0.027           |
| C <sub>26</sub>      | 0.258           | 0.104           | 0.082           | 0.046           | 0.113           | 0.121           | 0.275           | 0.407           | 0.362           | 0.290           | 0.153           |
| C <sub>27</sub>      | 0.044           | 0.024           | 0.016           | 0.011           | 0.023           | 0.026           | 0.042           | 0.045           | 0.041           | 0.034           | 0.022           |
| C <sub>28</sub>      | 0.129           | 0.074           | 0.048           | 0.033           | 0.076           | 0.088           | 0.142           | 0.174           | 0.167           | 0.137           | 0.092           |
| C <sub>29</sub>      | 0.036           | 0.020           | 0.013           | 0.003           | 0.014           | 0.014           | 0.033           | 0.038           | 0.036           | 0.031           | 0.022           |
| C <sub>30</sub>      | 0.039           | 0.026           | 0.017           | 0.024           | 0.021           | 0.024           | 0.035           | 0.040           | 0.036           | 0.031           | 0.026           |

\*recovery standard

\*\*internal standard for methylation efficiency

APPENDIX A: INDIVIDUAL COMPOUND CONCENTRATIONS (cont'd)

ACID-RELEASED LIPIDS, fatty acid methyl esters

| DEPTH (cm)           | 1.5   | 7.5   | 16.5  | 19.5  | 22.5  | 25.5  | 28.5  | 31.5  | 34.5  | 37.5  | 44.5  |
|----------------------|-------|-------|-------|-------|-------|-------|-------|-------|-------|-------|-------|
|                      | µg/g  | µg/g  | µg/g  | µg/g  | µg/g  | µg/g  | µg/g  | µg/g  | µg/g  | µg/g  | µg/g  |
| C <sub>14</sub>      | 0.109 | 0.055 | 0.046 | 0.019 | 0.048 | 0.044 | 0.107 | 0.166 | 0.112 | 0.079 | 0.057 |
| iC <sub>15</sub>     | 0.059 | 0.021 | 0.016 | 0.007 | 0.014 | 0.014 | 0.026 | 0.045 | 0.032 | 0.026 | 0.015 |
| aiC <sub>15</sub>    | 0.073 | 0.031 | 0.021 | 0.011 | 0.024 | 0.026 | 0.036 | 0.055 | 0.041 | 0.036 | 0.026 |
| C <sub>15</sub>      | 0.053 | 0.029 | 0.038 | 0.013 | 0.028 | 0.023 | 0.047 | 0.069 | 0.050 | 0.044 | 0.027 |
| iC <sub>16</sub>     | 0.068 | 0.020 | 0.024 | 0.010 | 0.017 | 0.016 | 0.038 | 0.075 | 0.051 | 0.044 | 0.024 |
| C <sub>16</sub>      | 0.678 | 0.319 | 0.316 | 0.186 | 0.350 | 0.265 | 0.474 | 0.684 | 0.532 | 0.468 | 0.311 |
| iC <sub>17</sub>     | 0.073 | 0.023 | 0.030 | 0.014 | 0.022 | 0.016 | 0.042 | 0.083 | 0.059 | 0.051 | 0.026 |
| aiC <sub>17</sub>    | 0.045 | 0.020 | 0.024 | 0.014 | 0.021 | 0.018 | 0.034 | 0.056 | 0.044 | 0.039 | 0.023 |
| ??                   | 0.018 | 0.016 | 0.021 | 0.026 | 0.010 | 0.014 | 0.009 | 0.011 | 0.091 | 0.024 | 0.020 |
| C <sub>17</sub>      | 0.047 | 0.023 | 0.025 | 0.015 | 0.026 | 0.018 | 0.039 | 0.061 | 0.053 | 0.046 | 0.024 |
| C <sub>18</sub>      | 0.325 | 0.152 | 0.162 | 0.098 | 0.196 | 0.125 | 0.219 | 0.281 | 0.250 | 0.224 | 0.181 |
| C <sub>19</sub>      | 0.021 | 0.000 | 0.013 | 0.010 | 0.013 | 0.009 | 0.017 | 0.022 | 0.023 | 0.019 | 0.012 |
| iC <sub>20</sub> *   | 0.040 | 0.037 | 0.039 | 0.036 | 0.036 | 0.040 | 0.033 | 0.031 | 0.038 | 0.034 | 0.032 |
| C <sub>20</sub>      | 0.106 | 0.060 | 0.058 | 0.043 | 0.054 | 0.050 | 0.068 | 0.103 | 0.096 | 0.085 | 0.056 |
| aiC <sub>21</sub> ** | 0.045 | 0.041 | 0.062 | 0.044 | 0.044 | 0.345 | 0.037 | 0.046 | 0.040 | 0.039 | 0.039 |
| C <sub>21</sub>      | 0.021 | 0.000 | 0.014 | 0.012 | 0.013 | 0.011 | 0.019 | 0.023 | 0.023 | 0.018 | 0.011 |
| C <sub>22</sub>      | 0.112 | 0.055 | 0.073 | 0.051 | 0.063 | 0.050 | 0.095 | 0.155 | 0.141 | 0.124 | 0.065 |
| C <sub>23</sub>      | 0.025 | 0.014 | 0.017 | 0.013 | 0.015 | 0.012 | 0.022 | 0.031 | 0.029 | 0.025 | 0.014 |
| C <sub>24</sub>      | 0.132 | 0.066 | 0.092 | 0.058 | 0.078 | 0.062 | 0.117 | 0.202 | 0.168 | 0.155 | 0.082 |
| C <sub>25</sub>      | 0.028 | 0.017 | 0.020 | 0.014 | 0.019 | 0.016 | 0.025 | 0.035 | 0.031 | 0.028 | 0.018 |
| C <sub>26</sub>      | 0.140 | 0.079 | 0.105 | 0.065 | 0.088 | 0.077 | 0.139 | 0.222 | 0.180 | 0.177 | 0.096 |
| C <sub>27</sub>      | 0.023 | 0.000 | 0.013 | 0.009 | 0.019 | 0.007 | 0.018 | 0.023 | 0.017 | 0.018 | 0.011 |
| C <sub>28</sub>      | 0.050 | 0.032 | 0.039 | 0.025 | 0.033 | 0.029 | 0.052 | 0.071 | 0.057 | 0.060 | 0.036 |
| C <sub>29</sub>      | 0.000 | 0.000 | 0.000 | 0.000 | 0.003 | 0.000 | 0.000 | 0.000 | 0.000 | 0.000 | 0.000 |
| C <sub>30</sub>      | 0.005 | 0.000 | 0.003 | 0.000 | 0.004 | 0.003 | 0.000 | 0.000 | 0.000 | 0.000 | 0.023 |

\*recovery standard

\*\*internal standard for methylation efficiency

APPENDIX A: INDIVIDUAL COMPOUND CONCENTRATIONS (cont'd)

EASILY-EXTRACTABLE LIPIDS, long-chain alkenones

| DEPTH (cm)         | 1.5   | 7.5   | 16.5  | 19.5  | 22.5  | 25.5  | 28.5  | 31.5  | 34.5  | 37.5  | 44.5  |
|--------------------|-------|-------|-------|-------|-------|-------|-------|-------|-------|-------|-------|
|                    | µg/g  | µg/g  | µg/g  | µg/g  | µg/g  | µg/g  | µg/g  | µg/g  | µg/g  | µg/g  | µg/g  |
| K <sub>37:3</sub>  | 0.008 | 0.002 | 0.004 | 0.004 | 0.005 | 0.005 | 0.015 | 0.027 | 0.032 | 0.042 | 0.017 |
| K <sub>37:2</sub>  | 0.192 | 0.050 | 0.063 | 0.065 | 0.090 | 0.096 | 0.246 | 0.406 | 0.392 | 0.454 | 0.239 |
| EE                 | 0.004 | 0.000 | 0.002 | 0.002 | 0.003 | 0.003 | 0.004 | 0.006 | 0.005 | 0.007 | 0.003 |
| K <sub>38:3e</sub> | 0.000 | 0.000 | 0.000 | 0.000 | 0.000 | 0.000 | 0.000 | 0.000 | 0.000 | 0.000 | 0.000 |
| K <sub>38:3m</sub> | 0.000 | 0.001 | 0.006 | 0.006 | 0.002 | 0.002 | 0.004 | 0.008 | 0.010 | 0.014 | 0.007 |
| K <sub>38:2e</sub> | 0.119 | 0.023 | 0.034 | 0.034 | 0.049 | 0.052 | 0.145 | 0.226 | 0.227 | 0.000 | 0.136 |
| K <sub>38:2m</sub> | 0.000 | 0.010 | 0.012 | 0.001 | 0.015 | 0.021 | 0.044 | 0.089 | 0.088 | 0.337 | 0.050 |
| K <sub>39:2</sub>  | 0.010 | 0.002 | 0.003 | 0.004 | 0.005 | 0.006 | 0.016 | 0.027 | 0.023 | 0.030 | 0.016 |

# APPENDIX B: SEDIMENT PROPERTIES

| DEPTH | AGE               | CaCO <sub>3</sub> | TOC                | DRY SAMPLE WEIGHT |                  |
|-------|-------------------|-------------------|--------------------|-------------------|------------------|
| (cm)  | (ka) <sup>1</sup> | (wt%)             | (wt%) <sup>2</sup> | (g) <sup>3</sup>  | (g) <sup>4</sup> |
| 1.5   | 1.19              | 80.12             | 1.781              | 7.80              | 7.36             |
| 7.5   | 4.44              | 83.18             | 1.068              | 8.97              | 8.59             |
| 16.5  | 9.78              | 84.32             | 1.467              | 8.98              | 8.59             |
| 19.5  | 11.54             | 85.44             | 1.532              | 9.04              | 8.64             |
| 22.5  | 13.31             | 89.00             | 2.000              | 9.56              | 9.01             |
| 25.5  | 15.09             | 86.66             | 1.716              | 9.48              | 8.80             |
| 28.5  | 16.86             | 86.35             | 2.506              | 9.58              | 9.09             |
| 31.5  | 18.64             | 87.67             | 3.488              | 9.61              | 9.22             |
| 34.5  | 20.40             | 88.92             | 2.798              | 9.46              | 8.89             |
| 37.5  | 22.13             | 89.07             | 2.818              | 9.86              | 9.48             |
| 44.5  | 25.72             | 89.98             | 2.156              | 10.19             | 9.82             |

(1) interpolated from data by Murray (1987). (2)carbonate-free.  
 (3)easily-extractable lipids. (4)acid-released lipids.